Integrated water quality and coastal groundwater monitoring to assess nutrient impacts to coral reef health

Photo by University of Hawai‘i at Hilo

This report was prepared by The Nature Conservancy under Award NA14NMF4630259 from the National Oceanic and Atmospheric Administration (NOAA) National Marine Fisheries Service, as administered by the NOAA Restoration Center’s Office of Habitat Conservation. The statements, findings, conclusions, and recommendations are those of the authors and do not necessarily reflect the views of NOAA or the U.S. Department of Commerce.

Integrated water quality and coastal groundwater monitoring to assess nutrient impacts to coral reef health

Kim Falinski[1], Tracy Wiegner[2], Courtney Couch[3,4], Steven Colbert[2], Stuart Goldberg[4], Jamison Gove[4], Jazmine Panelo[2], Leilani Abaya[2], Cherie Kauahi[2], Chad Wiggins[1], Rebecca Most[1], Eric Conklin[1]

1. The Nature Conservancy, Hawai‘i
923 Nu‘uanu Avenue
Honolulu, HI 96817

2. University of Hawai‘i at Hilo,
Marine Science Department
200 W. Kawili St.
Hilo, HI, USA 96720

3. Hawai‘i Institute of Marine Biology, University of Hawai‘i at Mānoa,
46-007 Lilipuna Road
Kāne‘ohe, HI 96744

4. NOAA/Pacific Islands Fisheries Science Center
Ecosystem Sciences Division
NOAA Inouye Regional Center
1845 Wasp Blvd, Bldg. # 176
Honolulu, HI 96818

July 27, 2019

Suggested Citation:
Falinski, K., Wiegner, T., Couch, C., Colbert, S., Goldberg, S., Gove, J., Panelo, J., Abaya, L., Kauahi, C., Wiggins, C., Most, R., and Conklin, E. 2019. Integrated water quality and coastal groundwater monitoring to assess nutrient impacts to coral reef health. Technical report prepared for NOAA (NA14NMF4630259). 90 pp.

Cover Image: University of Hawai‘i at Hilo students collecting algae samples at Kūki‘o.

Table of Contents

1.0 Executive Summary

Hawai‘i’s coral reefs are declining due to multiple stressors (Friedlander et al. 2008, Gombos et al. 2010, Rodgers et al. 2015), with coral cover in the Puakō and Mauna Lani reef system declining by at least 50 % over the last 40 years (Minton et al. 2012, Maynard et al. 2016). Many factors have contributed to these declines, with increasing concern for and attention to the potential role of land-based pollution (Couch et al. 2014a, Yoshioko et al. 2016, Abaya et al. 2018a,b). Land-based pollution can generally reach coastal waters via streams, overland flow, and groundwater, but in West Hawai‘i submarine groundwater discharge (SGD) at the coastal interface is the only major source of freshwater to the coastal marine ecosystem and serves as the main conduit delivering anthropogenic nutrients and pollutants to coral reefs. Understanding the sources and fluxes of nutrients and other pollutants from anthropogenic sources to reefs is key to informing appropriate management actions to protect these resources (i.e., the first step in developing an effective management strategy is correctly identifying the source of the problem).

While considerable attention has been focused on the role of sewage inputs in one West Hawai‘i community, the goal of this study was to determine if other sources of nutrient inputs were causing degraded coral reef health in other areas of West Hawai‘i, and, if so, from what sources and at what spatial scale. Our approach was to investigate the relationship between nutrients, groundwater and coral health in two coastal resort communities, Kūki‘o in North Kona and Pau‘oa Bay in South Kohala, by examining nutrient sources to coral reefs and their potential impacts on coral reef health. This was a collaborative effort among University of Hawai‘i at Hilo, The Nature Conservancy, Hawai‘i Institute of Marine Biology at University of Hawai‘i at Mānoa, and National Oceanic and Atmospheric Administration staff and researchers applying a multidisciplinary approach that examined the physical oceanography, chemistry and biology of two small-scale, nearshore systems in West Hawai‘i.

There was considerable variation between the two sites, but there were clear signals at both sites that elevated nutrient inputs were entering coastal waters and were associated with declines in coral recruitment and/or condition. SGD supplied nutrients to the bays studied, and low salinity events resulted in the reefs being exposed to elevated nutrient concentrations, which could result in excess algal and bacterial growth. Shoreline and benthic stable isotope values suggested fertilizer inputs were enhancing nutrients for at least one site, and nutrient enriched groundwater was among the strongest predictors of less healthy coral, more disease, higher coral-algal competition and less recovery potential (fewer coral juveniles). These results indicate SGD along the West Hawai‘i coastline connects land use to coral reefs, and that land use practices that effect nutrient groundwater nutrient loading can influence the condition of nearshore coral reefs.

2.0 Introduction & Objectives

Hawai‘i’s coral reefs are declining due to multiple stressors (Friedlander et al. 2008, Gombos et al. 2010, Rodgers et al. 2015), with coral cover in the Puakō and Mauna Lani reef system declining by at least 50 % over the last 40 years (Minton et al. 2012, Maynard et al. 2016). Many factors have contributed to these declines, with increasing concern for and attention to the potential role of land-based pollution (Couch et al. 2014a, Yoshioko et al. 2016, Abaya et al. 2018a,b). This pollution type includes elevated dissolved nutrient concentrations in coastal waters from fertilizers, sewage, animal manure, storm water, soil erosion, fossil fuel combustion, and invasive species (Dudley et al. 2014, USEPA 2017).

Land-based pollution can generally reach coastal waters via streams, overland flow, and groundwater, but in West Hawai‘i submarine groundwater discharge (SGD) at the coastal interface is the only major source of freshwater to the coastal marine ecosystem and serves as the main conduit delivering anthropogenic nutrients and pollutants to coral reefs. While SGD is naturally enriched with nutrients, along its transit from mountain to sea submarine groundwater can acquire additional nutrients and pollutants from anthropogenic sources such as cesspools and fertilizers. Because the residence time of submarine groundwater can be long, often decades, and because groundwater flows bypass treatment in estuarine areas, its sources have the potential to discharge freshwater with elevated concentrations of dissolved macronutrients (e.g., nitrate and phosphate) and pollutants (e.g., pathogenic bacteria, endocrine disruptors, petroleum products, trace metals, etc.) directly to the marine surface waters and benthic areas (Johnson 2008, Peterson, Burnett, Glenn, & Johnson 2009) where they may negatively affect the health of nearshore ecosystems.

Understanding the sources and fluxes of nutrients and other pollutants from anthropogenic sources to reefs is key to informing appropriate management actions to protect these resources (i.e., the first step in developing an effective management strategy is correctly identifying the source of the problem). As such, it is important to characterize upland groundwater concentrations as well as downstream values in order to differentiate natural nutrient enrichment from the impacts of anthropogenic nutrients and other pollutants. Understanding the flow paths of submarine groundwater flow is difficult in West Hawai‘i, however, because the local geology with many overlaid volcanic flows and porous volcanic sediments create challenges for accurately predicting how submarine groundwater flows through the system.

A large scale study completed in 2013 investigated nutrient-driven invasive algae blooms along the West Hawai‘i coast and found evidence in some areas that wastewater contributions near wastewater facilities and resorts contributed to algal growth (Dailer, Glenn, & Smith, 2011).

While the correlation between nutrients and invasive algae has been established, less work has been done to link nutrients by way of groundwater to coral health. In South Kohala coastal waters, primarily Puakō, previous and ongoing NOAA-supported research and monitoring activities have demonstrated the presence of sewage and elevated nutrients and pathogens delivered via submarine groundwater discharge along reefs, and that coral disease increases with elevated nutrient input (Couch et al. 2014a,b, Yoshioka et al. 2016, Abaya et al. 2018a,b).

The goal of this study was to expand the geographic extent of this work beyond Puakō to determine if nutrient inputs were causing degraded coral reef health in other areas of West Hawai‘i, and, if so, from what sources and at what spatial scale. Our approach was to investigate the relationship between nutrients, groundwater and coral health in two coastal resort communities in North Kona and South Kohala (Fig. 1) by examining nutrient sources to coral reefs and their potential impacts on coral reef health. This was a collaborative effort among University of Hawai‘i at Hilo (UHH), The Nature Conservancy (TNC), Hawai‘i Institute of Marine Biology at University of Hawai‘i at Mānoa, and National Oceanic and Atmospheric Administration (NOAA) staff and researchers applying a multidisciplinary approach that examined the physical oceanography, chemistry and biology of two small-scale, nearshore systems in West Hawai‘i.

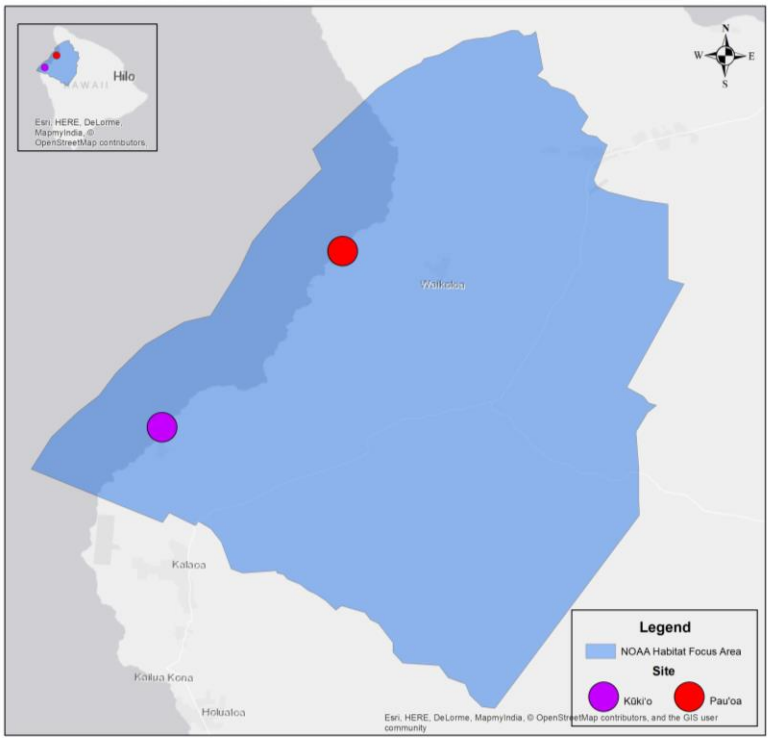

Figure 1. Study site locations on Hawai‘i Island at Fairmont Orchid (Pau‘oa Bay, red circle) and Kūki‘o (Uluweuweu Bay, purple circle) resorts in South Kohala and North Kona, respectively. These resort areas are in the NOAA Habitat Blueprint West Hawai‘i Focus Area.

Study Objectives

1: Determine nitrate sources and their percent contribution to nitrate in reef waters

2: Predict residence time and benthic area coverage of nutrients at reef sites

3: Estimate submarine groundwater discharge flux and nutrient loads

4: Assess link between coral health and nutrient inputs

5: Share information to natural resource managers and communities

3.0 Methods

3.1 Site Selection & Description

3.1.1 West Hawai‘i Watershed Hydrology and Geology

The island of Hawai‘i is the youngest and largest of the Hawaiian islands. Much of the western, leeward part of the island north of Kailua-Kona, known as West Hawai‘i, is formed by volcanic rocks from Mauna Kea, Mauna Loa and Hualalai volcanoes (Stearns & Macdonald 1946). The coastline of West Hawai‘i is very arid, receiving a mean annual rainfall of only 35 to 70 cm (Giambelluca et al. 2013). All streams along this coast are ephemeral, thus the majority of meteoric water reaching the shoreline is groundwater. Groundwater recharge likely happens within 10km of the coastline and on mountain slopes that receive an annual average of 102 cm to 160 cm of rainfall between 1,000 and 3,000 feet elevation (Peterson et al. 2009). Recharge in the higher, wet elevational areas occurs from rainfall, fog drip, and irrigation (Oki 1999, Bauer 2003). Groundwater flows through an unconfined aquifer comprised of young, porous basalt (0 – 10 kyr) (Kay et al. 1977, Oki et al. 1999). It is estimated that groundwater travels through rock at a rate of about one kilometer per year (Peterson et al. 2009).

The groundwater system for the region consists of a buoyant, freshwater lens on top of denser, oceanic seawater with a brackish transition zone between (Oki 1999). The brackish coastal aquifer extends inland for varying distances depending on development and in response to tides, seasonal changes in groundwater recharge, and bedrock structure and topography (Oki et al. 1999, Lau and Mink 2006). The system, however, is complicated by mixing processes that are spatially and temporally variable due to variations in precipitation and hydraulic conductivity. Oceanic tidal forcing drives the recirculated seawater component of SGD, and at low tides discharge rates at coastal seeps are more prevalent than at high tides. Heterogeneity of lava flow structure and porosity influence the distribution and magnitude of SGD along the Kona coast (Street et al. 2008).

3.1.2 Site Selection

In October 2016, the project team assessed the potential of several master-planned resort developments within the NOAA-designated West Hawai‘i Habitat Blueprint and Focus Area along the Kona-Kohala coast of Hawai‘i Island. Four criteria were used to select the two developments studied in this project: the extent and health of appropriate habitat, proximity to existing marine monitoring sites, accessibility for research activities, and the interest and support of the community and management to consider management actions in response to any issues identified through this research.

We chose sites with embayments due to the water quality and benthic habitat that they support. Embayments appear to be sites where SGD is prevalent, as is the presence and cover of habitat-forming coral reef. Proximity to existing marine monitoring sites was evaluated based on prior and current coral disease and water quality research conducted by collaborators on this project to maximize the potential for results to be informed by prior research. We chose to eliminate sites without paved paths to a safe ingress/egress shoreline for transport of sampling equipment, such as the Hilton Waikoloa. Finally, we considered the potential that further data may help coastal managers at the sites. The management staff of the Fairmont Orchid at Pau‘oa Bay and the Kūki‘o resort development at Uluweuweu Bay (Fig. 1) were interested in understanding more about their coastal resources and the potential for partnership, and as these sites also met all of the criteria discussed above, they became ideal sites for this study.

3.1.3 Pau‘oa Bay

Pau‘oa Bay (Fig. 2) is in the South Kohala district of West Hawai‘i and was formed from the 1859 lava flow of Mauna Loa Volcano. It receives 225 mm of rain annually (Giambelluca et al. 2013). Point source is used to described SGD input to the bay, which has a plume area of 44,000 m2, and a daily flux of 4489 m3 (Johnson 2008). There are also many anchialine ponds along Pau‘oa Bay’s coastline (Maciolek and Brock 1974). This shoreline is considered a high erosion area (Fletcher et al 2002). The dominant benthic substrate in Pau‘oa Bay is boulder (Pacific Island Benthic Habitat Mapping Center 2018). Local residents and visitors primarily use this bay for snorkeling, with the Fairmont Orchid Resort located along the northern edge of the bay. Wastewater effluent for the development is R2 treated and disposed of through an injection well.

Figure 1. Photo of Pauʻoa sites, looking to the north.

3.1.4 Kūkiʻo

The Kūkiʻo ahupuaʻa (a traditional land division) is located in the North Kona district of West Hawaiʻi and contains Uluweuweu Bay (Figure 3). Uluweuweu Bay was formed as a result of the 1801 lava flow originating from Hualālai Volcano (Clark 2002, Rubin and Doo 2004). Within a 5-km radius of the beach, land cover is primarily barren (70%), with forest/natural areas (29%), kiawe trees (Prosopis pallida, 8%), and development (2%) comprising the remainder (Knee et al. 2010). The population density is < 1/km2 (Knee et al. 2010). Uluweuweu Bay receives 275 mm of rain annually (Giambelluca et al. 2013). Like Pauʻoa Bay, point source is used to describe SGD input into Uluweuweu Bay, which has a plume area of 90,000 m2, and daily flux rate of 9089 m3 (Johnson 2008). There are also many anchialine ponds along the Kūkiʻo coastline (Phillips, Brandt, Reddick, and Assoc., Inc. 1986) and the area aquifer is diverse and highly permeable due to alternating layers of ʻaʻa and pāhoehoe lava (Duarte 2002). This shoreline is classified as a high erosion area (Fletcher et al. 2002). The dominant benthic substrate for Uluweuweu is complex reef (Pacific Island Benthic Habitat Mapping Center 2018). The residential resort development runs along the entire shoreline of the bay and is comprised of 193 private residences with 45 ha of lawn, two large luxury developments, and one golf course (190 ha) (Delevaux et al. 2018). The development disposes of their R2 treated wastewater effluent through an injection well. The bay is located within the Kaʻūpūlehu Marine Reserve, where all harvest of marine organisms is prohibited from the shoreline to a depth of 120ft from 20016 to 2026. For the remainder of this report, the study site in

Figure 3. Photos of Kūkiʻo sites including a) anchialine ponds and beach locations looking (b) south and (c) north.

Uluweuweu Bay will be referred to as Kūkiʻo, the name of the ahupuaʻa and resort development.

3.1.5 Survey Station Selection

In January 2017 we generated a high-resolution map of surface salinity to provide data on the spatial variability of SGD plumes and improve site selection (Fig. 4). Pauʻoa Bay and Kūkiʻo were surveyed on January 12, 2018 and January 13, 2018, respectively. For salinity assessments, a Yellow Springs Incorporated (YSI) sonde (YSI 6920 V2) was attached horizontally to the bottom of a kayak and towed across the study region in a grid pattern from shore to reef. In shoreline areas inaccessible by kayak, snorkelers towed the YSI by hand. Continuous salinity data were collected at 5 second intervals and GPS

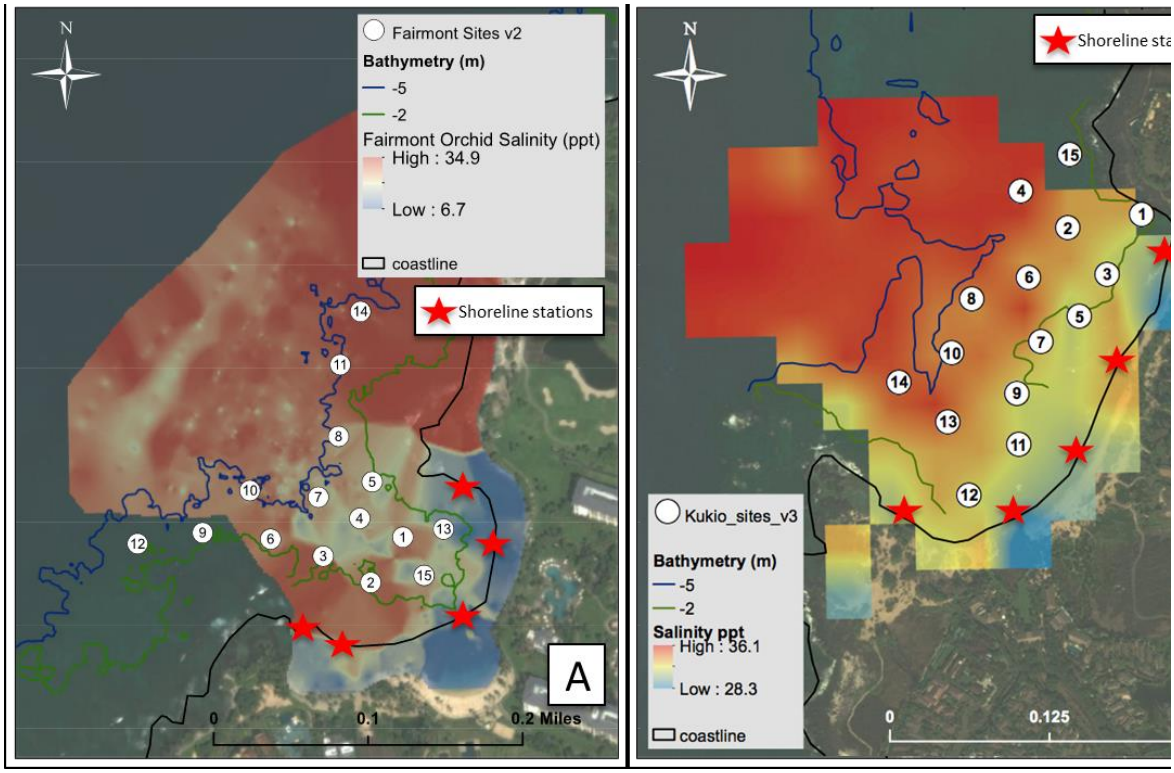

Figure 4. Offshore surface/benthic (numbered) and shoreline (red stars) collection stations for conductivity/temperature sensor deployments, as well as water and macroalgal collection, at Pau‘oa Bay (A) and Kūki‘o (B).

location measurements were simultaneously collected using a handheld Garmin GPS. The composite surface salinity contour map was created by interpolating 5753 survey points using the Kriging method in ArcMap (ESRI). Using these maps and data from coral reef surveys to assess coral cover, we identified 15 benthic stations across a range of salinity values and along an offshore gradient in each bay (Fig. 4); depths ranged between 3 and 4m at each site. Additionally, five shoreline, two anchialine pond, and two to three upper and lower elevational drinking and irrigation wells were selected at each resort to capture and characterize groundwater inputs to the coastal waters (Fig. 4-6).

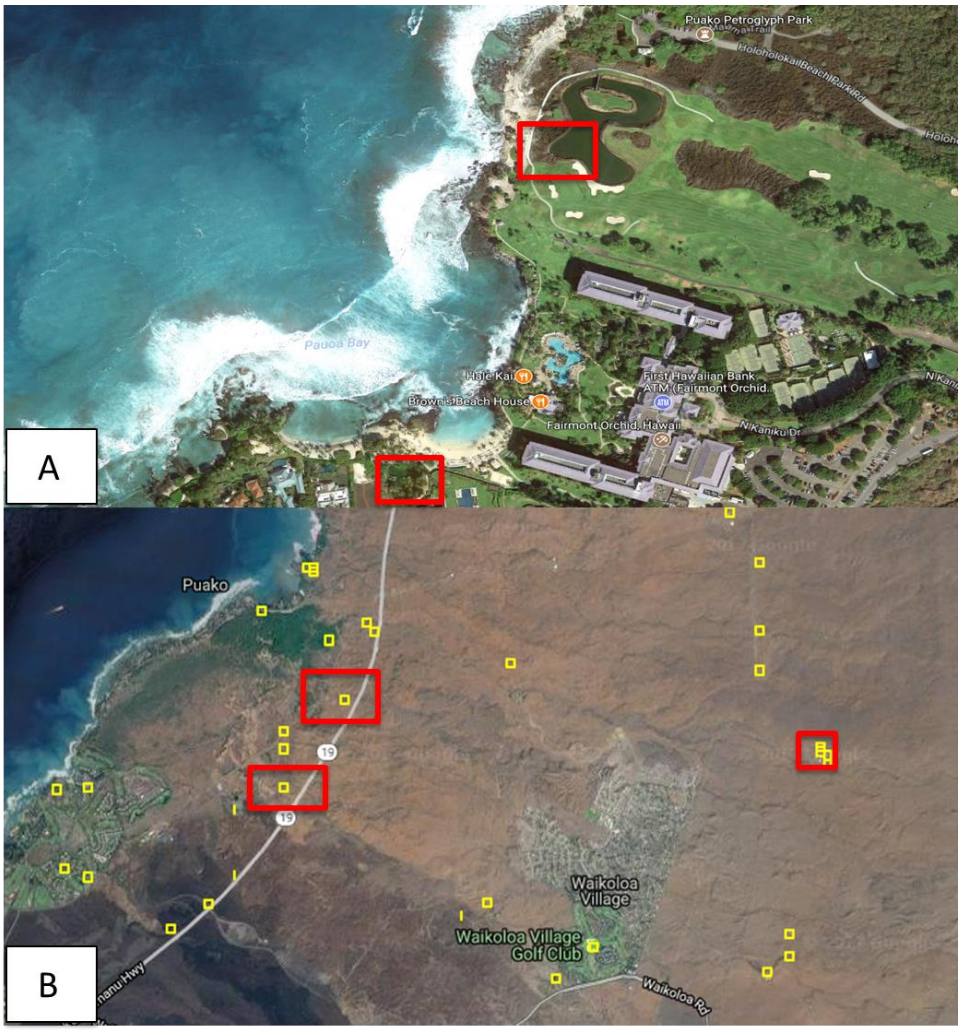

Figure 5. Groundwater collection areas (red squares) in the Pau‘oa Bay watershed: A) anchialine ponds and B) mid and high elevation wells.

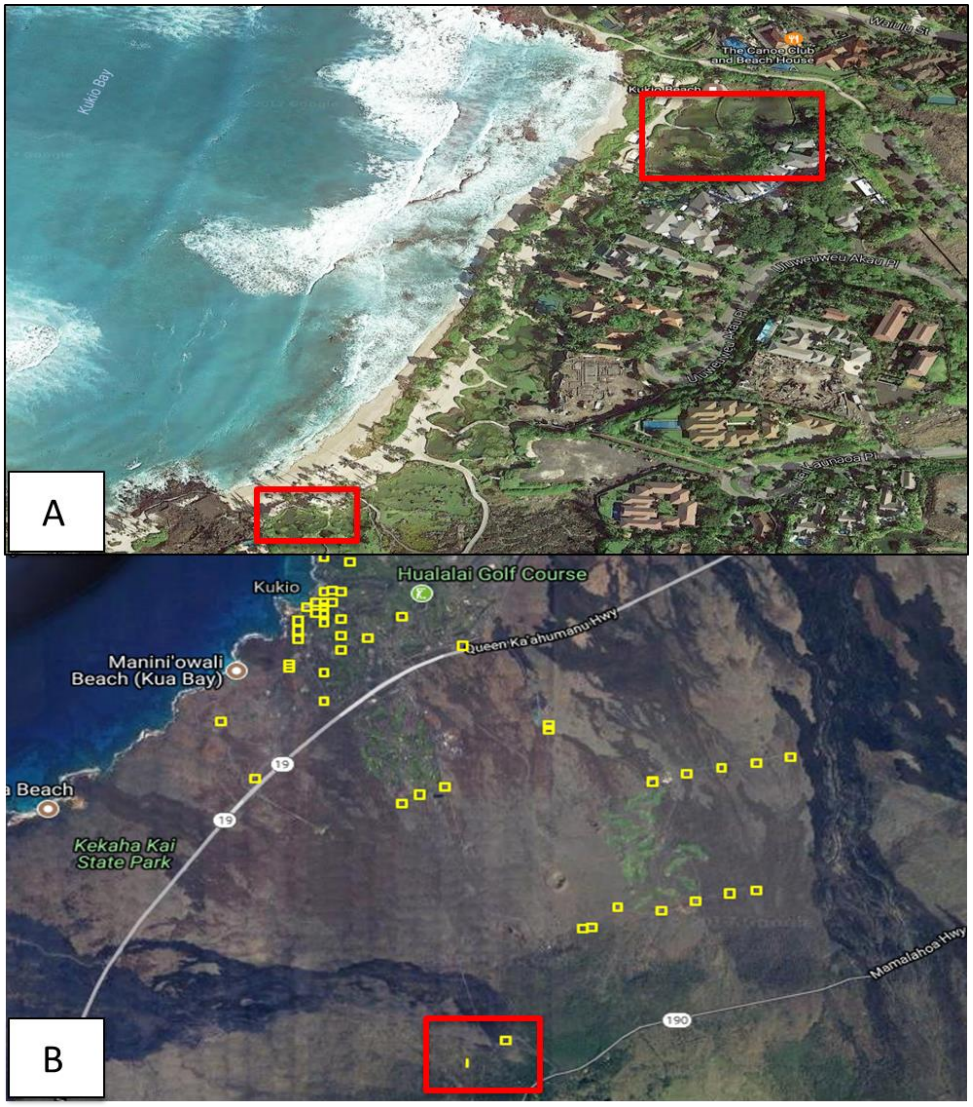

Figure 6. Groundwater collection areas (red squares) in the Kūkiʻo watershed: A) anchialine ponds and B) high elevation wells.

3.2 Approach & Sampling Design

In order to address the study objectives, five types of sampling and monitoring were conducted. Physical surveys including 1) coastal and well nutrient sampling, 2) nitrogen isotope sampling, 3) in situ salinity and temperature, 4) coral health and benthic assessment, and 5) current monitoring. In addition, we used a nutrient model called InVEST Nutrient Delivery Ratio model to estimate nitrogen source areas. Sampling and monitoring occurred over the project period from June 2017 to January 2018.

Table 1: Parameters assessed, types of analyses, and the frequency and timing of sampling summarized in this report.

Parameter	Analysis	Frequency	Dates	Instrument/Lab/Modeling
Physical surveys				
Surface salinity and temperature	Kayak surveys with a YSI probe	Once per site	January 2018	YSI
Benthic salinity and temperature	Anchored sensors	Every 15 min	June-August 2017	Odyssey
Current profiles	In situ monitoring of current direction	Every 5 minutes	August 2017	Acoustic Doppler Profiler (Nortek)
Chemical surveys				
Nutrients	Total Nitrogen, nitrate+nitrite, Total Phosphorus, Phosphate, Silicate	Monthly	Kūkiʻo: 7/25/2017, 8/18/2017; Pauʻoa: 5/23/2017, 6/22/2017, 7/28/2017, 8/3/2017	University of Hawaiʻi at Hilo Analytical Lab
Nitrogen isotopes	macroalgae samples for $\delta^{15}NO_3^-$	Monthly	Kūkiʻo: 7/25/2017, 8/18/2017; Pauʻoa: 5/23/2017, 6/22/2017, 7/28/2017, 8/3/2017	

Parameter (cont)	Analysis	Frequency	Dates	Instrument/Lab/Modeling
Oxygen and Nitrogen isotopes of Nitrate	$\delta^{15}N$ $\delta^{18}O_2$		Kūkiʻo: 7/25/2017, 8/18/2017; Pauʻoa: 5/23/2017, 6/22/2017, 7/28/2017, 8/3/2017	
Biological surveys				
Benthic surveys	Discrete sampling at the shoreline	Once	7/28/17-8/1/17	
Modeling analysis				
Nutrient export	InVEST NDR	-	-	

3.2.1 Water Quality Sampling

3.2.1.1 Well Sampling

Contacts for well operators within the Pauʻoa Bay watershed were established for groundwater water collection and wells were selected in April 2017 (Fig. 5). Potential wells within the Kūkiʻo watershed were identified for groundwater collection in May 2017 (Fig. 6), but obtaining contact information for well operators and permission to sample was challenging and limited our ability to collect samples. Permission to sample groundwater wells in Kūkiʻo was granted in July and September 2017.

Water quality samples from groundwater wells were collected within the Pauʻoa Bay watershed at three developments. The two mid-elevation wells were collected within the Mauna Lani development on May 23 and June 22, 2017. Access to these wells was granted by Mauna Lani. High-elevation well water was collected above Waikoloa Village, and access to this development was granted by the Hawaiʻi Water Supply Company on July 6 and July 13, 2017. Within the Kūkiʻo watershed, water quality samples from groundwater wells were collected from two wells on July 25 and August 18, 2017. Access was granted by the Hawaiʻi Water Supply Company.

All water quality (nutrients) were analyzed at the UHH Analytical Laboratory using methods described below.

3.2.1.2 Coastal Water Sampling

From May through August 2017 at morning low tide, water samples were collected in 1-L sterilized Polypropylene bottles twice at each site at all twenty-five stations; five shoreline, fifteen offshore stations, 2 anchialine ponds, and 2 to 3 upper and lower drinking and irrigation wells. Low tide was targeted as this is the time of day when groundwater has the greatest influence on nearshore water quality. At offshore stations, both surface and benthic water were collected. Benthic samples were collected just above the substrate (< 5 cm). Salinity and temperature were measured at the time of collection using a YSI 2030 multi-parameter probe at the shoreline. Additionally, conductivity/temperature sensors were deployed at each benthic station (*see In Situ Salinity and Temperature* section below).

3.2.1.3 Nutrient Analyses

Water samples were filtered through pre-combusted (500°C for 6 hours), 0.7 GF/F filters (Whatman™), and stored frozen until analysis at the UHH Analytical Laboratory. Nutrients were analyzed on a Pulse TechniconTM II autoanalyzer using standard methods as described in Table 2. Nutrients were analyzed on a Pulse TechniconTM II autoanalyzer using standard methods (NO_3- + NO_2- [Detection Limit (DL) 0.07 µmol/L, USEPA 353.4], NH_4+ (DL 0.36 µmol/L, USGS I-2525], PO_4^3- [DL 0.03 µmol/L, Technicon Industrial Method 155-71 W], total dissolved phosphorous (TDP) [DL 0.5

µmol/L, USGS I-4650-03], and H_4SiO_4 [DL 1 µmol/L, USEPA 366]) and reference materials (NIST; HACH 307-49, 153-49, 14242-32, 194-49). Total dissolved nitrogen (TDN) was analyzed by high-temperature combustion, followed by chemiluminescent detection of nitric oxide (DL 5 µmol/L, ASTM D5176, Shimadzu TOC-V, TNM-1) (Sharp et al. 2002).

Table 2: Methods used for nutrient analysis

Parameter	Detection Limit	Method
Nitrate, NO_3^- + NO_2^{--}	0.07 µmol L^{-1}	US EPA 353.4
Ammonium, NH_4+	0.36 µmol L^{-1}	USGS I-2525
Phosphate, PO_4^{3-}	0.03 µmol L^{-1}	
Total dissolved phosphorous (TDP)	0.50 µmol L^{-1}	USGS I-4650-03
Silicate, H_4SiO_4	1.00 µmol L^{-1}	USEPA 366

3.2.1.4 $\delta^{15}N$ Analyses

Macroalgal samples were collected at benthic and shoreline stations at each development, concurrently with water sample collection. Benthic samples were collected once at each development, while shoreline samples were collected twice. The samples were transported on ice to the laboratory where they were rinsed with deionized water and dried at 60ºC until dry weight was constant. Samples were processed using a Wig-L-Bug grinding mill until the sample was homogeneous. About 2 mg of the macroalgal tissue were folded in 4x6 mm tin capsules for $\delta^{15}N$ isotope analysis. Samples were analyzed on a Thermo-FinniganTM Delta V Advantage isotope ratio mass spectrometer (IRMS) with a Conflo III interface and a CostechTM ECS 4010 Elemental Analyzer located at the UHH Analytical Laboratory. Data were normalized to United States Geological Survey (USGS) standard NIST 1547. Isotopic signatures were expressed as standard (δ) values, in units of parts per mil (‰), and calculated as:

$$[(R_{sample} - R_{standard}) / R_{standard}] \times 1000, \text{ where } R = {}^{15}N/{}^{14}N.$$

Additionally, water samples were filtered through a 0.22-µm cellulose acetate filter (Whatman™) and frozen until analysis. Samples were analyzed on a Thermo-Finnigan™ Delta Plus IRMS with data normalized to USGS standards (USGS32, USGS34, USGS53) at Northern Arizona University Stable Isotope Laboratory. IAEA-NO3 was used as a reference standard.

3.2.1.5 Data Analyses

Gaussian general linear models were used to assess differences among water types within each development for all water quality parameters. Data sets for each parameter were tested for normality and equality of variance. Transformations were performed on data sets with non-normal distributions. Post hoc analyses were conducted using the Tukey's test. Regression analysis was used to examine the relationship between NO_3^-+NO_2^- concentrations. All statistical tests were conducted in R (v. 1.1) or MiniTab17, with $\alpha = 0.05$.

Nutrient concentration data on mixing plots were compared to a theoretical mixing line connecting the freshwater and ocean end members (Officer 1979). When nutrient concentration data overlaid the mixing line, the nutrient was characterized as having conservative behavior, where only dilution with seawater is affecting the nutrient concentration in the nearshore waters. When data fell above or below the mixing line, the nutrient was described as behaving non-conservatively, with some source adding the nutrient to the water or some process removing it during mixing.

To estimate relative contribution of different NO_3^- sources to the NO_3^- pool within different water types (anchialine ponds, shoreline, offshore surface and benthic waters) at the two developments, we used measurements of $\delta^{15}N^-$ and $\delta^{18}O^-$ NO_3^- for these water types and potential NO_3^- sources (sewage, groundwater, soil, and ocean water) in the statistical program SIAR (Stable Isotope Analyses in R, v. 4.0). The SIAR mixing model uses a Bayesian framework which takes into account natural variability and uncertainty within a system by allowing multiple sources of uncertainty to be incorporated (Parnell et al. 2010). The Shapiro-Wilk test for normality was used to verify that isotope data for the four NO_3^- sources were normally distributed. $\delta^{15}N^-$ and $\delta^{18}O^-$ NO_3^- data were normally distributed for all sources. Multiple mixing models were examined for each development: 1) among water types (anchialine ponds, shoreline, surface, and benthic waters), 2) within anchialine ponds, 3) within shoreline waters, 4) within surface waters, and 5) within benthic waters. We are also looked at models with and without sewage, and also with and without ocean water as NO_3^- sources, as we were uncertain how much they may actually contribute to the NO_3^-pools in these different water types. Also for ocean water, sometimes it is excluded from coastal water models as its NO_3^-concentrations are often below detection limits for stable isotope analysis (> 2 µmol/L, Coplen et al. 2012).

3.2.2 In Situ Salinity and Temperature Profiles

Odyssey temperature-conductivity sensors (operating range: 3 to 60 mS/cm) collecting data at 5-min intervals were deployed at the 15 sites at each Pauʻoa Bay and Kūkiʻo described above (Fig. 4). Snorkelers temporarily affixed sensors to rocks and/or dead

coral at each site using cable ties; each location was photographed for documentation. To calibrate the loggers *in situ*, vertical profiles from the surface to the seafloor adjacent to the logger were collected at the beginning and end of deployment using a Sontek Castaway. The Pauʻoa deployment was 28 April to 23 June 2017 (56 days), and the Kūkiʻo deployment was 26 June to 19 August 2017 (54 days). The number of loggers deployed at each development varied, with 10 and 8 loggers deployed for the entire period at Pauʻoa and Kūkiʻo, respectively. Six loggers were either lost or malfunctioned and then recovered. Upon recovery, each station had one temperature logger that had malfunctioned, resulting in 14 usable datasets for temperature. For salinity, three and two conductivity sensors failed at Pauʻoa and Kūkiʻo, respectively.

Logger temperature did not experience any drift, with final logger temperatures differing from Castaway temperatures by -0.05± 0.10 °C. Conductivity experienced both biofouling and drift. Biofouling was evident by periodic step decreases followed by similar magnitude increases in salinity, which were likely due to organisms (e.g., young sea urchins) crawling into the sensor and altering the electric field when conductivity was measured. Step decreases lasting less than 18 hours were removed from the data by identifying the range of the step decrease in conductivity and applying a constant offset. Step offsets that lasted the remainder of deployment were adjusted using a constant offset. Spikes in salinity lasting only one time step and > 1 mS/cm were removed from the records. Long-term drift was accounted for by determining the offset at each point based on a polynomial fit and assuming no long-term change in salinity at the station, which was consistent with the calibration data. Specific conductivities were converted to Practical Salinity based on PSS-78 algorithm. From hereon, salinity will be used to describe the conductivity data.

3.2.3 Coral Health & Benthic Assessments

Benthic assessments were conducted at each resort from July 28 - August 1, 2017. Each station was assessed along one 15 m transect line surveyed parallel to shore. All coral colonies within a 1-m wide belt were identified to species and enumerated. The condition of each colony was assessed and any signs of disease (growth anomalies, trematodiasis, and tissue loss syndrome) or compromised health, (algal overgrowth, discoloration, bleaching, physical damage, gastropod predation and crown-of-thorns predation) were recorded (**Error! Reference source not found.**7). To calculate average colony size, the m aximum colony diameter was recorded in colonies within the first and last two meters of the transect (4m2 total). The overall disease and compromised health prevalence was calculated as follows: number of colonies with at least one disease or compromised health lesion/total number of colonies on a transect. The prevalence of each condition was also calculated as the number of colonies with a given condition/total number of

colonies. The prevalence of several

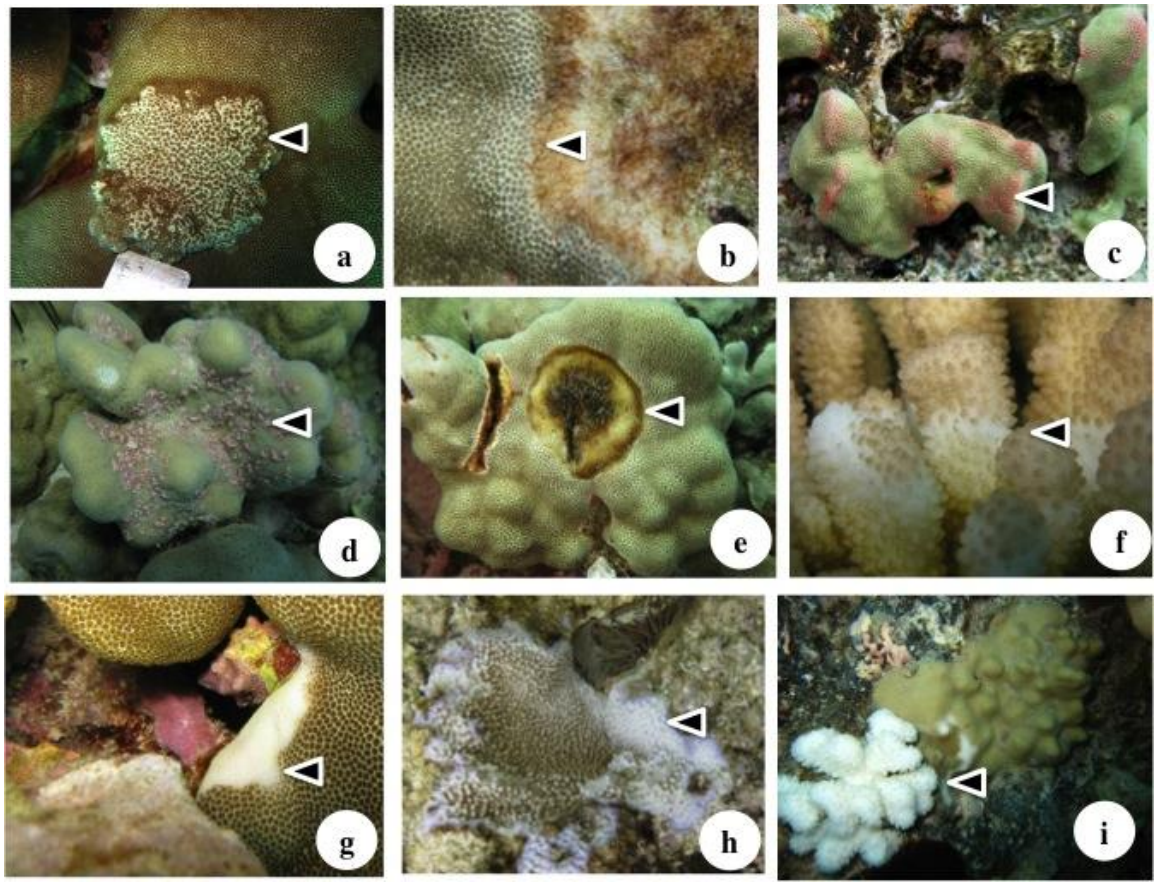

Figure 7. Coral health conditions included in coral health surveys along West Hawai'i (Top left down to bottom right): (a) growth anomalies; (b) algal overgrowth; (c) discoloration; (d) trematodiasis; (e) tissue loss disease on the coral genus Porites; (f) tissue loss disease on the coral genus Pocillopora; (g) gastropod predation; (h) bleaching; and (i) Crown-of-thorns predation.

genus-specific diseases were also calculated (e.g., *Porites* growth anomalies: number of *Porites* colonies growth anomalies/total number of *Porites.*

To quantify percent cover of coral, macroalgae, and crustose coralline algae, benthic photographs were taken every meter along the transect line using a Canon Powershot camera mounted on a 0.8-m PVC monopod. This generated 15 images for each site, with each photo covering approximately 0.5 m^2 of the bottom. Photos were analyzed using CoralNet (Beijbom et al. 2015). Thirty random points were overlaid on each photo and the benthic component under each point was identified to the lowest possible taxonomic level. Corals were primarily identified to species and algae were identified to a higher taxonomic resolution (e.g., red, green, brown, turf, and crustose coralline). All photographs were processed by the same analyst to reduce potential observer variability. Once completed, the raw point data from each photograph was combined to calculate the percent cover of each station's benthic component. The reef builder ratio was calculated

to assess the abundance of reef builders (CCA and coral) relative to fleshy algae (turf and macroalgae) (Smith et al. 2016).

3.2.3.1 Data Analyses

Benthic data were analyzed in R (version 3.2.4). Separate generalized linear models using a binomial distribution were used to determine whether the proportion of healthy colonies, and the two most prevalent conditions (*Porites* growth anomalies and algal overgrowth) were correlated with a combination of demographic (colony density and size) and environmental (temperature, salinity, dissolved inorganic nutrient concentration, and stable nitrogen isotopes in field-collected algae) variables. To identify drivers of coral juvenile density and reef-builder ratio, we used linear models after log or square root transforming the data to meet assumptions of normality and equal variances. All predictor variables were checked for multicollinearity (correlation coefficient > 0.8), scaled and centered. Due to the high correlation between the individual nutrient parameters PO_4 was dropped from the analyses. Model selection comparing Akaike's information criterion (AICc, ΔAICc and AIC weight) were used to determine which factor or combination of factors best fit each condition (Burnham and Anderson 2002). ΔAIC > 4 suggests substantial evidence for the model and Akaike weights (w_i) provide another measure of the strength of evidence for each model (Burnham and Anderson 2002). The "best-fit" models were then averaged together and the standardized parameter estimates for each predictor variable were compared to identify the strength and direction of the relationships.

3.2.4 Nutrient Modeling

The InVEST nutrient delivery model estimates nitrogen retention using the concept of nutrient delivery ratio (NDR). The technique provides quantitative values to a risk-based approach and considers both an estimate of nutrient loading rates and a calculated probability that a nutrient load will reach a stream. Additionally, two transport processes are modeled, nutrient transported by surface flow and by subsurface flow (Sharp et al. 2015). For this work in West Hawai'i, we only considered subsurface flow. The model uses a digital elevation model (DEM) to calculate flow paths from the Hawai'i Statewide Geographic Information System program. The DEM was additionally processed to remove pits (abnormal holes in the DEM created during processing) using TauDEM (TauDEM 5.0, http://hydrology.usu.edu/taudem/taudem5/downloads5.0.html).

A key component of the NDR model is the ability to use any land use map and to estimate nitrogen loading at the coast. We used the Coastal and Climate Adaptation Program's (C-CAP) 2010 high resolution (2.4m) imagery as a base and modified the layer to include other land uses that might be important for nitrogen inputs. Specifically, we delineated kiawe forest, golf courses, and hotel landscaping areas, and added sites

with on-site disposal systems, which had more detailed nitrogen loading information and were able to add resolution. Each resort complex was parameterized separately for golf course and hotel landscaping, although lacking information we used standard golf course export estimates for all hotels. Different golf course practices, including irrigation type, fertilizer application method, type of fertilizer, and fertilizer application frequency, would affect the capacity of the landscaping to retain nitrogen.

This study developed total nitrogen loading rates and retention parameters (efficiency) for each land use type using literature and local sources (Beaulac & Reckhow 1982; Cobo, Dercon, & Cadisch 2010; Johnes 1996; Lin 2004; Line, White, Osmond, Jennings, & Mojonnier 2002; Ling & El-Kadi 1998; Markewitz, Davidson, Moutinho, & Nepstad 2004; Young, Marston, & Davis 1996). The biophysical parameters presented in this study are included in Appendix 21.

In addition to loading rates by land use, additional parameters for the model include the critical length, defined as the distance after which it is assumed that a patch of land use land cover (LULC) retains nutrient at its maximum capacity, and the proportion of subsurface N as a measure of dissolved nutrients over the total amount of nutrients. Following the work of Kwong *et al* (2002), we assumed that most (90%) of the nitrogen was exported in the subsurface rather than through surface runoff. We also explored the work of Street et al. (2008) to assist in calibration.

Lastly, we wanted to be able to address the question: Are the nutrients concentrations in coastal SGD correlated with inputs close to the coast or from the entire watershed? Or, put another way, does the speed of groundwater affect what the concentrations are at the coast? To answer this, we considered three different types of watersheds, watersheds that fed from 2k from the coastline, 10km from the coastline, and the full watershed. We used ArcGIS 10.2 Basins function and eliminated and combined slivers. Using the 3 different sizes of watersheds, we ran the NDR model for the entire West Hawai‘i coast, and compared the results to coral health data and known nutrient concentrations.

3.2.5 Mapping

Maps were created using ArcMap 10.3. Data were imported and spatially referenced to the geographic coordinate system and world grid system of 1984 (WGS1984). A graduated color renderer was then used to group the data into ordered classes, using the natural breaks method. The natural breaks (Jenks) standard classification divides data into natural groups, allowing the greatest differences among data to be detected (de Smith et al. 2015). Each map was created using this method for each parameter. Maps were then saved and exported as a JPEG/TIFF file.

3.2.6 Ocean Currents

Two 1 MHz Nortek Aquadopp acoustic Doppler profilers (ADP; https://www.nortekgroup.com/) were deployed in Kūkiʻo and Pauʻoa in 7.3 and 6 m of water, respectively. Both sensors were configured to collect current information at 0.5 m depth bins for up to 5.5 m from the bottom with a sampling interval of 5 min from 21-July2017 to 21-August-2017.

4.0 Results and Discussion

4.1 WATER QUALITY

4.1.1 Salinity and Nutrient Concentrations

Average water quality results for both sites are presented in Table 3. Notably, average surface and benthic nitrogen concentrations were higher at Pauʻoa than at Kūkiʻo.

Table 3. Average ±SE of salinity, nutrient concentrations (µmol/L), estimated (Est.) % nitrogen (N) and δ15N in macroalgal tissue (‰), and $\delta^{15}N$ (‰) and $\delta^{18}O$ (‰) in NO_3^- in well, pond, shoreline, surface, and benthic water samples in Pauʻoa and Kūkiʻo in June and July 2017. N/A – not applicable. Algal samples were only collected from the shoreline and benthos.

Site	Water Type	Salinity	$NO_2^- + NO_3^-$	NH_4^+	PO_4^{3-}	H_4SiO_4	Est. %N (algae)	$\delta^{15}N$ (algae)	$\delta^{15}N$ (NO_3^-)	$\delta^{18}O$ (NO_3^-)
Pauʻoa	Wells	1.2 ± 0.4	113.73 ± 9.14	1.53 ± 0.74	1.74 ± 0.21	768 ± 20	N/A	N/A	5.22 ± 1.15	0.88 ± 1.17
	Ponds	7.2 ± 1.9	95.52 ± 32.55	9.15 ± 5.35	1.30 ± 0.76	651 ± 24	N/A	N/A	6.43 ± 0.58	0.27 ± 0.57
	Shoreline	11.1 ± 2.6	93.17 ± 20.16	2.35 ± 0.27	1.24 ± 0.16	496 ± 56	1.94 ± 0.22	4.66 ± 0.14	5.30 ± 0.27	0.81 ± 0.54
	Surface	33.2 ± 0.2	10.89 ± 1.52	1.79 ± 0.35	0.18 ± 0.02	69 ± 9	N/A	N/A	6.38 ± 0.27	4.70 ± 0.81
	Benthic	34.3 ± 0.1	2.28 ± 0.24	1.17 ± 0.22	0.10 ± 0.01	12 ± 3	0.96 ± 0.05	3.15 ± 0.15	7.52 ± 0.52	10.91 ± 1.22
Kūkiʻo	Wells	1.1 ± 0.2	73.59 ± 1.47	1.20 ± 0.54	8.22 ± 0.88	740 ± 70	N/A	N/A	6.01 ± 3.98	8.89 ± 7.27
	Ponds	6.8 ± 0.4	50.14 ± 7.19	4.47 ± 2.64	0.78 ± 0.31	564 ± 35	N/A	N/A	6.25 ± 0.48	6.96 ± 2.00
	Shoreline	23.5 ± 1.6	30.66 ± 5.32	1.46 ± 0.47	0.78 ± 0.10	143 ± 20	1.81 ± 0.17	4.67 ± 0.15	5.21 ± 0.33	3.88 ± 0.87
	Surface	34.0 ± 0.1	6.46 ± 1.45	1.00 ± 0.20	0.23 ± 0.02	29 ± 3	N/A	N/A	5.59 ± 0.29	6.28 ± 0.64
	Benthic	34.3 ± 0.1	1.66 ± 0.18	0.62 ± 0.13	0.14 ± 0.02	7 ± 1	1.14 ± 0.07	2.41 ± 0.16	6.29 ± 0.55	10.03 ± 0.97

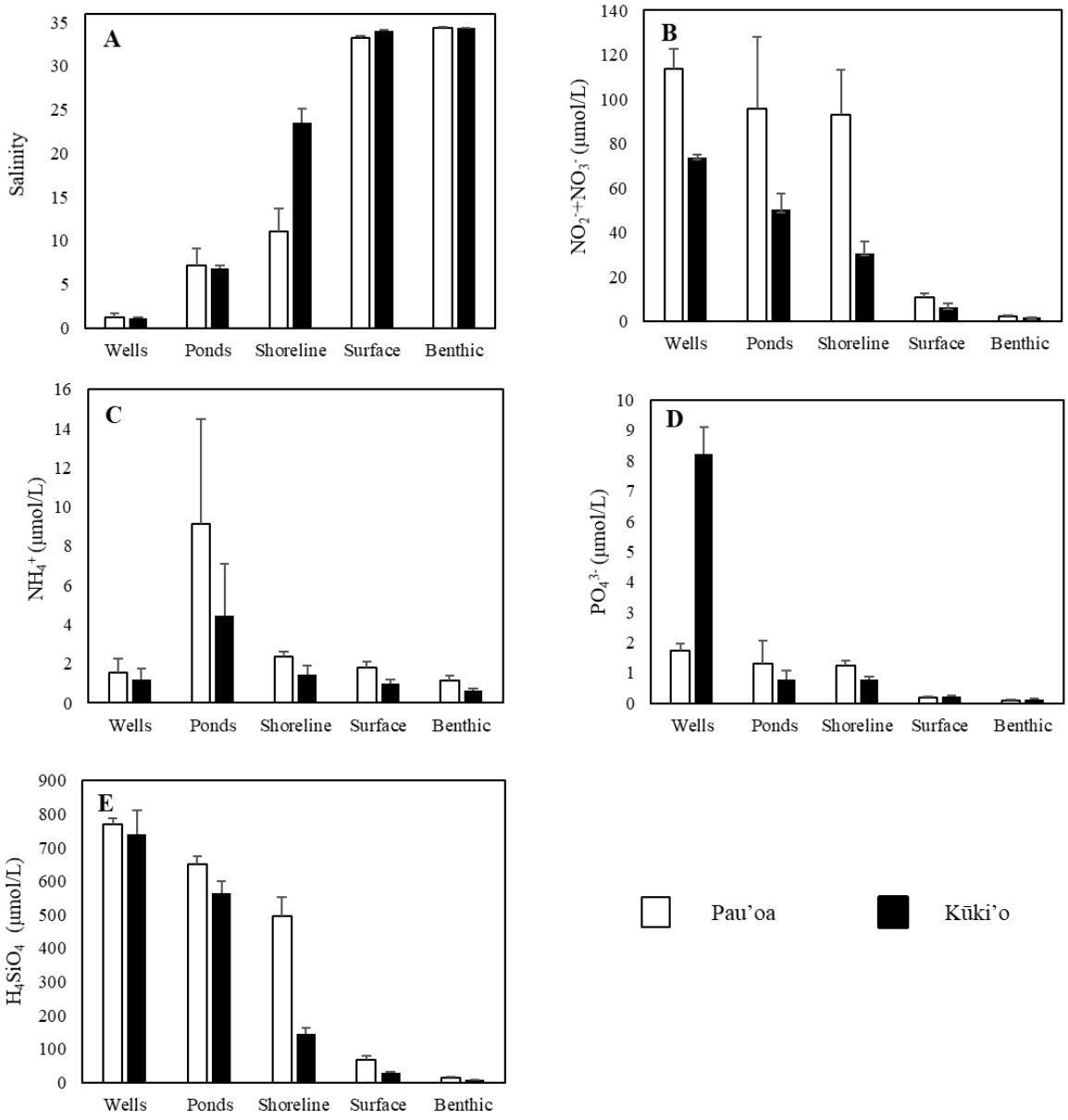

Figure 8. Average ±SE salinity and nutrient concentrations at Pau‘oa and Kūki‘o.

Salinity increased from groundwater wells to offshore stations for each development, ranging from 0.2 to 35.0 at Pau'oa, and 0.7 to 35.0 for Kūki'o (Fig. 8, Table 3). Most water types had significantly different salinities from each other at both developments ($p \leq 0.0185$, Table 4). There were two exceptions: 1) surface and benthic waters had similar salinities at both developments, and 2) anchialine pond and shoreline salinities were

similar at Pau‘oa. Groundwater wells and anchialine ponds had similar salinities between developments (Table 4). In contrast, shoreline and surface waters had lower salinities at Pau‘oa ($p \leq 0.004$), while benthic waters at Kūki‘o had lower salinities ($p = 0.022$).

Table 3. Results (p-values) of Mann Whitney/Wilcoxon Rank Sum tests comparing salinity and nutrient concentrations between water types (groundwater wells, anchialine ponds, shoreline, surface and benthic waters) at Pau‘oa and Kūki‘o in June and July 2017 ($\alpha = 0.05$).

		Salinity	$NO_2^- + NO_3^-$	PO_4^{3-}	NH_4^+	H_4SiO_4
Water Type	Well	1	0.01421	0.01421	0.8307	1
	Pond	1	0.3123	0.8852	0.665	0.1124
	Shoreline	0.002202	0.009108	0.03756	0.02575	0.0003298
	Surface	0.004316	0.02462	0.09871	0.05454	0.006669
	Benthic	0.02165	0.08231	0.02872	0.01466	0.3938

In contrast to salinity, $NO_2^- + NO_3^-$, NH_4^+, PO_4^{3-}, and H_4SiO_4 concentrations decreased from groundwater wells to offshore stations for each development (Fig. 8, Table 3). Pau'oa had consistently greater ranges for $NO_2^- + NO_3^-$, NH_4^+, and H_4SiO_4 across all water types than those at Kūki‘o (Fig. 8, Table 3). For $NO_2^- + NO_3^-$, anchialine ponds and benthic waters had similar concentrations, respectively (Table 4). However, concentrations in groundwater wells, shoreline, and surface waters were significantly higher at Pau‘oa ($p \leq 0.025$). For NH_4^+, anchialine ponds and wells had similar concentrations between the two developments, respectively (Table 4). Shoreline ($p = 0.026$), surface ($p = 0.054$), and benthic ($p = 0.014$) waters' NH_4^+ concentrations were higher at Pau‘oa compared to Kūki‘o (Fig. 8). For PO_4^{3-}, anchialine ponds and surface waters had similar concentrations between developments, respectively (Table 4). Concentrations in groundwater wells at Kūki‘o were significantly higher ($p = 0.014$), while concentrations in shoreline ($p = 0.038$) and benthic waters at Pau‘oa were higher ($p = 0.029$, Fig. 8). H_4SiO_4 concentrations were similar between the two developments for groundwater wells, anchialine ponds, and benthic waters (Table 4). Shoreline ($p = 0.0003$) and benthic ($p = 0.0067$) water concentrations were significantly higher at Pau‘oa compared to Kūki‘o.

At Pau‘oa, $NO_3^- + NO_2^-$ and PO_4^{3-} concentrations were similar among groundwater wells, anchialine ponds, and the shoreline (Table 5). Concentrations in these previous water types were significantly higher ($p \leq 0.0185$) than those in the surface and benthic waters,

whose concentrations were comparable (Table 5). In contrast, NH_4^+ concentrations were similar among all water types except for anchialine ponds, whose concentrations were the highest (Fig. 8, Tables 3 and 5). For H_4SiO_4, all water types had significantly different concentrations, except for the groundwater wells and anchialine ponds (Tables 3 and 5). H_4SiO_4 concentrations decreased from groundwater wells to offshore benthic waters (Fig. 8).

Table 5. Results from one-way ANOVAs and Tukey's post hoc tests (p-values) comparing salinity and nutrient concentrations among water types (groundwater wells, anchialine ponds, shoreline, surface and benthic waters) at Pau'oa in June 2017 (α = 0.05).

		Salinity	$NO_2^- + NO_3^-$	PO_4^{3-}	NH_4^+	H_4SiO_4
Water Type	Well-Pond	0.0185	0.819	0.3732	$< 1 * 10^{-4}$	0.07841
	Well-Shoreline	< 0.001	0.552	0.0785	0.9717	< 0.001
	Well-Surface	< 0.001	$< 1 * 10^{-4}$	< 0.001	0.9994	< 0.001
	Well-Benthic	< 0.001	$< 1 * 10^{-4}$	< 0.001	0.9978	< 0.001
	Pond - Shoreline	0.1746	1.00	0.9987	0.0001	0.00234
	Pond - Surface	< 0.001	$< 1 * 10^{-4}$	< 0.001	$< 1 * 10^{-4}$	< 0.001
	Pond - Benthic	< 0.001	$< 1 * 10^{-4}$	< 0.001	$< 1 * 10^{-4}$	< 0.001
	Shoreline - Surface	< 0.001	$< 1 * 10^{-4}$	< 0.001	0.9746	< 0.001
	Shoreline - Benthic	< 0.001	$< 1 * 10^{-4}$	< 0.001	0.7129	< 0.001
	Surface - Benthic	0.6178	0.7090	0.9304	0.8820	0.0189

At Kūki'o, all water types had significantly different $NO_3^- + NO_2^-$ concentrations, except for surface and benthic waters, whose concentrations were comparable (Tables 3 and 6). Concentrations decreased from groundwater wells to offshore benthic waters (Fig. 8). For PO_4^{3-}, groundwater wells had significantly higher concentrations compared to all other water types (Fig. 8). Anchialine ponds had similar PO_4^{3-} concentrations with shoreline and surface waters (Table 6), and surface and benthic water concentrations were also comparable (Table 6). Benthic waters had significantly lower PO_4^{3-} concentrations than shoreline ($p < 0.001$) and surface waters ($p = 0.021$). Like at Pau'oa, NH_4^+

concentrations were significantly higher in anchialine ponds compared to all other water types (Fig. 8), which had similar concentrations (Table 6). Lastly for H_4SiO_4, all water types had significantly different concentrations, except for surface and benthic waters which were comparable (Table 6). H_4SiO_4 concentrations decreased from groundwater wells to offshore benthic waters (Fig. 8).

Table 6. Results from one-way ANOVAs and Tukey's post hoc tests (p-values) comparing salinity and nutrient concentrations among water types (groundwater wells, anchialine ponds, shoreline, surface and benthic waters) at Kūki'o in July 2017 (α = 0.05).

		Salinity	$NO_2^- + NO_3^-$	PO_4^{3-}	NH_4^+	H_4SiO_4
Water Type	Well-Pond	0.000148	< 0.001	< 0.001	0.01317	< 0.001
	Well-Shoreline	$< 1 * 10^{-4}$	< 0.001	< 0.001	0.99819	< 0.001
	Well-Surface	$< 1 * 10^{-4}$	< 0.001	< 0.001	0.99892	< 0.001
	Well-Benthic	$< 1 * 10^{-4}$	< 0.001	< 0.001	0.94301	< 0.001
	Pond - Shoreline	$< 1 * 10^{-4}$	< 0.001	1.00	0.00456	< 0.001
	Pond - Surface	$< 1 * 10^{-4}$	< 0.001	0.06933	< 0.001	< 0.001
	Pond - Benthic	$< 1 * 10^{-4}$	< 0.001	0.02113	< 0.001	< 0.001
	Shoreline - Surface	$< 1 * 10^{-4}$	< 0.001	0.00142	0.90633	< 0.001
	Shoreline - Benthic	$< 1 * 10^{-4}$	< 0.001	< 0.001	0.50691	< 0.001
	Surface - Benthic	0.9783	0.1530	0.9022	0.8500	0.2030

Mixing plots revealed that $NO_3^- + NO_2^-$, PO_4^{3-}, and H_4SiO_4 in groundwater largely mixed conservatively with seawater at Kūki'o, much more so than at Pau'oa (Fig. 9). Groundwater wells, pond, and shoreline stations for Pau'oa fell above the theoretical mixing line for $NO_3^- + NO_2^-$, NH_4^+, and H_4SiO_4 (Fig. 9). Shoreline, surface, and benthic stations for $NO_3^- + NO_2^-$ at Kūki'o fell above the mixing line (Fig. 9). The mixing line for PO_4^{3-} and H_4SiO_4 at Kūki'o had a greater slope than at Pau'oa (Fig. 9). A majority of stations at both developments fell above the mixing line for NH_4^+ (Fig. 9). PO_4^{3-} displayed non-conservative mixing for both developments, with almost all sampling stations falling below the theoretical mixing line (Fig. 9).

Mixing plot analysis revealed $NO_3^- + NO_2^-$, PO_4^{3-}, and H_4SiO_4 in groundwater mixed conservatively with seawater at Kūki'o, but there were indications of nutrients added into the hydrologic system between the upland wells and the shoreline samples at Pau'oa (Figure 2). Groundwater wells, pond stations, and shoreline stations, for Pau'oa fell above

the theoretical mixing line for NO_3^- + NO_2^-, NH_4^+, and H_4SiO_4. Shoreline, surface, and benthic stations for NO_3^- + NO_2^- at Kūki'o fell above the mixing line (Fig. 9). The mixing line for PO_4^{3-} and H_4SiO_4 at Kūki'o had a greater slope than at Pau'oa (Fig. 9). A majority of stations at both developments fell above the mixing line for NH_4^+ (Fig. 9). PO_4^{3-} displayed non-conservative mixing for both developments, with almost all sampling stations falling below the theoretical mixing line.

4.1.2 Nutrient sources

The $\delta^{15}N$ in macroalgal tissues ranged from 1.60‰ to 5.54‰ across shoreline and benthic stations at Pauʻoa and Kūkiʻo (Fig. 10, Table 3). These $\delta^{15}N$ algal values did not fall within the $\delta^{15}N$ range for sewage (Fig. 10). Shoreline and benthic $\delta^{15}N$ macroalgal tissue values at both developments were within the $\delta^{15}N$ range for high elevation groundwater, fertilized/kiawe soil NO_3^-, and ocean water (Fig. 10).

To further examine sources of NO_3^- to anchialine ponds, shoreline, surface and benthic waters at both developments, bi-plots of $\delta^{15}N$- and $\delta^{18}O$-NO_3^- were created, plotting averages for each station relative to averages for all potential NO_3^- sources (Fig. 11). This step allows for the stable isotope data for samples to be visualized relative to values for the sources. These figures are used to decide on which sources to include in the SIAR mixing models. They also allow us to determine if different sources have overlapping stable isotope values. This is important because if there is overlap, it is harder to distinguish each source's contribution to a sample from one another in the modeling effort. Ocean and sewage sources have overlapping $\delta^{15}N$ and $\delta^{18}O$-NO_3^- values, with the ocean source having a wider $\delta^{15}N$ range (Fig. 11). Likewise, fertilized/kiawe soil NO_3^- stable isotope values overlapped with those for high elevational groundwater, with soils having broader $\delta^{15}N$ and $\delta^{18}O$ ranges (Fig. 11). Models to be examined were determined using information displayed on the bi-plots (Fig. 11).

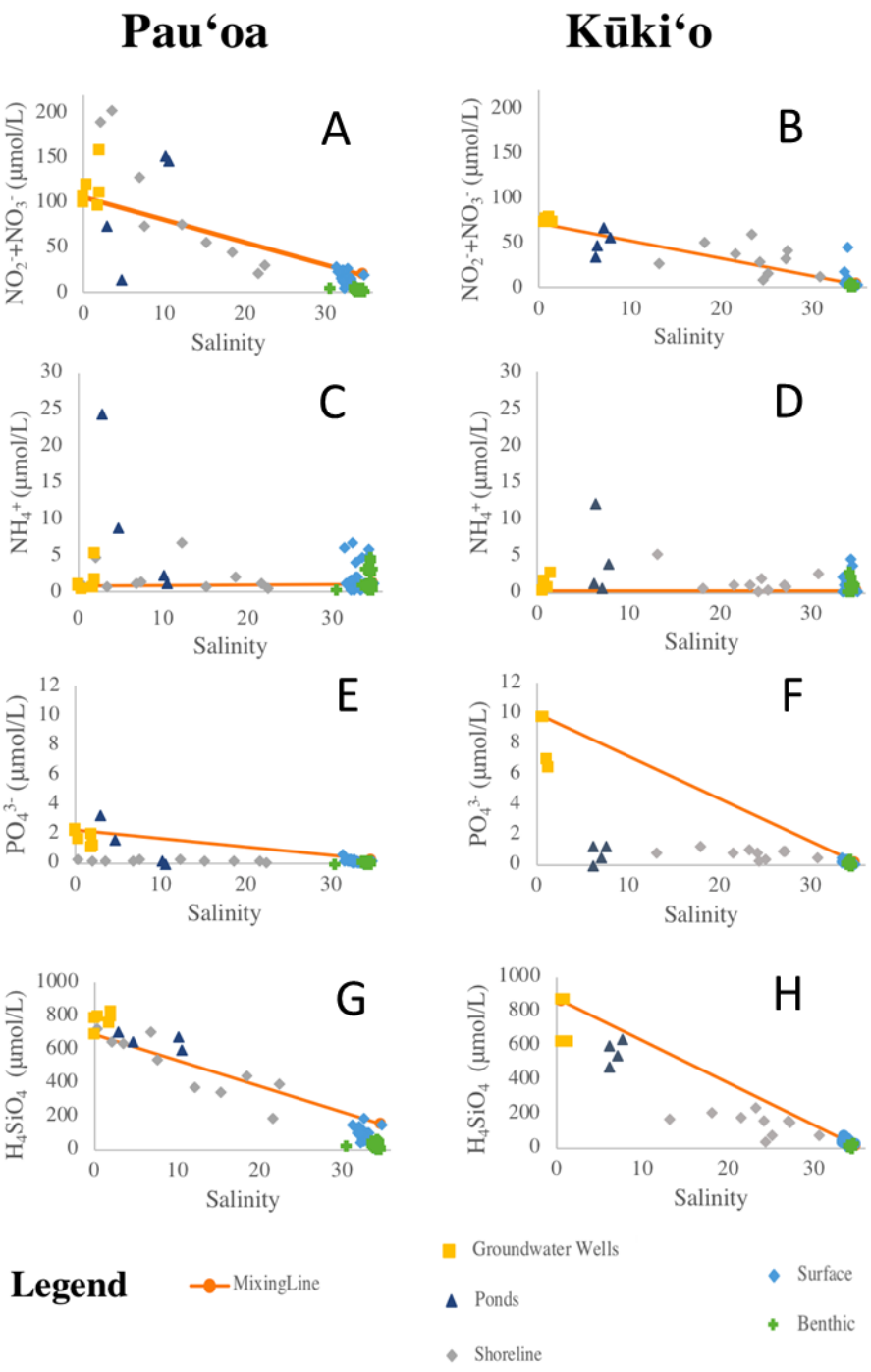

Figure 2. Mixing models for both sites, categorized by type of site. Mixing plots of nutrient concentrations for Pau‘oa and Kūki‘o: (A, B) NO_3^- + NO_2^-, (C, D) NH_4^+, (E, F) PO_4^{3-}, and (G, H) H_4SiO_4. Line represents theoretical mixing line, connecting freshest and saltiest samples at each location

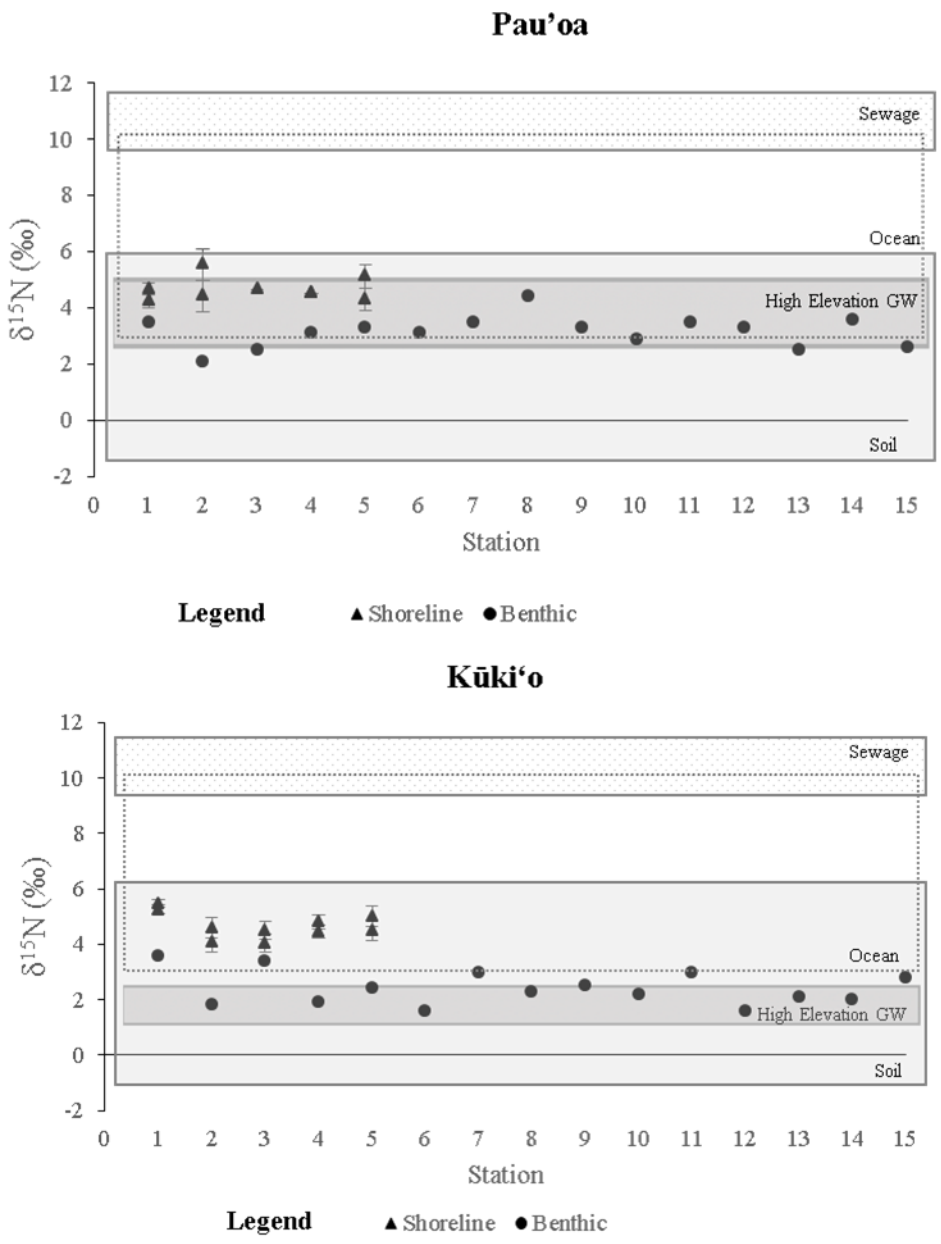

Figure 10. Average ± SE $\delta^{15}N$ (‰) of wild macroalgae collected from shoreline and benthic stations at (A) Pau'oa and (B) Kūki'o. Outlined background areas represent (average ± SE) $\delta^{15}NO_3^-$ of the N sources (soil, ocean, high elevation groundwater wells, and sewage) measured as part of this study. Fertilizer values are from previous sewage study on Hawai'i Island (Wiegner et al. 2016).

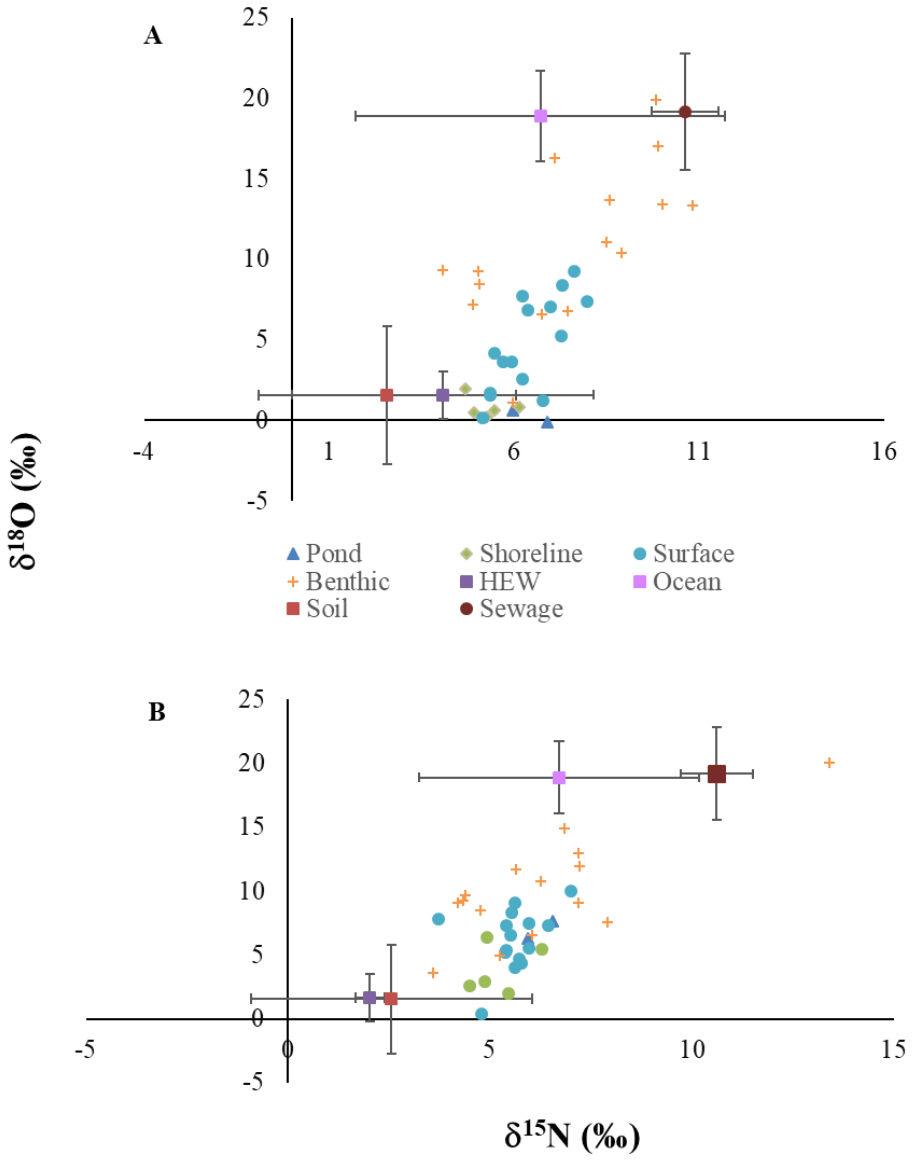

Figure 11. Bi-plot of $d^{15}N$ and $d^{18}O$ of NO_3^- in different water types at (A) Pau‘oa and (B) Kūki‘o, and potential NO_3^- sources. Averages are shown for each station (n = 2, no error bars) and each NO_3^- source (±SE).

4.1.2 Discussion

At both Pau‘oa and Kūki‘o, nutrient concentrations decrease from upland groundwater wells to the ocean, and were higher in surface waters than benthic ones (Fig. 8, Table 3). This pattern suggests that terrestrial groundwater supplies nutrients to the bays at shoreline and benthic SGD seeps. This pattern has been observed at other developments

along the West Hawai‘i shoreline (*e.g.,* Street et al. 2008, Knee et al. 2010, Abaya et al. 2018a, Delevaux et al. 2018).

While concentration patterns from upland wells to nearshore waters were similar between Pau‘oa and Kūki‘o, overall nutrient concentrations and ranges were greater at Pau‘oa (NO_3^-+NO_2^-, NH_4^+, PO_4^{3-}, H_4SiO_4). One notable difference in this pattern was a higher average PO_4^{3-} concentration in Kūki‘o’s wells.

To examine mixing behavior and determine nutrient sources (freshwater vs. ocean) at Pau‘oa and Kūki‘o, we used mixing plots of nutrient concentrations and salinity (Officer 1979). Both conservative and non-conservative mixing of groundwater nutrients with ocean water were observed at both developments (Fig. 9). At Pau‘oa, NO_3^-+NO_2^- displayed non-conservative mixing, with anchialine ponds and shoreline concentrations falling largely below the mixing line. This pattern suggests NO_3^-+NO_2^- maybe taken up by biota, such as bacteria, phytoplankton, and macroalgae, in the nearshore waters. Note, however, there were a few anchialine pond (PAP2) and shoreline (PSH4, PSH5) stations that had concentrations that fell above the mixing line, which is suggestive of an external nutrient source to the groundwater. This source could possibly be fertilizers as these stations were located either within or adjacent to the golf course and development landscaping (Figs. 4 and 5).

A similar pattern was observed for PO_4^{3-}, where a majority of the data points fell below the theoretical mixing line. There was one anchialine pond station (PAP1) which did fall above the mixing line which suggests an external nutrient source. This could also be fertilizers as the pond fronts landscaping adjacent to the beach (Figs. 4 and 5). Previous studies in Hawai‘i have documented higher concentrations in nearshore waters in close proximity to golf courses (Dollar and Atkinson 1992, Derse et al. 2007, Knee et al. 2010).

In contrast, H_4SiO_4 had a conservative mixing pattern, suggesting that groundwater H_4SiO_4 concentrations offshore were decreasing from dilution with ocean water. Data points for NH_4^+ fell above and below the theoretical mixing line suggesting that it was both being taken up by biota and introduced to the water by either internal (organic matter degradation) or external (fertilizers, sewage, etc.) sources.

At Kūki‘o, slopes of the mixing lines for the different nutrients were less steep than those at Pau‘oa, illustrating the smaller nutrient concentration differences between upland wells and nearshore waters. This pattern is consistent with the nutrient concentration patterns observed (Fig. 8). Additionally, nutrient mixing patterns at Kūki‘o were different from those observed at Pau‘oa. Here, NO_3^-+NO_2^- displayed conservative mixing, while PO_4^{3-} and H_4SiO_4 displayed non-conservative mixing, with most data points falling below the theoretical mixing line. For the latter two nutrients, concentrations precipitously dropped below the mixing line between upland groundwater well and anchialine pond samples.

These results suggest that PO_4^{3-} and H_4SiO_4 are being taken up by biota within the anchialine ponds.

To determine N sources to the nearshore waters of Pau‘oa and Kūki‘o, we measured stable N isotopes in macroalgae tissues, as different N sources often have distinct $\delta^{15}N$ values (reviewed in Wiegner et al. 2016). At both Pau‘oa and Kūki‘o, shoreline $\delta^{15}N$ macroalgal tissues were more enriched in $\delta^{15}N$ than benthic algae on the reef. However, both shoreline and benthic macroalgae values fell within the range reported for high elevational groundwater, fertilized/kiawe soil, and ocean water NO_3^- (Fig. 10). However, past studies have found that macroalgae assimilate N more rapidly under low NO_3^- concentrations (Fujita 1985), and that $\delta^{15}N$ in macroalgal tissue can be underestimated by up to 6‰ in waters with high NO_3^- concentrations (> 10 µmol/L) (Swart et al. 2014). All shoreline stations at Pau‘oa ($NO_3^-+NO_2^-$ range: 42 - 137 µmol/L), and 4 of 5 at Kūki‘o (32 – 39 µmol/L) had $NO_3^-+NO_2^-$ concentrations that exceeded this value. If the $\delta^{15}N$ macroalgal values are adjusted for possible increased N isotope discrimination at higher concentrations, then algal shoreline values fall within the range reported for sewage (> +7‰, *reviewed in* Wiegner et al. 2016). It is possible that sewage from the treatment plants is emerging at shoreline seeps as injection wells are used at both developments.

Studies from Maui have shown that treated sewage effluent disposed of using an injection well can reach shorelines and reefs (Hunt 2006, Smith and Smith 2006, Hunt and Rosa 2009, Glenn et al. 2013), and can stimulate ecologically and economically devastating algal blooms (Cesar and van Beukering 2004, van Beukering and Cesar 2004, Smith et al. 2005). A recent study which included Ka‘ūpūlehu (the development in which Kūki‘o is located) found that the primary source of nutrients to nearshore waters was fertilizers from golf courses and landscaping, as well as the sewage injection well, and that reefs were vulnerable to these inputs, resulting in increased benthic algae biomass (Delevaux et al. 2018).

Because $\delta^{15}N$ in macroalgal tissues can have values in between N sources, indicating uptake of N from different sources with differing isotopic compositions (Ochoa-Izaguirre and Soto-Jiménez 2015), we also measured stable N and O isotopes in NO_3^- and used mixing models to partition out N sources (Wiegner et al. 2016). These results are forthcoming.

4.2 In Situ Salinity and Temperature Profiles

4.2.1 Salinity

The daily mean salinity only differed slightly between Pau‘oa (34.1 ± 0.1‰) and Kūki‘o (34.2 ± 0.1‰) ($p < 0.001$). While occasional decreases in salinity were observed at some stations, the mean salinity did not change significantly from the beginning to the end of

the deployment ($p < 0.001$ for both developments) (Fig. 12). Daily mean salinities at individual stations differed ($p < 0.001$ for both developments, Fig. 13). The lowest salinities were measured at Kūkiʻo, with salinities below 31 at 5 stations (2, 8, 9, 12, 15), while Pau'oa only had one station with a salinity below 32‰ (Station F04) (Fig.13). These low salinity stations were the most affected by fresh groundwater.

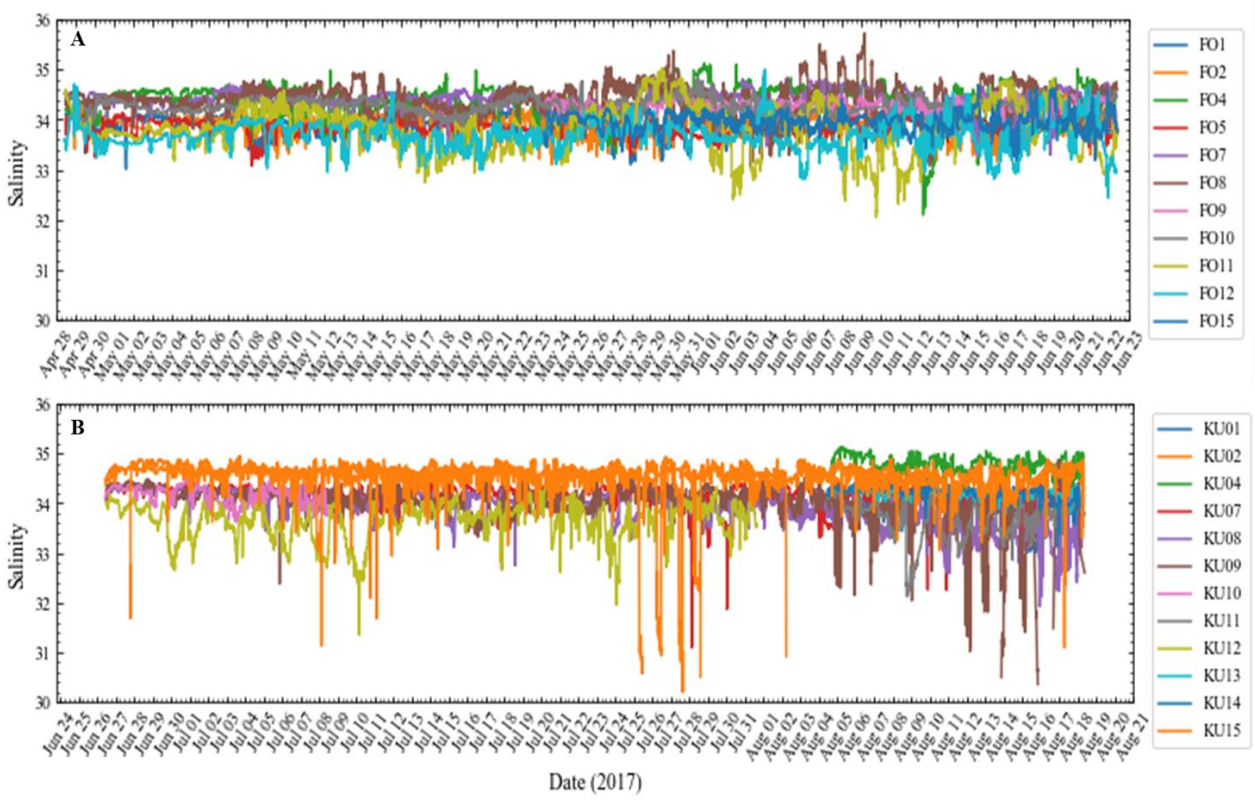

Figure 12. Time-series plot of benthic salinity at (A) Pauʻoa (April-June 2017) and (B) Kūkiʻo (June-August 2017).

Across both bays, low salinity was observed at 16 of the 23 stations (Fig. 13). Low salinity was defined as salinity < 33.5‰, which was greater than the logger precision of salinity = 0.5. At Pauʻoa, low salinity occurred less than 4% of the time at five stations, and FO11 and FO12 both experienced low salinity during 21% of their deployment time (Fig. 14). At Kūkiʻo, seven stations experienced low salinity less than 4% of the deployment time, three stations had low salinity between 5% and 13% of the deployment, and two, KU11 and KU12, experienced low salinity 28% and 23% of the deployment, respectively (Fig. 14).

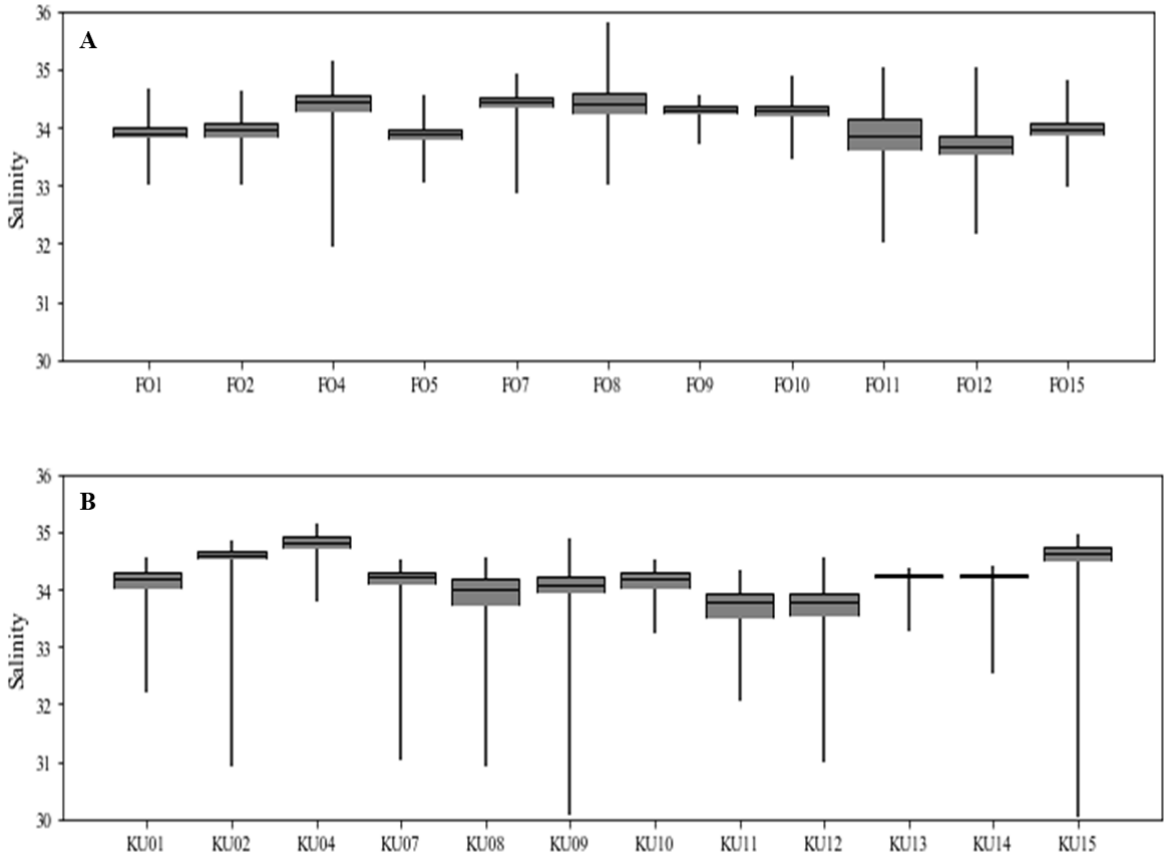

Figure 13. Distribution of salinity at each station (A) Pauʻoa and (B) Kūkiʻo. Whiskers are the maximum and minimum measured salinity, box is the 25th and 75th percentile, and the line within the box is the median.

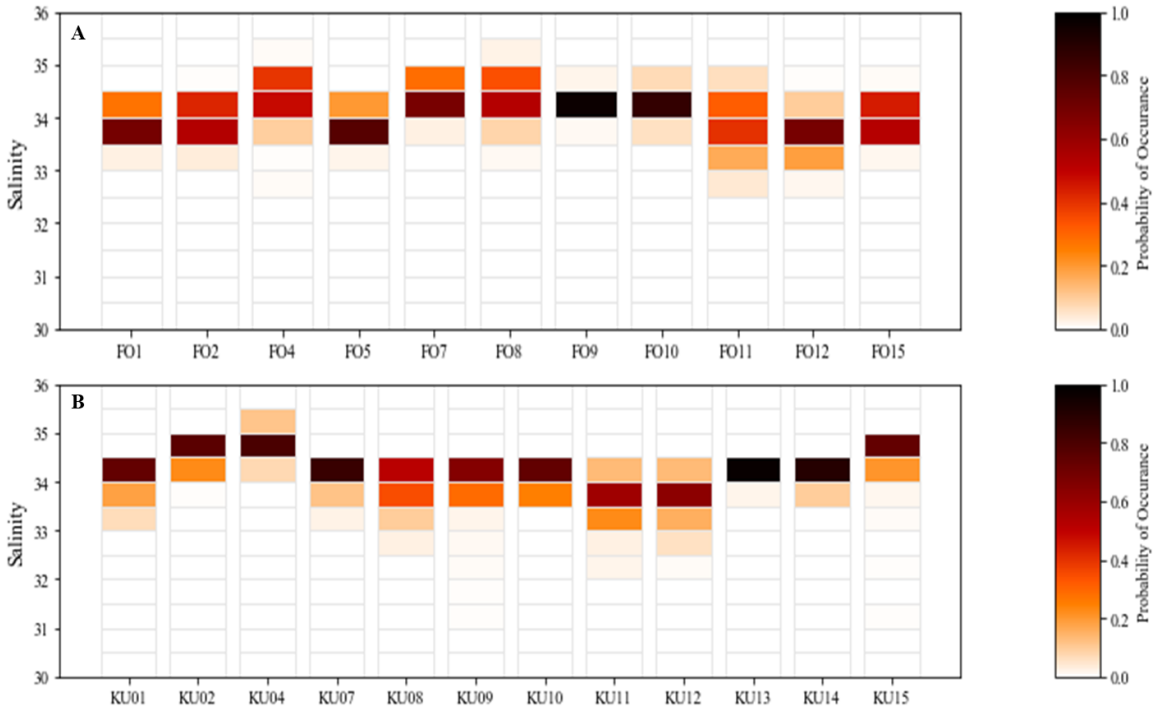

Figure 14. Fraction of total time during the temperature-conductivity sensor deployments that salinity was within a given salinity range (salinity bin size=0.5) at each station at each site, (A) Pauʻoa and (B) Kūkiʻo.

The length of time that low salinity events (S<33.5‰) occurred ranged from a few minutes up to more than 2 days, with most events lasting less than 12 hours (Fig. 15). At Pau'oa, two stations experienced reduced salinity 21% of the time (FO11 and FO12), but they experienced that low salinity in different ways. For example, at FO11, low salinity occurred in a few, persistent events (> 12 hours) (Fig. 15). Low salinity events at FO12 were typically less than 2 hours, while Stations FO4 and FO5 experienced low salinity less frequently but the exposure to low salinity was for longer durations.

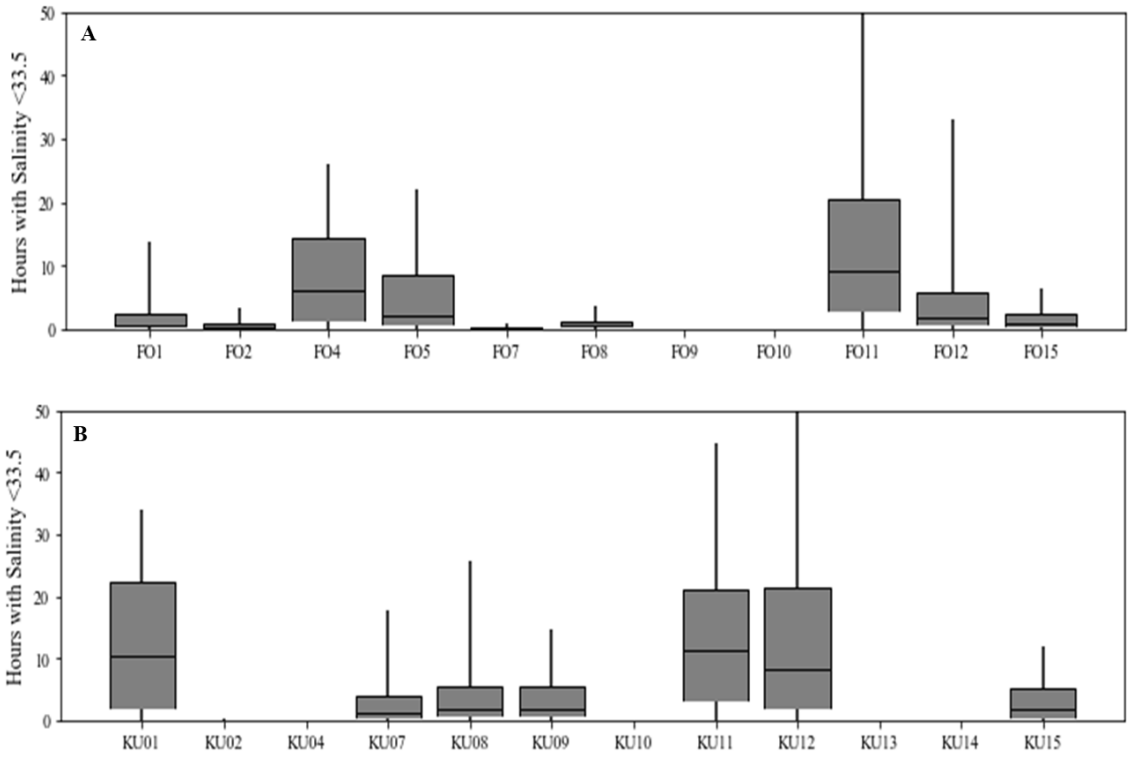

Figure 15. Distribution of the length of time that low salinity events (S<33.5) occurred at each station at each site (A) Pau'oa and (B) Kūki'o. Whiskers are the maximum and minimum length of time of these events, box is the 25th and 75th percentile, and the line within the box is the median.

Using the benthic and shoreline $NO_3^-+NO_2^-$-salinity relationships for each bay (Fig. 16), the average benthic nutrient concentration was almost five times higher at Kūki'o than at Pau'oa (5.0 ± 0.7 µmol/L vs. 1.4 ± 1.4 µmol/L, respectively) (Fig. 16). Across both developments, 5 of the 23 stations experienced $NO_3^-+NO_2^-$concentrations less than 1 µmol/L during > 50% of the deployment, and those stations were all deeper stations at Pau'oa (Fig. 17). At Pau'oa, $NO_3^-+NO_2^-$ concentrations greater than 7 µmol/L were predicted at several stations, but rarely occurred (0.14% of time).

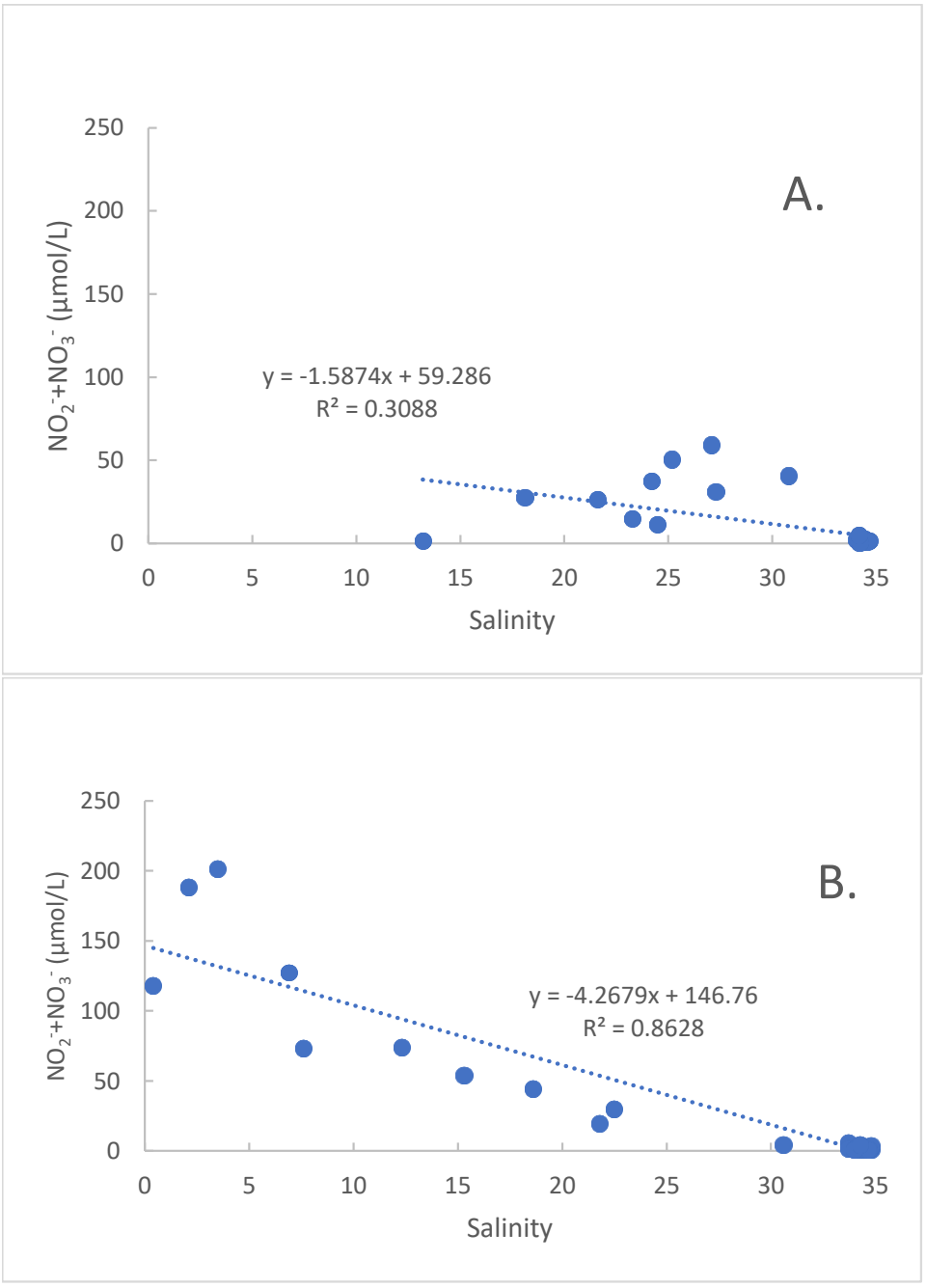

Figure 16. Linear regression models for NO_3^-+NO_2^-- and salinity at (A) Kūkiʻo and (B) Pauʻoa. Samples used in the regression were from the shoreline and benthic data.

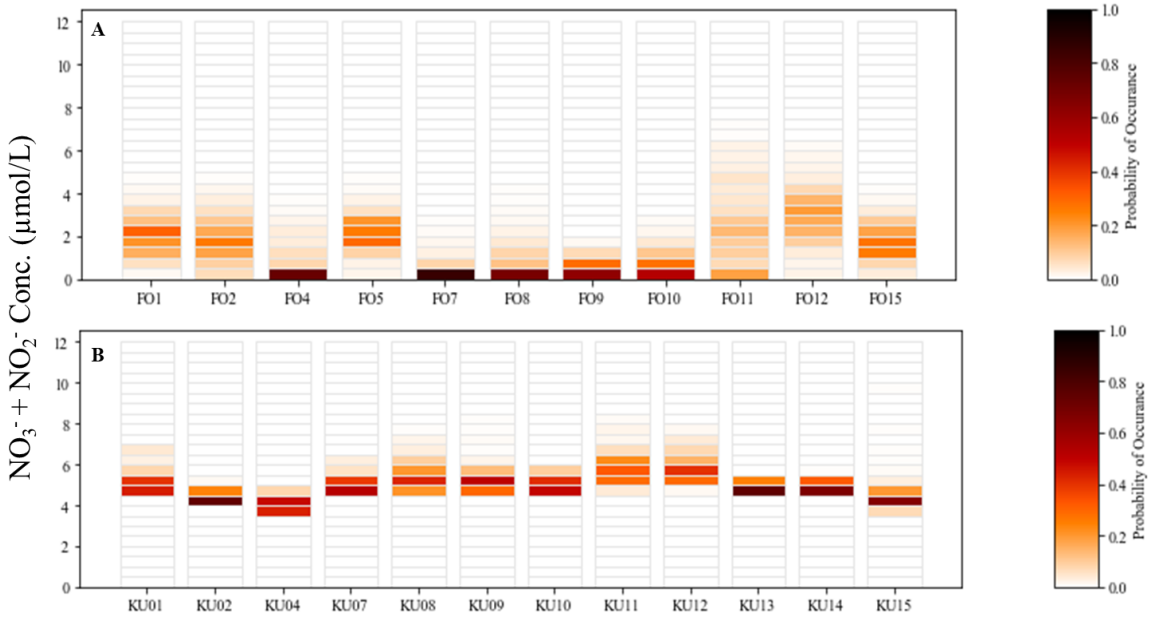

Figure 17. Fraction of total time predicted NO_3^- +NO_2^- concentration was within a given NO_3-+NO_2^- range (NO_3^-+NO_2^- bin size = 0.5 µmol/L) at each station at each site (A) Pau‘oa and (B) Kūki‘o.

4.2.2 Temperature

Temperatures were cooler at Pau‘oa (26.1 ± 0.4 °C) than at Kūki‘o (27.1 ± 0.5 °C) ($p < 0.001$), which was sampled later in the summer (Figs. 18 and 19). At Pau’oa, temperature displayed a strong diurnal fluctuation, with daily temperature fluctuations >1°C (Figs. 18 and 19). A notable pulse of cold water occurred during the nights of June 5-7, where temperatures across the bay decreased below 25.0 °C (Figs. 18 and 19). In contrast, at Kūki‘o the bay experienced a pulse of warming, where mean temperatures increased by 1.0 °C on July 10, 2017 (Figs. 18 and 19). Among stations, average temperature varied by less than 0.5°C at night, and by as much as 1°C during the daytime (Fig. 20). Warmer temperatures were observed at shallower sites closer to shore (Fig. 20).

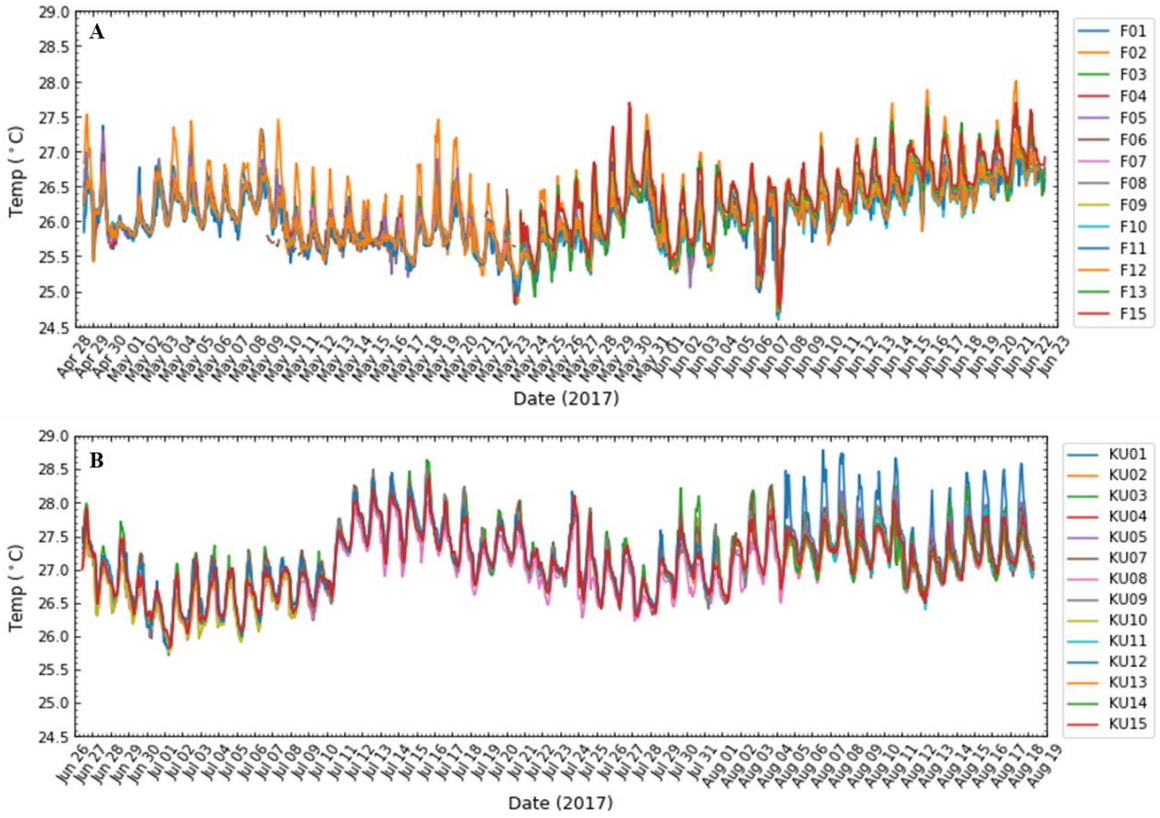

Figure 18. Time-series plot of benthic temperature at (A) Pau‘oa (April-June 2017) and (B) Kūki‘o (June-August 2017).

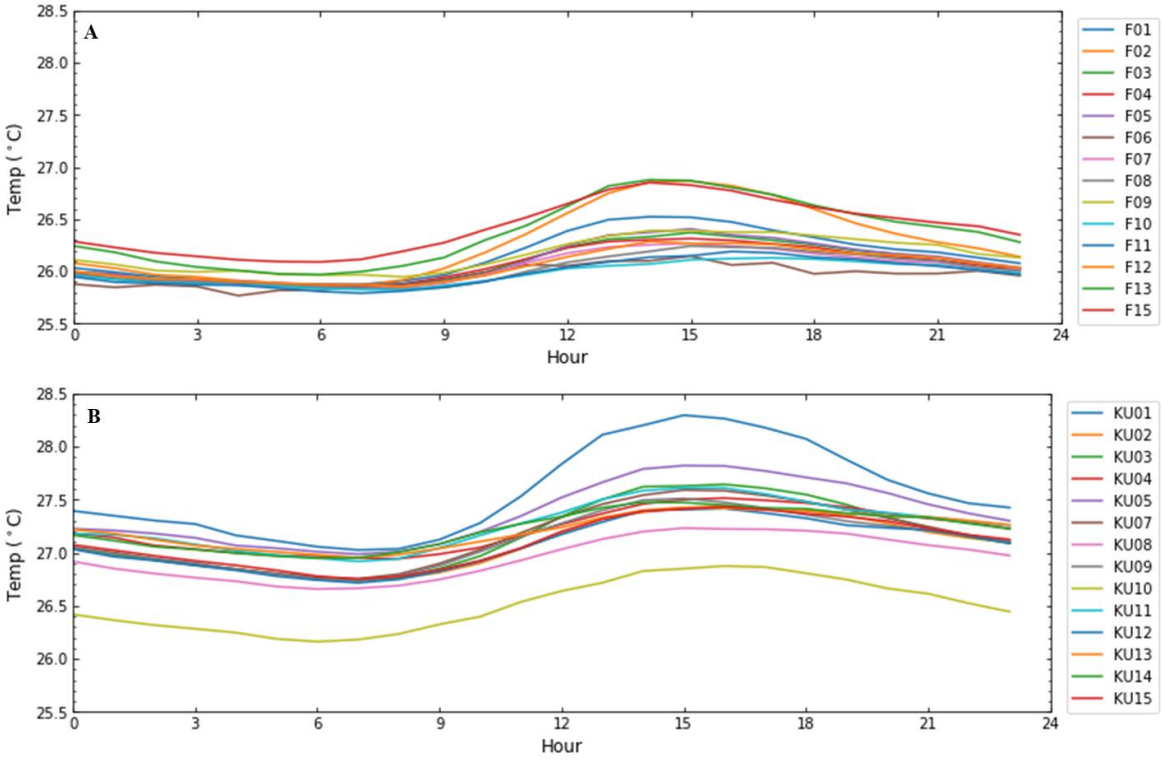

Figure 19. Time-series plot of benthic temperature at (A) Pauʻoa (April-June 2017) and (B) Kūkiʻo (June-August 2017).

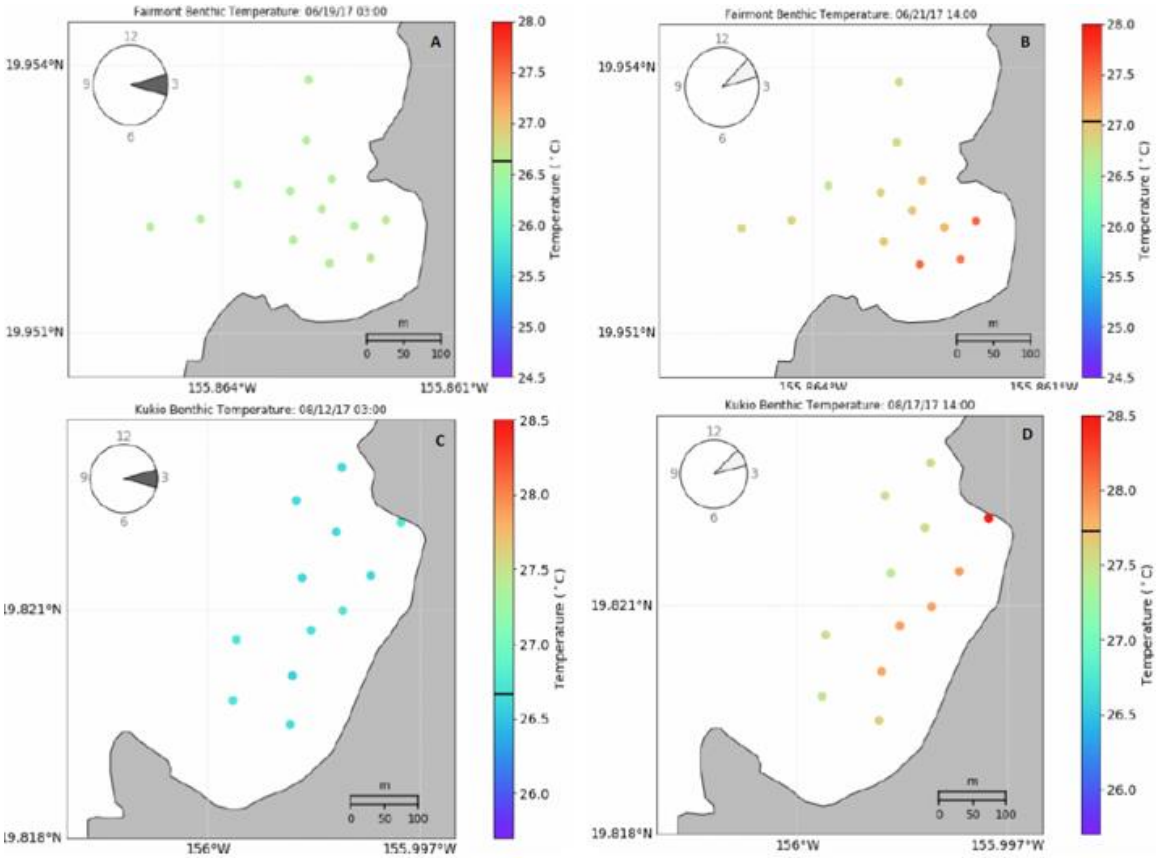

Figure 20. Typical benthic temperatures at (A,B) Pauʻoa and (C,D) Kūkiʻo during the early morning (left) and afternoon (right).

4.2.3 Discussion

While the mean salinity among the developments was similar, differences in the salinity at individual stations were observed. Seven stations (two at Pauʻoa and five at Kūkiʻo) did not experience salinities less than 33.5‰ and were likely free of any direct impacts of land-based sources of pollution during the study. Indirect impacts (e.g., productivity in surface water that then sinks down to the reef) were not assessed in this study.

The other 16 stations were impacted by fresh groundwater to different magnitudes. The exposure time of the seafloor to low salinity (< 33.5‰) was assessed in two ways. First, an overall probability of exposure to low salinity was calculated, with some stations experiencing no low-salinity events during more than 20% of the deployment time. Second, the length of time that salinity remained below 33.5‰ was also calculated. The majority of low salinity events at both developments lasted < 12 hours. Six stations had occurrences of low salinity events that exceeded 20 hours (two at Pauʻoa, four at Kūkiʻo). These longer duration low salinity events likely have a greater impact on benthic ecosystems. For example, longer duration events are more likely to include periods of

daytime, when algae can maximize their growth and uptake of nutrients. Based on the nitrate-salinity relationships, low salinity events corresponded to exposure to elevated nutrient concentrations, which can result in excess algal and bacteria growth.

4.3 Spatial Patterns in Coral Health and Benthic Communities

Overall, 31.8 ± 2.3 % of the corals at Pau‘oa and 27.1 ± 3.7% of corals at Kūki‘o showed signs of disease or compromised health. We observed three types of diseases, all of which are classified as slow progressing chronic or sub-acute. Growth anomalies were the most prevalent and only found on *Porites*, with 19 to 22% of colonies affected, followed by trematodiasis and tissue loss (Fig. 21). The most prevalent sign of compromised health was algal overgrowth, with 11 to 13% of all colonies affected, followed by discoloration, predation, physical damage and bleaching (Fig. 21).

At Pau‘oa Bay, corals affected by any condition decreased with distance from the inner bay adjacent to the resort (Fig 22). This pattern appears to be driven strongly by corresponding patterns in *Porites* growth anomalies (Fig 22). We also saw an offshore gradient in coral juvenile density and the reef builder ratio, with juveniles and reef builders relative to fleshy algae increasing with distance from the inner bay (Fig. 22).

At Kūki‘o Bay, there was no clear pattern in coral health across the bay (Figs 23). However, similar to Pau‘oa, there was an increase in juvenile density with distance from shore (Fig. 23). The abundance of reef builders relative to fleshy macroalgae increased from north to south (Fig. 23).

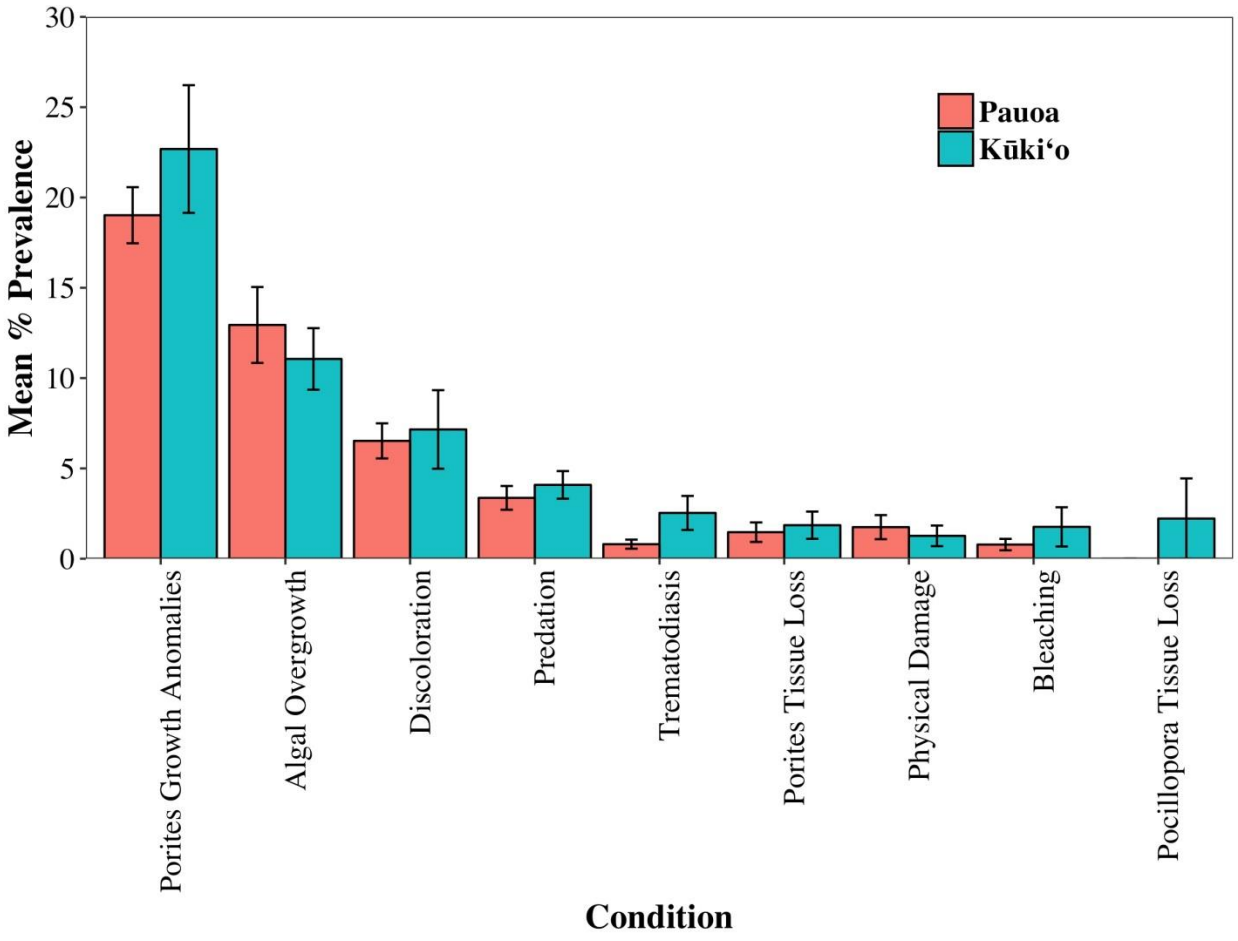

Figure 21. Mean ± SE prevalence (# of colonies with condition/total # of colonies) of conditions affecting colonies at both study sites (n=15 stations/site). See Figure 7 for condition descriptions.

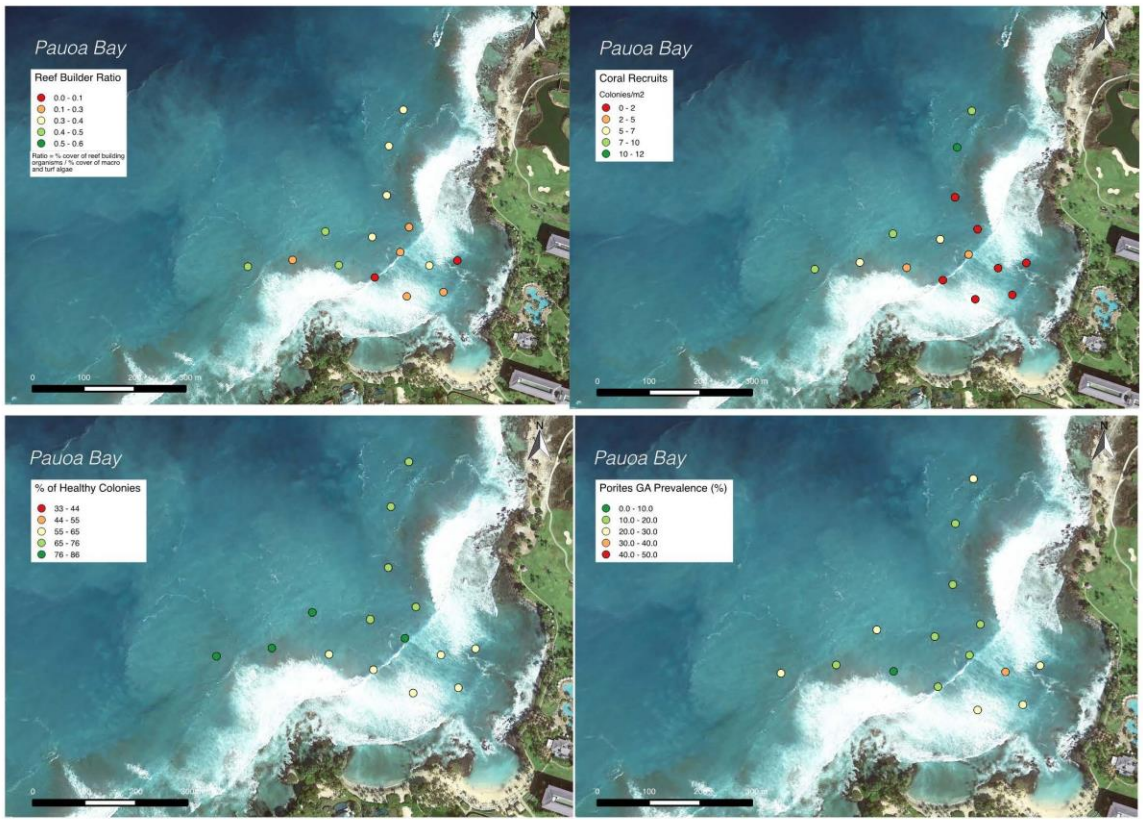

Figure 22. Reef builder ratio, coral recruits, % healthy colonies and prevalence of Porites growth anomalies in Pau‘oa Bay

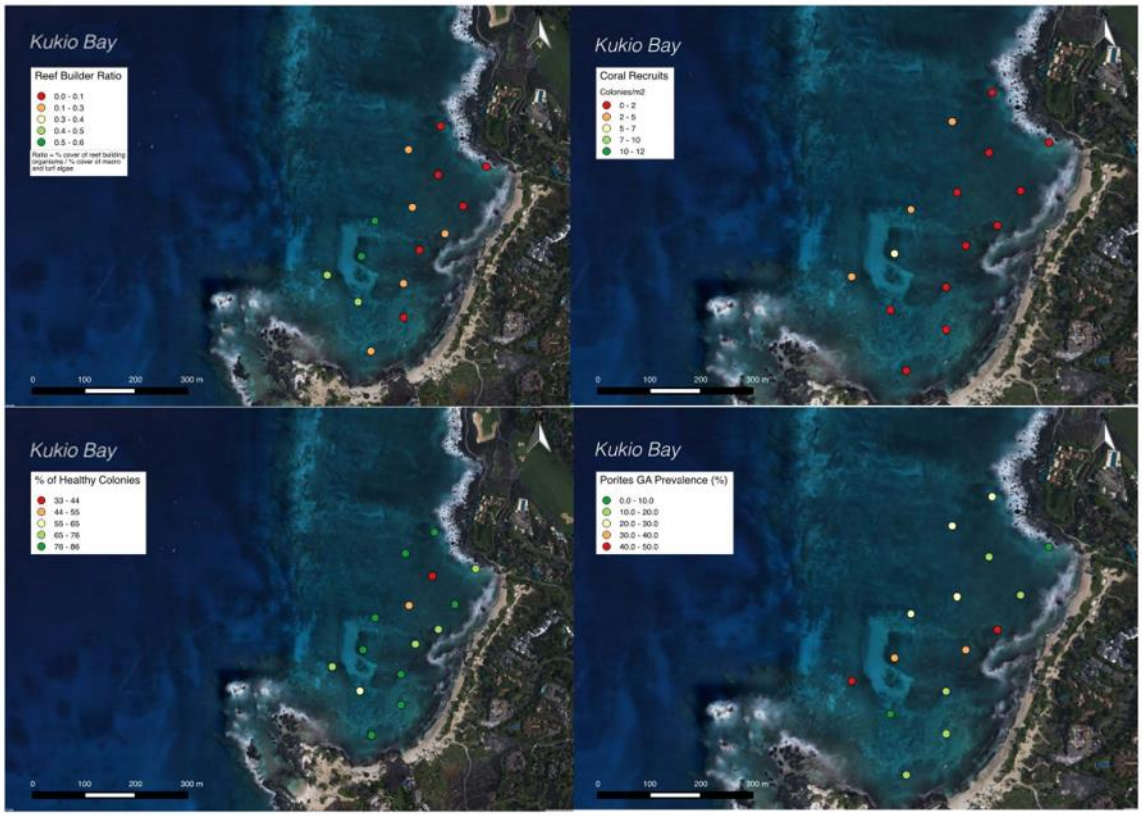

Figure 23. Reef builder ratio, coral recruits, % healthy colonies and prevalence of Porites growth anomalies in Kūkiʻo.

4.3.1 Drivers of Coral Communities and Health at Pauʻoa Bay

A separate set of generalized linear models for were computed for all permutations of the environmental and colony-level factors for our five benthic response variables (proportion of healthy colonies, *Porites* growth anomalies and direct coral-algal competition, coral juvenile density and the reef builder ratio). After selecting and averaging the "best-fit" models (ΔAIC <4), we compared the relative importance of the top drivers of each benthic factor by comparing the standardized predictor estimates. Overall, this approach suggests that each response variable is driven by a combination of factors with some factors being more important than others (Fig. 24). Results suggest that the proportion of healthy colonies increased when exposed to lower Si and NH_4^+, which were 2 to 3 times more influential than the other variables (Figs. 24 and 25). The proportion of *Porites* colonies with growth anomalies (GA) increased when exposed to higher $\delta^{15}N$ values and lower NH_4^+ concentration (Fig. 24). While Porites GAs appeared to increase with colony size and Si, their effect was more variable than the others and should be interpreted with caution. The factors correlated with the proportion of corals

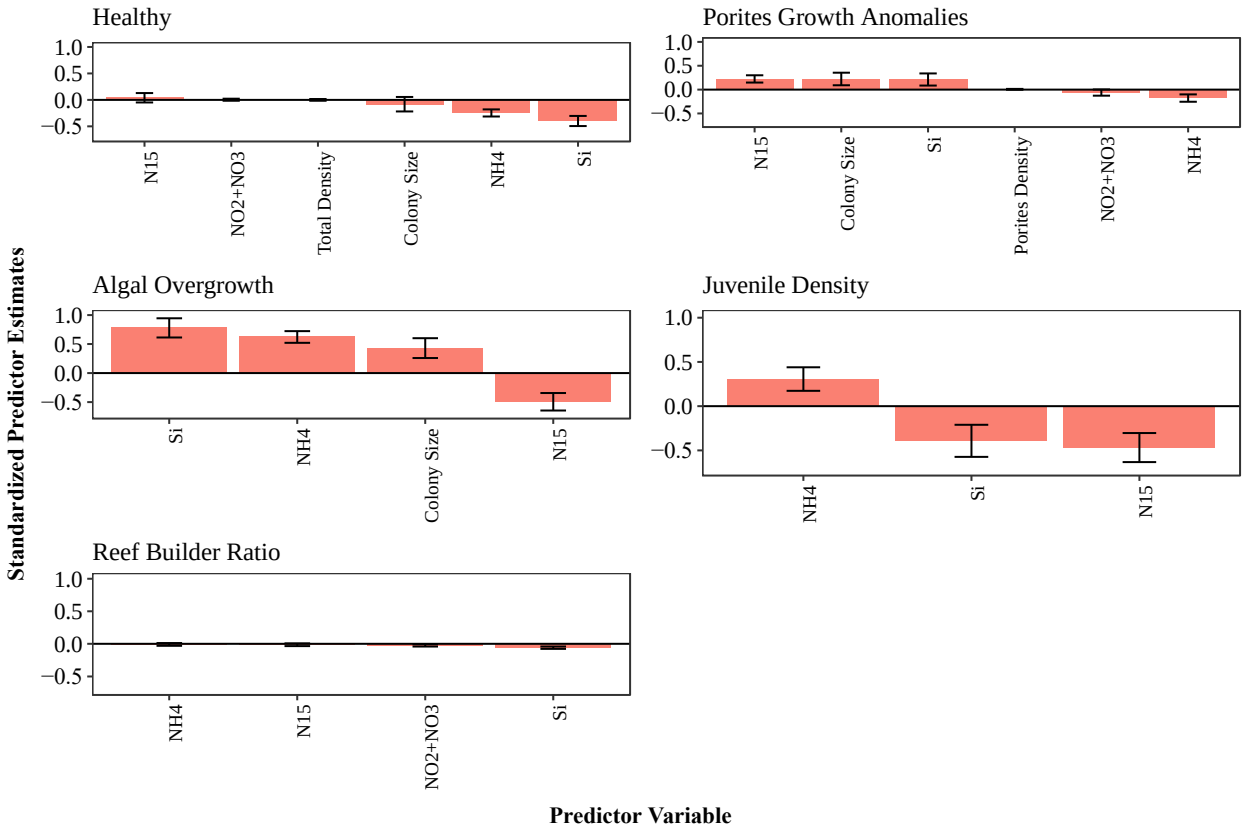

Figure 24. Explanatory variables of proportion of: health colonies, *Porites* colonies with growth anomalies, and direct coral-algal competition as well as coral juvenile density and reef builder ration (coral cover + algal cover/turf algae + macroalgae) at Pau'oa Bay and their standardized parameter estimates (±SE) from the average of the "best-fit" models ΔAIC_C <4. Only variables included in the "best-fit" models were included in model averaging.

experiencing direct competition with algae had similar importance but different relationships, with algal overgrowth (ALOG) increasing when exposed to higher Si, higher NH_4^+ concentration and lower $\delta^{15}N$ values on reefs with larger colonies (Fig. 24). Juvenile density increased when exposed to higher NH_4^+, lower Si and lower $\delta^{15}N$ values. For predictors of reef builder ratio, NH_4^+, $\delta^{15}N$, NO_3^- + NO_2^- and Si were all included in the "best fit" models, but these factors had a very small effect size compared to the other response variables suggesting that other factors not included in this study are likely driving reef builder ratio.

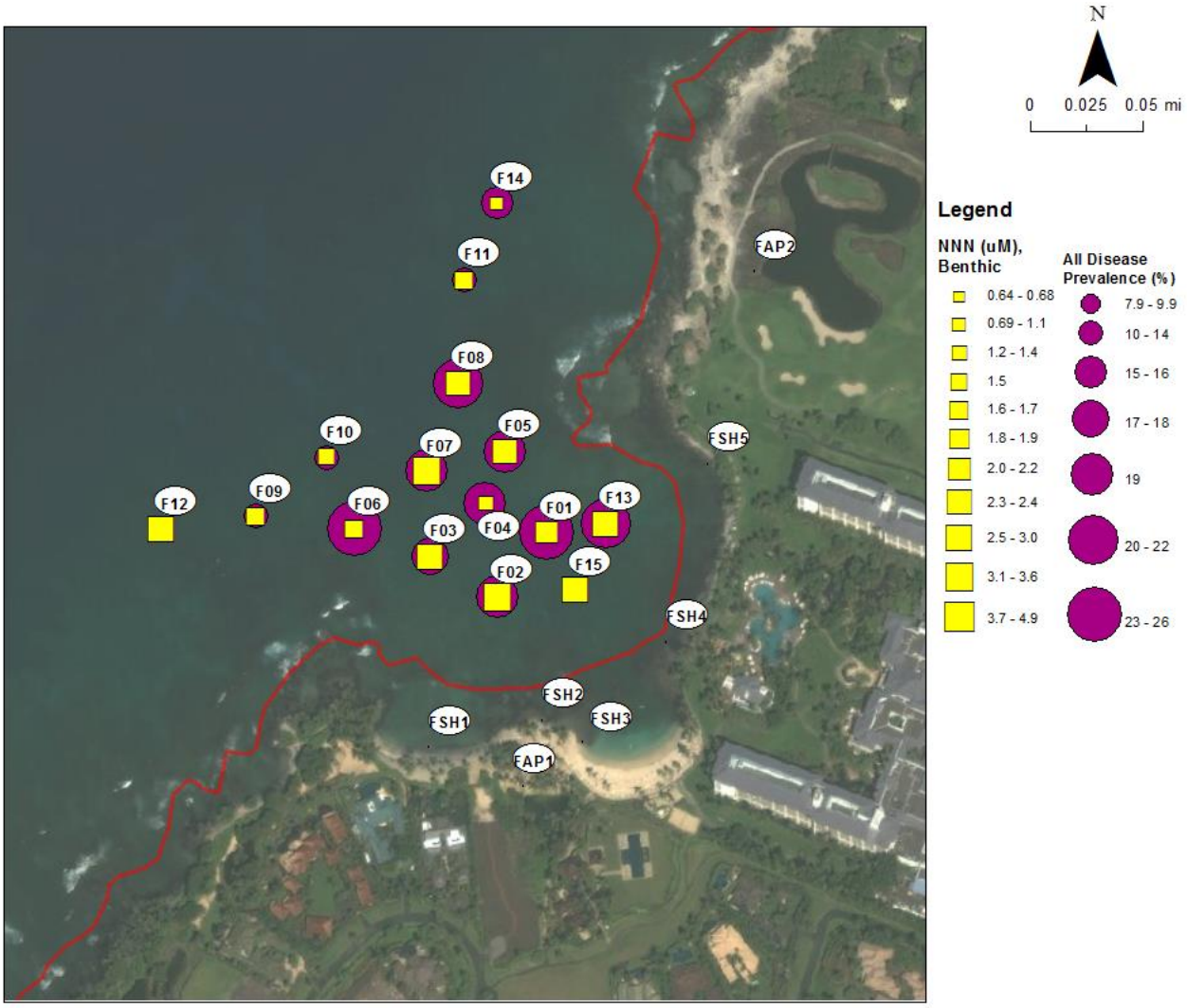

Figure 25: All disease prevalence compared with average benthic nitrate concentrations at Pau‘oa.

4.3.2 Drivers of Coral Communities and Health at Kūki‘o Bay

Similar to Pau‘oa Bay, our results suggests that each response variable is driven by a combination of factors with some factors being more important than others (Fig. 26). However, the relative predictive power of the environmental and benthic community factors was not as strong at Kūki‘o compared to Pau‘oa as evidenced by the smaller predictor estimates. Although six predictor variables were included in the “best-fit” models of the proportion of healthy colonies, colony size was the strongest driver with more healthy colonies on reefs with smaller colony size (Fig. 26). The proportion of *Porites* colonies with GAs was also strongly driven by colony size with more *Porites* colonies with GAs on reefs with larger colonies (Fig. 26). While *Porites* GAs appeared to also increase with NO_3^- + NO_2^- and decrease with $\delta^{15}N$ and Si, their effect was more variable and should be interpreted with caution (Fig. 27). The proportion of corals

experiencing direct competition was most strongly driven by colony size and Si concentration (Fig. 26). More specifically, ALOG was highest on reefs with large colonies and low Si. ALOG also increased with NH_4^+ concentration and $\delta^{15}N$ values, but with a smaller and more variable effect size (Fig. 26). Juvenile density increased when exposed to lower NO_3^- + NO_2^- concentration and lower $\delta^{15}N$ values. For predictors of reef builder ratio, NH_4^+, $\delta^{15}N$, NO_3^- + NO_2^- and Si were all included in the "best fit" models, but similar to Pau'oa these factors had a very small effect size compared to the other response variables suggesting that other factors not included in this study are likely driving reef builder ratio.

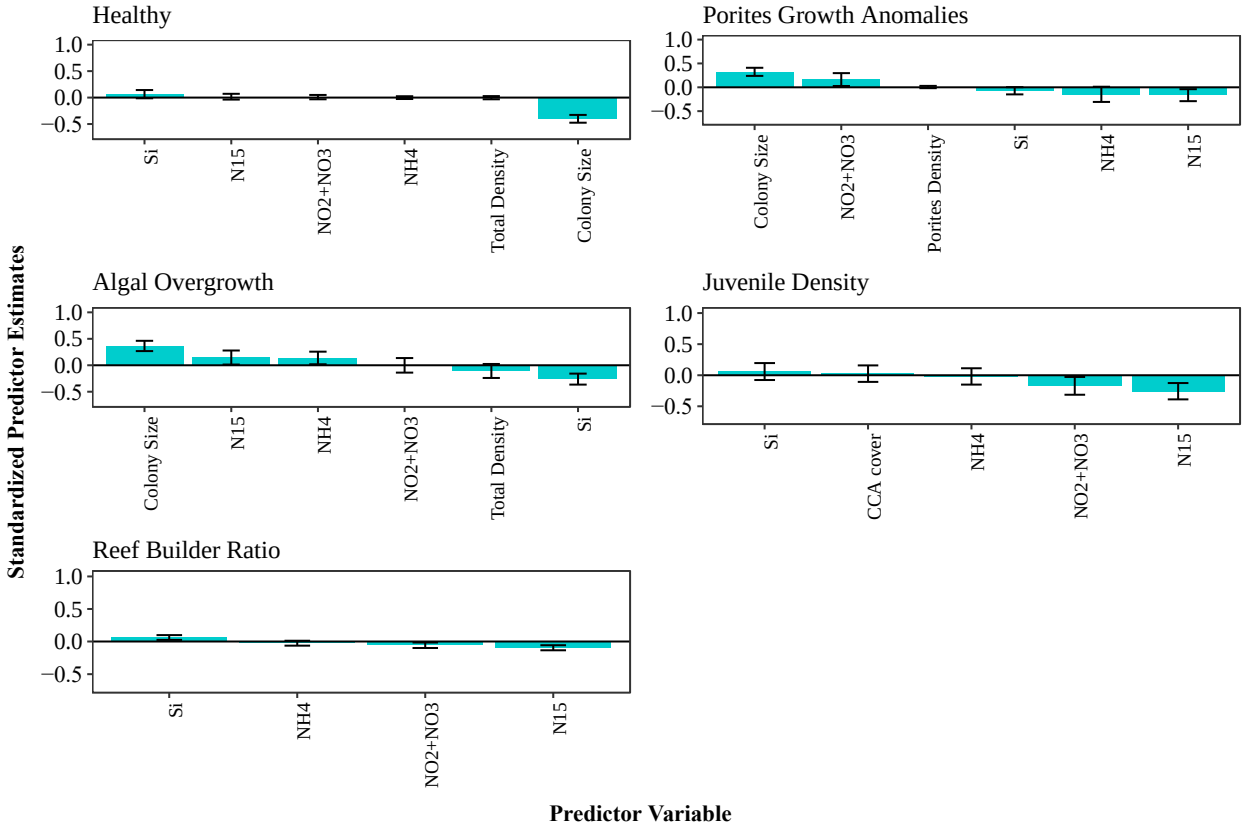

Figure 26. Explanatory variables of proportion of: health colonies, *Porites* colonies with growth anomalies, and direct coral-algal competition as well as coral juvenile density and reef builder ration (coral cover + algal cover/turf algae + macroalgae) at Kūki'o Bay and their standardized parameter estimates (±SE) from the average of the "best-fit" models ΔAIC_C <4. Only variables included in the "best-fit" models were included in model averaging.

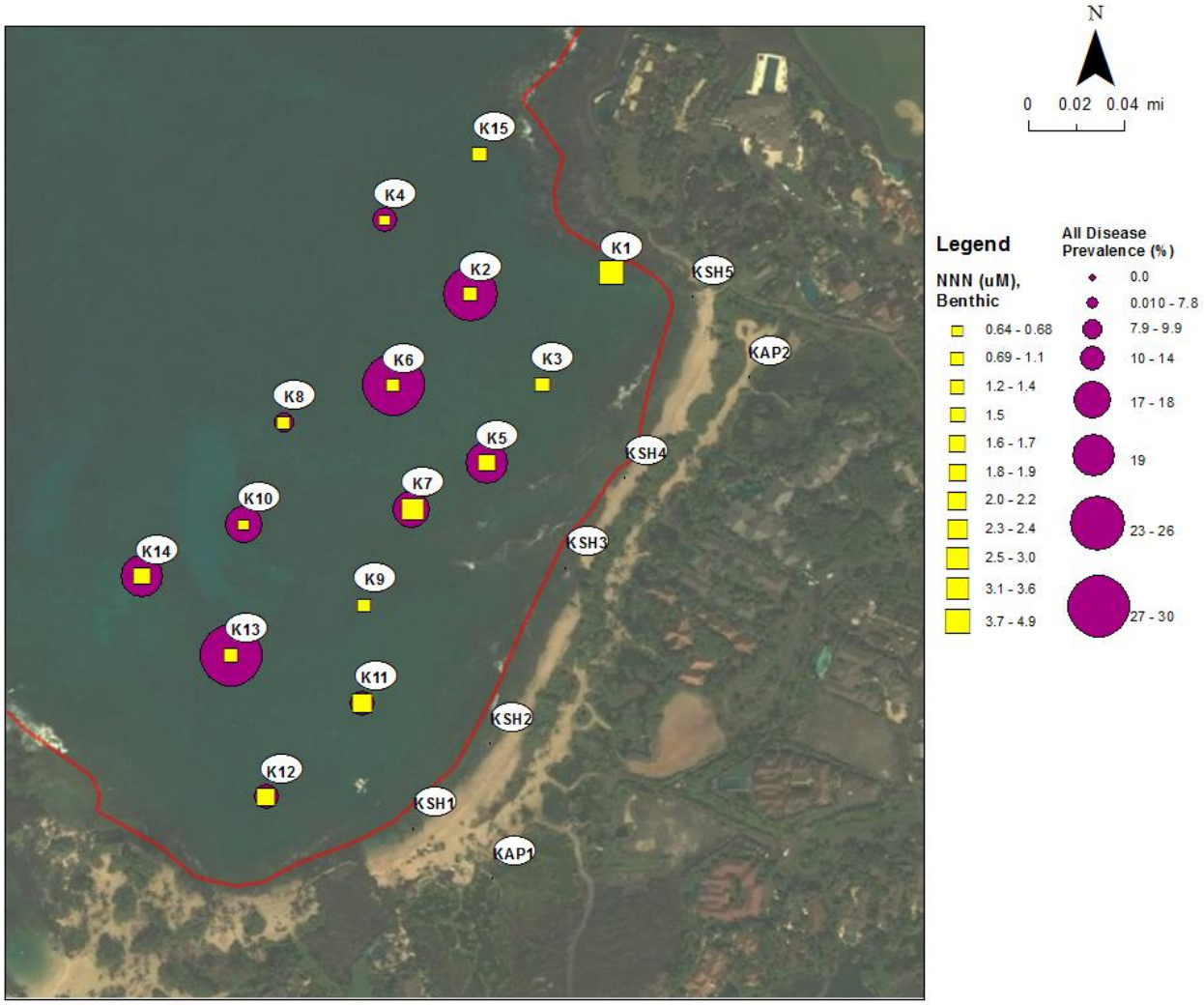

Figure 27. All disease prevalence compared with average benthic nitrate concentrations at Kūkiʻo.

4.3.3 Discussion

Benthic communities are likely influenced by a combination of nutrients and community factors. However, coral health, juvenile density and the amount of reef builders respond differently to these factors.

There is also a noticeable difference in how and the degree to which corals in these two regions respond to terrestrial inputs and community factors.

In Pauʻoa, higher Si concentrations, which is a proxy for groundwater input, was among the strongest predictors with less healthy coral, more disease, higher coral-algal competition and less recovery potential (fewer coral juveniles) in areas with high

groundwater input. Lower $\delta^{15}N$ values and higher NH_4 were also associated with areas with more coral algal competition, but more juveniles.

In Kūkiʻo, the relative importance of nutrients and community factors was lower than Pauʻoa Bay, suggesting that much of the variability on Kūkiʻo's benthic communities is still unaccounted for. Regardless, similar to Pauʻoa, more healthy colonies with fewer *Porites* growth anomalies and direct coral-algal competition were found on reefs dominated by small colonies. The role of groundwater input is less clear in Kūkiʻo, with only algal overgrowth showing a decline as a function of groundwater input. Juvenile density was also higher in areas with lower $\delta^{15}N$ values.

4.4 NUTRIENT MODELING

The results of the nutrient modeling are presented below in Figs. 28 and 29, representing 2km and 10km results, respectively. The land use land cover composition used for modeling of both 2km and 10km watersheds can be found in Table 7.

Notably, Pauʻoa Bay is located in a region that was predicted to have lower amounts of groundwater and was not directly connected to the larger watershed leading up to Mauna Kea. Observationally, the groundwater shifts seen in Pauʻoa contradict this modeling result. However, more broadly, the model did correctly reflect the hotspots of nutrients along the coast (Figs. 30 and 31).

Table 7: Land use percentages for both sites for 2km watersheds.

	Pauʻoa	Kūkiʻo
Developed High Intensity	20.64%	19.20%
Bare Land	18.16%	49.49%
Hotel Trees and Shrubs	15.35%	11.18%
Golf courses	14.63%	11.57%
Lawns and Gardens	12.18%	2.04%
Kiawe Forest	8.14%	0.00%
Open Water	3.94%	1.16%
Scrub/Shrub	3.04%	2.32%
Grassland/Herbaceous	2.53%	2.96%
Evergreen Forest	1.30%	0.02%
Cess pools	0.05%	0.01%
Developed Open Space	0.05%	0.06%

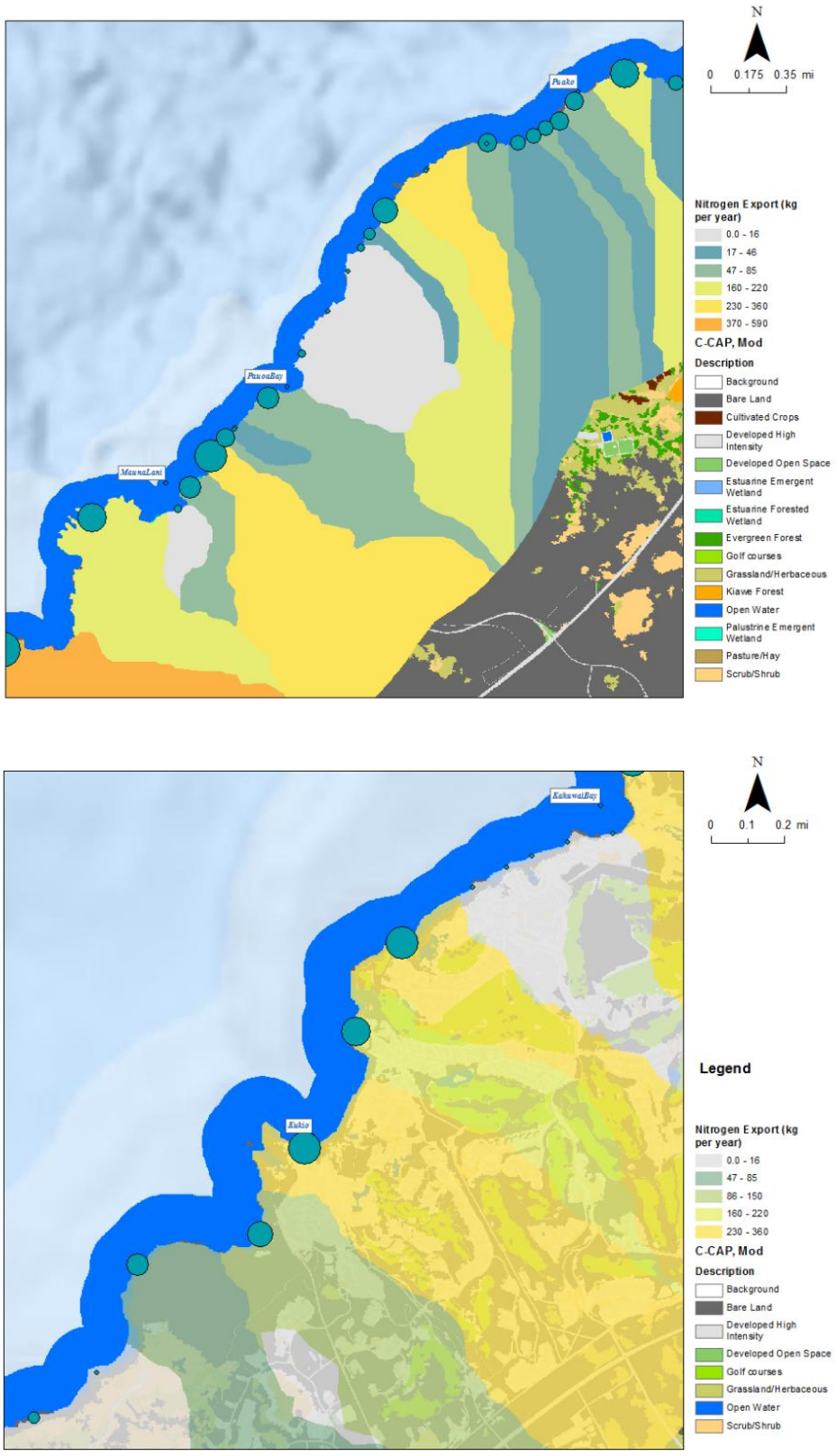

Figure 28. Pau‘oa (top) and Kūki‘o (bottom) predicted nitrogen export for 2km watersheds.

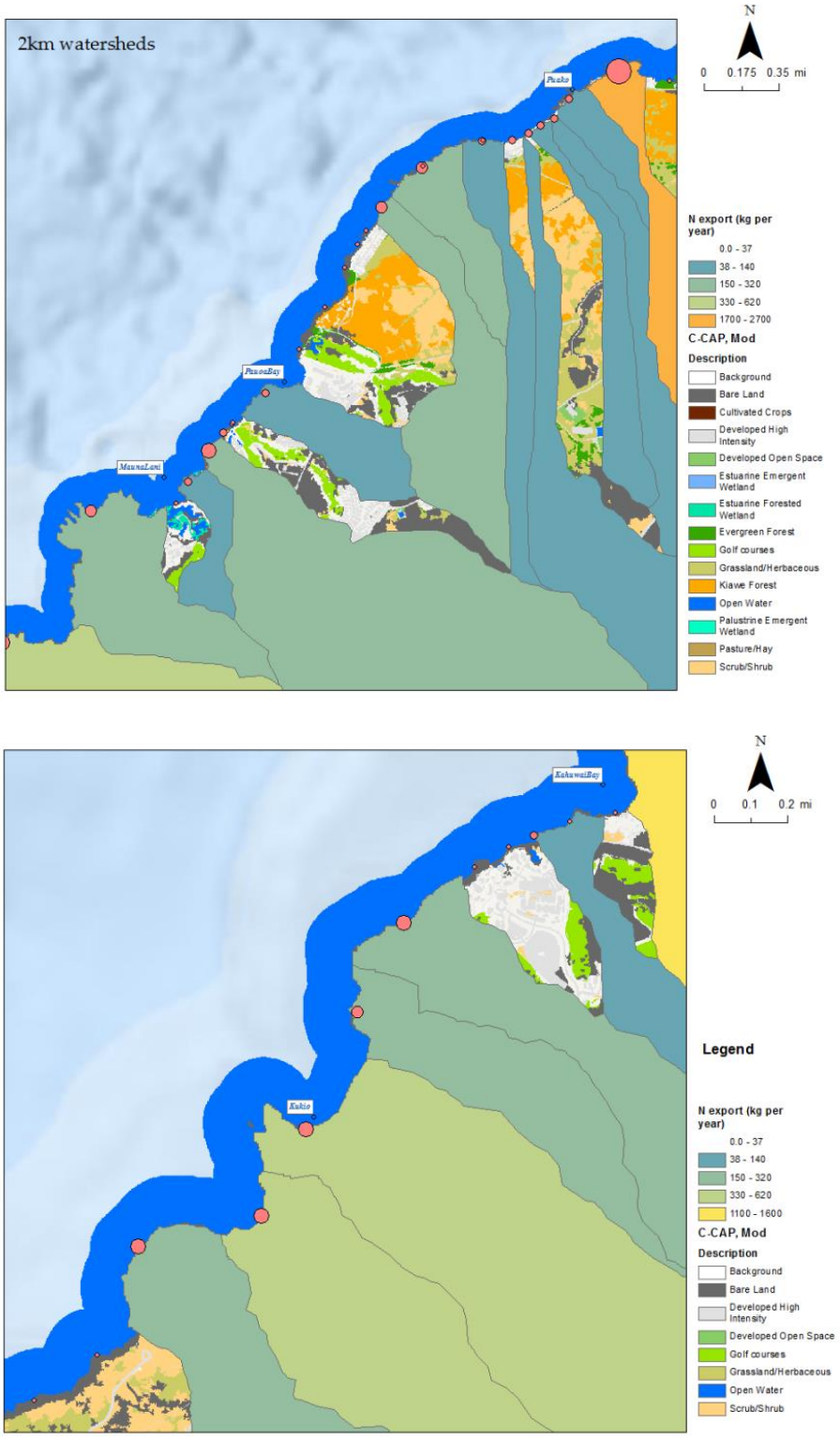

Figure 29: Pauʻoa (top) and Kūkiʻo (bottom) predicted nitrogen export for 10km watersheds.

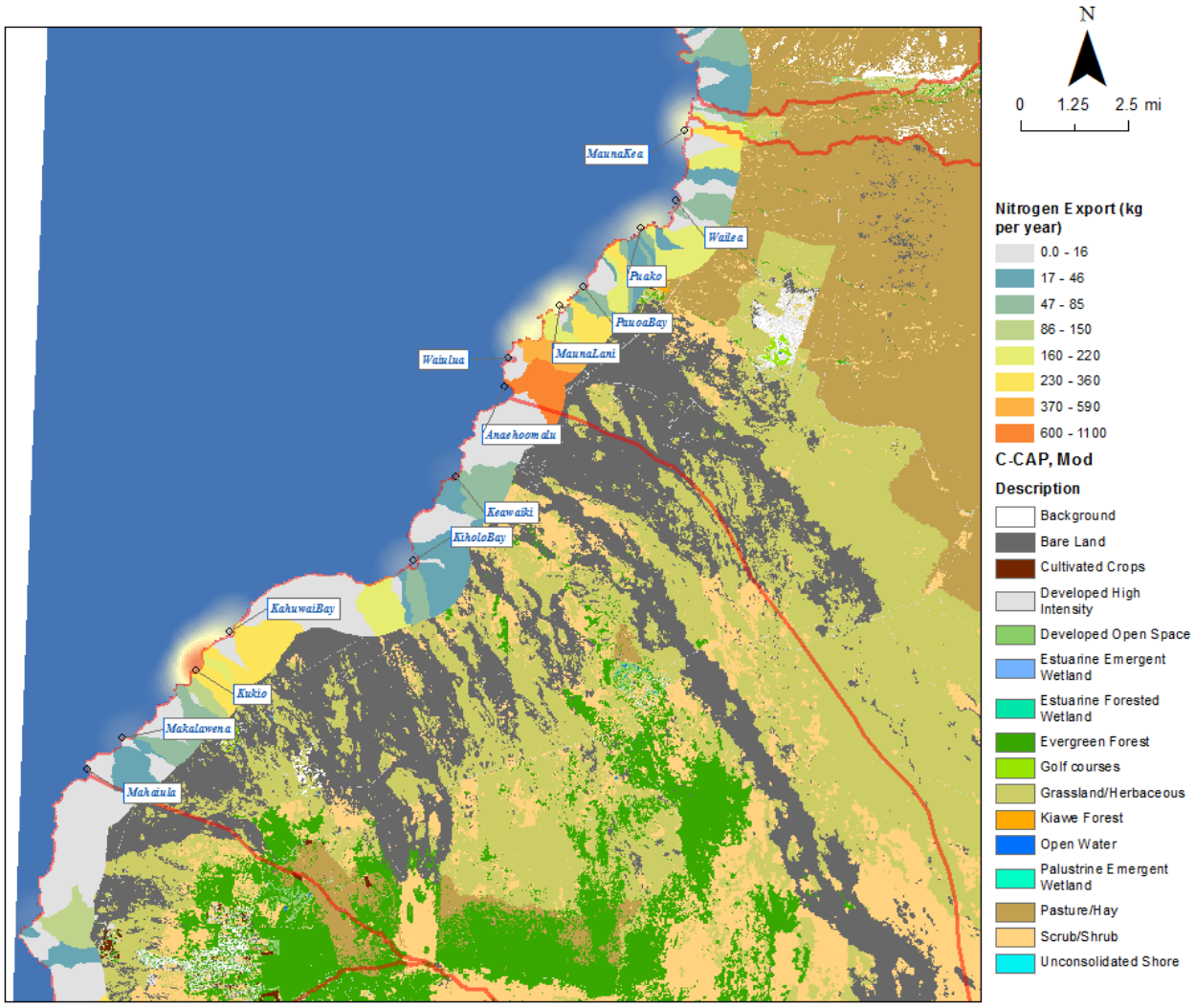

Figure 30: Predicted nitrogen export for 2km watersheds in North Kona and South Kohala coastline, with corresponding locations of coastal export.

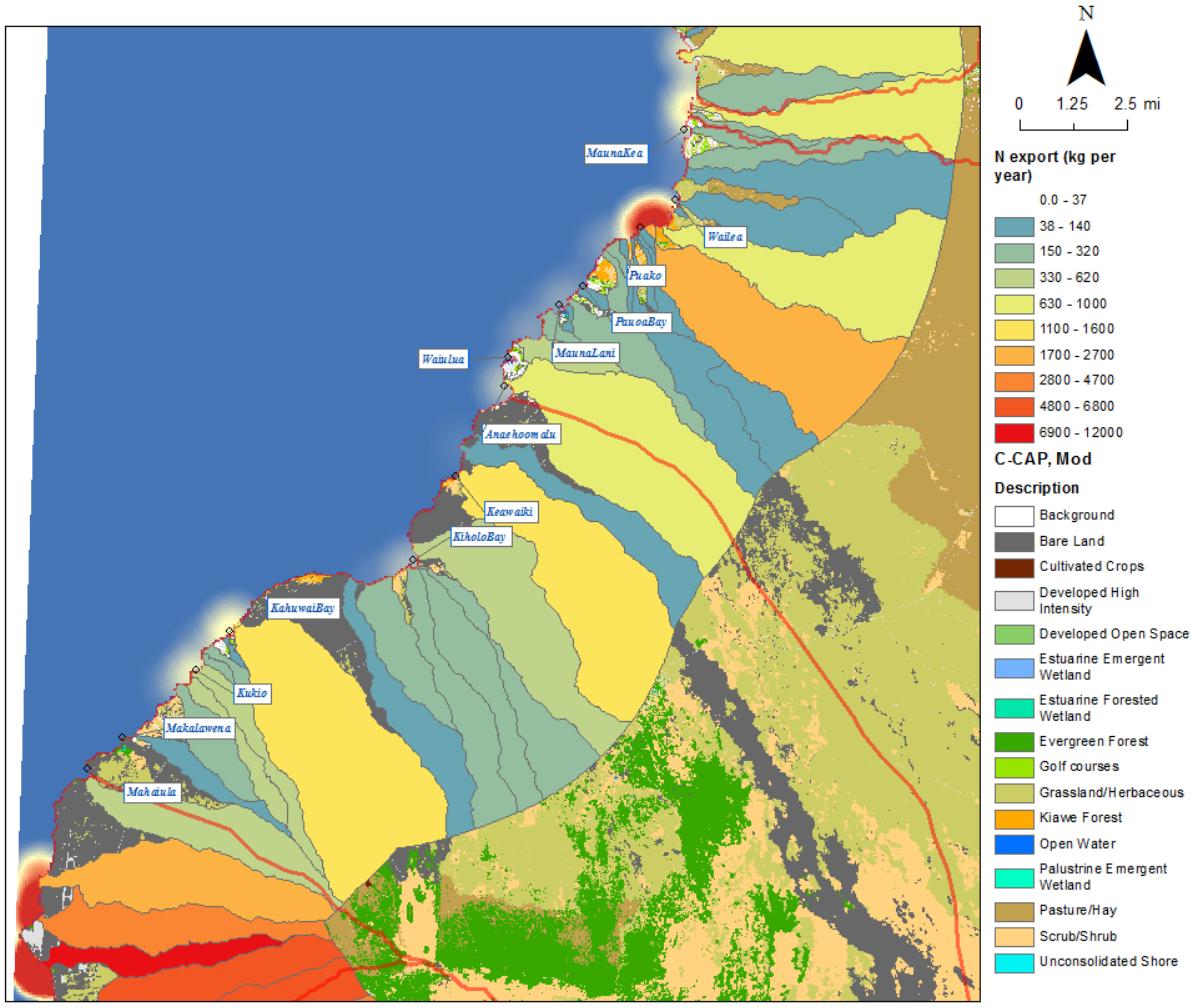

Figure 31: Predicted nitrogen export for 10km watersheds in North Kona and South Kohala coastline, with corresponding locations of coastal export.

The nutrient modeling shows that there are different spatial patterns for nutrient export if one considers the groundwater originating from 2km from shoreline versus 10km (Figs. 28 and 29). Given groundwater rates of flow through the substrate in West Hawai‘i, 1km takes approximately one year to move. It might also be more likely that nutrients originating from 2km from the coastline are more likely to stay shallow in the groundwater – thereby affecting the nearshore more than farther from the coast. The coral data presented here showed a correlation between coral health and distance from the coast. Given that Pau‘oa is an embayment, and that the physical oceanography tools presented here (below) demonstrate that there is not a strong current, it is likely that the 2km model is appropriate.

4.5 OCEAN CURRENTS

ADP results indicate that ocean currents at Kūkiʻo are generally uniform with depth and flow predominantly to the Northeast (Fig. 32). Flow is strongest (0.1 – 0.2 m/s) in the upper water column (-1.5 – -2 m) with fluctuations in strength driven principally by tidal forcing (Fig. 33). Currents deeper in the water column are generally weaker (0.5 – 0.1 m/s) than that observed towards the surface (Fig. 33).

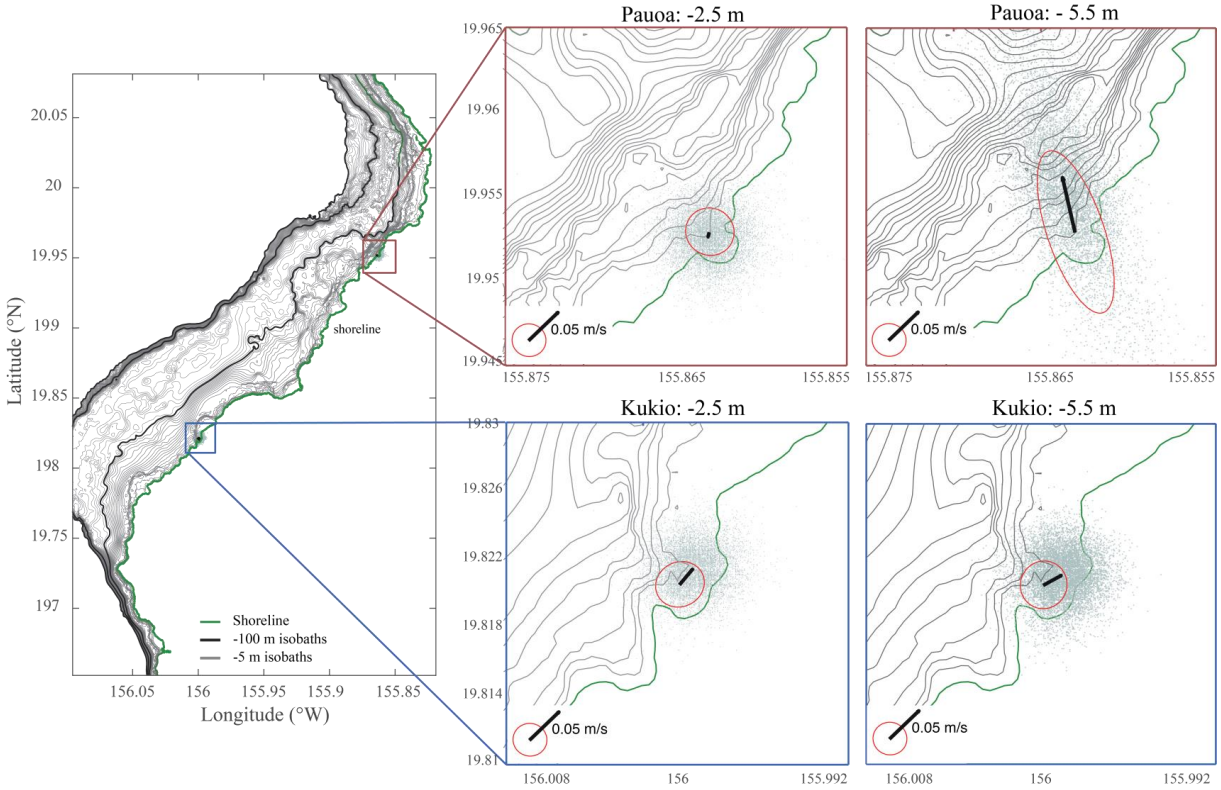

Figure 32: Map of the northwest portion of West Hawaiʻi indicating bathymetric contours from the shoreline (green line) to -300 m depth. Locations of in situ acoustic Doppler profilers (ADP) deployed at Pauʻoa (red box) and Kūkiʻo (blue box) from 21-July-2017 to 21-August-2017 (a). Variance ellipses and Mean current vectors (black arrow) and variance ellipses (red circle) calculated for ocean current obtained from -2.5 m and -5.5 m depth from their respective locations along West Hawaiʻi (b - e). Individual 5 min current observations are indicated by scatter points (gray); scaling is given by arrows and ellipses on the lower left of each plot. Vector scale arrows correspond to 0.05 m/s and error ellipse scales (red) correspond to standard deviation of 0.02 m/s.

Ocean currents at Pauʻoa are strongly non-uniform with flow varying in both strength and direction with depth (Fig. 32). Current is weakest (~0.05 m/s) with no dominant direction towards the upper surface (-2.5 m) while deeper, current strength is highly variable with peak flows that are significantly stronger (>0.2 m/s) and predominantly to the Northwest (Fig. 33).

Note that flow patterns can only be interpreted for the specific location of the deployments and are not necessarily representative of water velocities and direction across their respective locations.

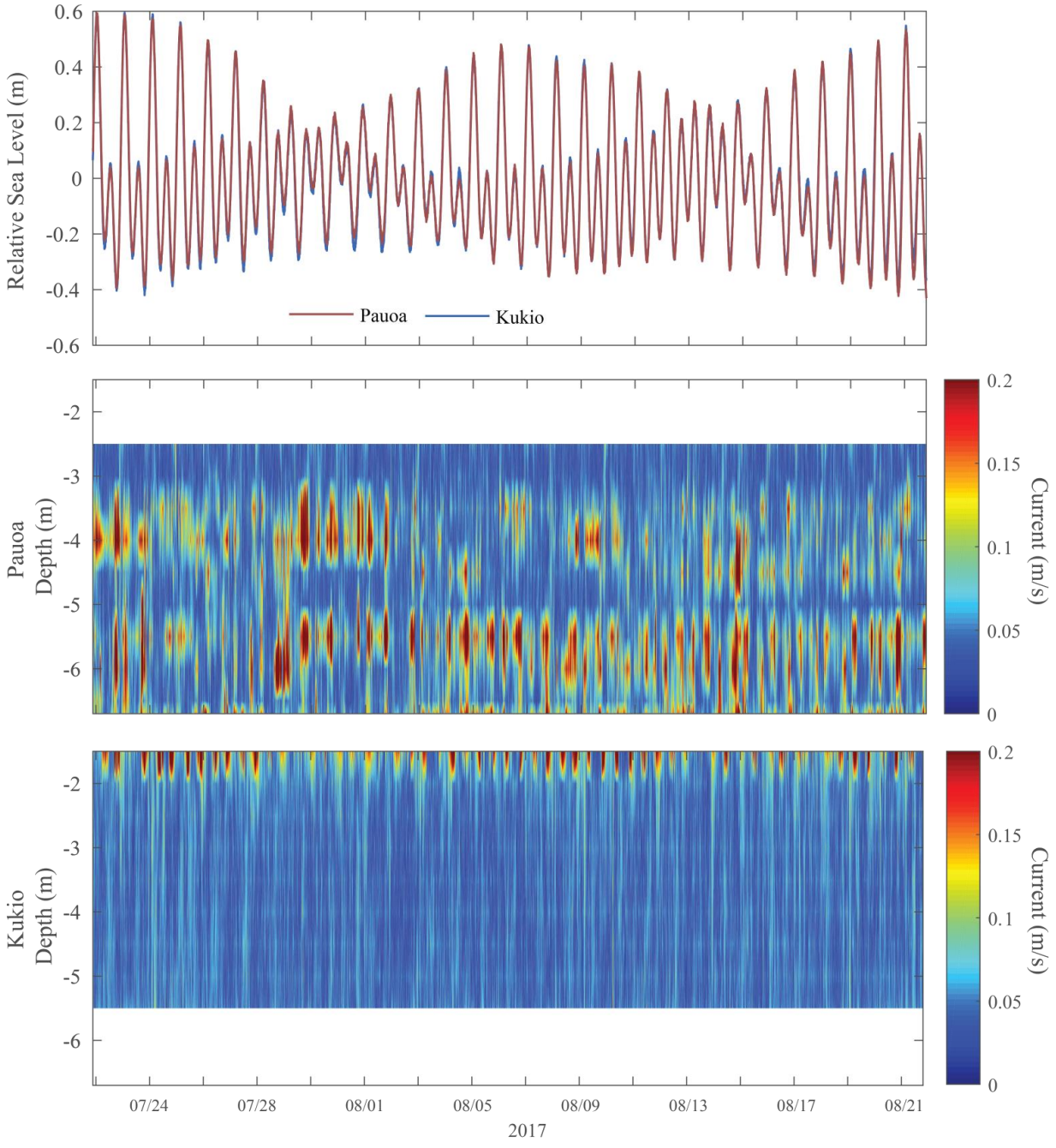

Figure 33. Relative sea level (m) measured from *in situ* ADPs deployed at Pauʻoa and Kūkiʻo in 7.3 and 6 m water depth, respectively. Water column current magnitude (m/s) from Pauʻoa (middle panel) and Kūkiʻo (bottom panel). In the middle and bottom panels, the y-axis represents depth from the surface. Note the differences in the depth range shown are attributed to differences in the depth of deployment and data acquisition.

5.0 Summary

The one site in West Hawai‘i that has received the greatest research attention to identify the sources of land-based inputs to coastal coral reefs is Puakō, where there is clear evidence that sewage is entering nearshore waters and that it is contributing to the degradation of coral condition (Couch et al. 2014a, Yoshioka et al. 2016, Abaya et al. 2018a,b). The research reported here was motivated in large part to examine the relationship between land-based inputs and reef condition in other areas within the West Hawai‘i Habitat Focus Area to determine what kind of effects other forms of coastal land use may have on nearshore waters and coral reefs. At the two resort developments studied here, there was no indication of sewage entering nearshore waters, but there were clear signals of elevated nutrient levels at the coast. While the extent, potential sources, and impacts of those elevated nutrients varied between the two areas, there were signs in both sites that nutrient inputs were associated with declines in coral recruitment and/or condition.

We shared our results with the resort managers at both Pau‘oa and Kūki‘o via a presentation and handouts summarizing key findings. As discussed above, these sites were selected in part because of the interest managers had in better understanding the condition of the waters and reefs they rely on, and a willingness to engage in conversations about potential changes to management actions to address any issues discovered. While the conversations initiated by the sharing of our results are still ongoing, it is hoped that providing this information will generate interest in collaboratively exploring options to continue to provide excellent experiences for resort visitors and improve the condition of the coastal waters and reefs so essential to the culture and economy of West Hawai‘i.

Below, please find a summary of our key findings:

- Excess coastal nutrient concentrations are most likely driven by coastal inputs, according to nutrient input models.
- Nutrient concentrations decreased from upland groundwater wells to the ocean and were higher in surface than benthic waters. Groundwater supplied nutrients to the bays, based on nutrient concentrations that increased with lower salinities.
- Shoreline and benthic $\delta^{15}N$ macroalgal tissue values at both developments were within the $\delta^{15}N$ range for high elevation groundwater, fertilized/kiawe soil, and ocean water NO_3^-.
- Pau'oa had consistently higher concentrations and greater ranges for $NO_2^- + NO_3^-$, NH_4^+, and H_4SiO_4 than those at Kūki‘o across most water types.
- A few anchialine pond and shoreline stations at Pau‘oa had $NO_2^- + NO_3^-$ and PO_4^{3-} concentrations that fell above the theoretical mixing line between ground and ocean water, which is suggestive of an external nutrient source to the

groundwater. The likely source is fertilizers as these stations were located either within or adjacent to the golf course and development landscaping.

- Groundwater reached the reef at both developments, with the majority of stations experiencing low salinity (< 33.5‰) events that lasted < 12 hours, and in some cases > 20 hours. Based on nitrate-salinity relationships, low salinity events resulted in the reefs being exposed to elevated nutrient concentrations, which could result in excess algal and bacterial growth.
- Tidal fluctuations are important for current variability, at both sites. However, current strength does not appear well correlated with the magnitude of tidal change, so clearly other forcings (e.g., wind) are contributing to currents at both of these locations. Currents at Kūkiʻo flows predominantly NE whereas it has no strong directionality at Pauʻoa.
- Benthic communities are likely influenced by a combination of nutrients and community factors. However, coral health, juvenile density and the amount of reef builders respond differently to these factors.
- In Pauʻoa, higher of Si concentration, which is a proxy for groundwater input, was among the strongest predictors with less healthy coral, more disease, higher coral-algal competition and less recovery potential (fewer coral juveniles) in areas with high groundwater input. Lower $\delta^{15}N$ values and higher NH_4^+ were also associated with areas with more coral algal competition, but more juveniles.
- In Kūkiʻo, the relative importance of nutrients and community factors was lower than Pauʻoa Bay, suggesting that much of the variability on Kūkiʻoʻs benthic communities is still unaccounted for. Regardless, similar to Pauʻoa, more healthy colonies with fewer Porites growth anomalies and direct coral-algal competition were found on reefs dominated by small colonies. The role of groundwater input is less clear in Kūkiʻo, with only algal overgrowth showing a decline as a function of groundwater input. Juvenile density was also higher in areas with lower $\delta^{15}N$ values.

7.0 Acknowledgements

This project could not have been completed without the assistance of many people. For assistance with field work and sample processing, we wish to thank University of Hawai‘i at Hilo graduate students Kailey Pascoe, Ashley Pugh, and Michael Fox, and undergraduate volunteers Tyler Gerken, Adel Sharif, Melia Takakusagi, Amy Olsen, Bryan Tonga, Kaikea Nakachi, Candice Miner-Ching (U‘i), Kainalu Steward, Kelsey Johnson-Sapp, Kevin Nolan, Romance Romero, Alexander Hernandez, Braysen Kainoa Libed, Madison Byers, Nicholas Galliani, Michele Peterson, and Kahoruko Kajiya. The support and excellent communication of Kūki‘o, Fairmont Orchid, and Hawai‘i Water Supply, Alaka‘i Nalu, and Outdoor Pursuits especially the following staff, were instrumental in our ability to conduct this work: Scott Nair, Paola Pagan, Jaisy Jardine, Ryan Priest, Jolene Hinds, Ka‘uhane Morton, Wil Suliban, Mewlan Seto, Trent Fischer, Daniel Dochin, Stephen Green, Ellen Frosch, and Kimber Deverse. Sampling at Uluweuweu was assisted by Jenny Kalmbach and greatly informed by the Ka‘ūpūlehu Marine Life Advisory Committee’s Conservation Action Planning Team, particularly Hannah Kihalani Springer, Leina‘ala Lightner, Ku‘ulei Keakealani, David Chai, Vern Yamanaka, Natalie Kurashima, Wayne Tanaka, Mike Nakachi, Ulalia Woodside, John Kahiapo, Cynthia Nazara, Kekaulike Tomich, Reggie Lee, Nahaku Kalei, Kirsten Fujitani, Pua‘ala Pascua, Bradd Stubbs, Kalisi Mausio, Kalani Quiocho, Annick Cros, Cecile Walsh, and Emily Fielding. Sampling at Pau‘oa was assisted by Bill Ferreira (Mauna Lani) and informed by the Puakō Community Association and research conducted by Kona’s Division of Aquatic Resources and the University of Hawai‘i at Hilo in conjunction with the good-will demonstrated by the Fairmont Orchid Resort. We would also like to acknowledge the additional support provided by UH Hilo Marine Science Department, UH Hilo Analytical Laboratory (https://hilo.hawaii.edu/~analab/), and several UH Hilo internship programs: PIPES (https://hilo.hawaii.edu/uhintern/), SHARP (http://www.uhhilo-sharp.org/), and NSF EPSCoR Ike Wai (https://www.hawaii.edu/epscor).

8.0 References

Abaya LM, Wiegner TN, Colbert SL, Beets J, Carlson KM, Kramer KL, Most R, Couch C. (2018a) A multi-indicator approach for identifying shoreline sewage pollution hotspots adjacent to coral reefs. Mar Pollut Bull 129(1):70-80.

Abaya LM, Wiegner TN, Beets JP, Colbert SL, Carlson KM, Kramer KL (2018b) Spatial distribution of sewage pollution on a Hawaiian coral reef. Mar Pollut Bull 31:130:335-47.

Bauer GR (2003) A study of the ground-water conditions in North and South Kona and South Kohala districts, Island of Hawai‘i, 1991-2002. Department of Land and Natural Resources, Commission on Water Resource Management.

Beaulac, Michael N, & Reckhow, Kenneth H. (1982). An examination of land use: nutrient export relationships. *Journal of the American Water Resources Association, 18*(6), 1013-1024.

Beijbom, O., Edmunds, P. J., Roelfsema, C., Smith, J., Kline, D. I., Neal, B. P., et al. (2015). Towards automated annotation of benthic survey images: Variability of human experts and operational modes of automation. PLoS One 10, 1–22. doi:10.1371/journal.pone.0130312.

Cesar HS, van Beukering P (2004) Economic valuation of the coral reefs of Hawai'i. Pac Sci 58(2):231-42

Clark JRK (2002) Kūki‘o. Hawai‘i place names shores, beaches, and surf developments

Cobo, Juan Guillermo, Dercon, Gerd, & Cadisch, Georg. (2010). Nutrient balances in African land use systems across different spatial scales: a review of approaches, challenges and progress. Agriculture, ecosystems & environment, 136(1), 1-15.

Coplen, T.B., Haiping, Q., Kinga, R., Casciotti, K., Hannon, J.E., 2012. Determination of the □15N and □18O of nitrate in water; RSIL lab code 2900, chap. 17 of Stable isotope-ratio methods, sec. C of Revesz, Kinga, and Coplen, T.B. eds, Methods of the Reston Stable Isotope Laboratory; U.S. Geologic Survey Techniques and Methods, book 10, 35 p.

Couch CS, Most R, Wiggins C, Minton D, Conklin E, Sziklay J, Amimoto R, Pollock K, Caldwell Z (2014a) Understanding the consequences of land-based pollutants on coral health in South Kohala. Final Report to Hawai‘i Division of Aquatic Resources

Couch, CS, Garriques, JD, Barnett, C, Preskitt, L, Cotton, S, Giddens, J, & Walsh, W. (2014b). Spatial and temporal patterns of coral health and disease along leeward Hawai’i Island. Coral Reefs, 33(3), 693-704.

Dailer, M. L., Glenn, C. R., & Smith, C. (2011). Preventing the introduction and spread of nutrient driven invasive algal blooms and coral reef degradation in West Hawai`i (pp. 24).

Delevaux JM, Whittier R, Stamoulis KA, Bremer LL, Jupiter S, Friedlander AM, Poti M, Guannel G, Kurashima N, Winter KB, Toonen R, Conklin E, Wiggins C, Knudby A, Goodel W, Burnett K, Yee S, Htun H, Oleson KLL, Wiegner T, Ticktin T (2018) A linked land-sea modeling framework to inform ridge-to-reef management in high oceanic islands. PloS one 13(3):e0193230

Derse E, Knee KL, Wankel SD, Kendall C, Berg Carl J, Paytan A (2007) Identifying sources of nitrogen to Hanalei Bay, Kauai, utilizing the nitrogen isotope signature of macroalgae. Environ Sci Technol 41: 5217-5223

de Smith MJ, Goodchild MF, Longley PA (2009) Geospatial analysis: A comprehensive guide to principles, techniques and software tools, 3rd ed.. Troubador Ltd., Leicester, UK.

Dollar SJ, Atkinson MJ (1992) Effects of nutrient subsidies from groundwater to nearshore marine ecosystem off the Island of Hawai‘i. Estuar Coast Shelf Sci 35: 409-424

Dudley BD, Hughes RF, Ostertag R (2014) Groundwater availability mediates the ecosystem effects of an invasion of Prosopis pallida. Ecol Appl 24(8):1954-71

Fletcher CH, Grossman EE, Richmond BM, Gibbs AE (2002) Atlas of natural hazards in the Hawaiian coastal zone. United States Geological Survey Report No. 2761

Friedlander A, Aeby G, Brainard R, Brown E, Chaston K, Clark A, McGowan P, Montgomery T, Walsh W, Williams I, Wiltse W (2008) The state of coral reef ecosystems of the main Hawaiian Islands. pp. 222-269. In: Waddell, J. and A.M. Clarke (eds.), The State of Coral Reef Ecosystems of the United States and Pacific Freely Associated States. NOAA Technical Memorandum NOS NCCOS 73. NOAA/NCCS Center for Coastal Monitoring and Assessment’s Biogeography Team. Silver Springs, MD. 569 pp.

Fujita RM (1985) The role of nitrogen status in regulating transient ammonium uptake and nitrogen storage by macroalgae. J Exp Mar Biol Ecol 92:283-301

Giambelluca, Thomas W, Chen, Qi, Frazier, Abby G, Price, Jonathan P, Chen, Yi-Leng, Chu, Pao-Shin, . . . Delparte, Donna M. (2013). Online rainfall atlas of Hawai'i. Bulletin of the American Meteorological Society, 94(3), 313-316.

Glenn CR, Whittier RB, Dailer ML, Dulaiova H, El-Kadi AI, Fackrell J, Kelly JL, Waters CA, Sevadjian J (2013) Lahina groundwater tracer study, Lahaina, Maui. Final report to HDOH, USEPA, and US Army Engineer and Research Development Center

Gombos M, Komoto J, Lowery K, MacGowen (2010) The State of Hawai‘i. Hawai‘i coral reef strategy in the main Hawaiian Islands. 2010-2020. Honolulu, HI

HDAR (Hawai‘i Division of Aquatic Resources) (2013) South Kohala reefs are in dire straits. Public handout.

HDOH (Hawai‘i Department of Health) (2014) Amendment and compilation of chapter 11-54 Hawai‘i administrative rules

Hunt CD (2006) Ground-water nutrient flux to coastal waters and numerical simulation of wastewater injection at Kihei, Maui, Hawai‘i . USGS Scientific Investigations Report 2006-5283

Hunt CD, Rosa SN (2009) A multi tracer approach to detect wastewater plumes from municipal injection wells in nearshore marine waters in Kihei and Lahaina, Maui, Hawai‘i . USGS Scientific Investigations Report 2009-5253

Kay EA, Lau LS, Stroup ED, Dollar SJ, Fellows DP, Young RHF (1977) Hydrologic and ecologic inventories of the coastal waters of west Hawai‘i. Technical Report 105. Sea Grant Cooperative Report. UNIHI-SEA-GRANT-CR-77-02

Knee K, Street JH, Grossman EG, Paytan A (2010) Nutrient inputs to the coastal ocean from submarine groundwater discharge in a groundwater-dominated system:

Relation to land use (Kona coast, Hawai‘i, U.S.A.). Limnol Oceanogr 55:1105–1122
Johnes, P. J. (1996). Evaluation and management of the impact of land use change on the nitrogen and phosphorus load delivered to surface waters: The export coefficient modelling approach. Journal of Hydrology, 183(3-4). doi: 10.1016/0022-1694(95)02951-6
Johnson, Adam G. (2008). Groundwater discharge from the leeward half of the Big Island, Hawaii. Masters in Science Thesis, University of Hawai ‘i.
Kwong, Kfnk, Bholah, A., Volcy, L., & Pynee, K. (2002). Nitrogen and phosphorus transport by surface runoff from a silty clay loam soil under sugarcane in the humid tropical environment of Mauritius. Agriculture Ecosystems & Environment, 91(1-3), 147-157.
Lau LS, Mink JF (2006) Hydrology of the Hawaiian Islands. University of Hawai‘i Press, Honolulu, HI
Lin, Jeff P. (2004). Review of published export coefficient and event mean concentration (EMC) data. (ERDC-TN-WRAP-04-3). Vicksburg, MS: Engineer Research and Development Center.
Line, Daniel E, White, Nancy M, Osmond, Deanna L, Jennings, Gregory D, & Mojonnier, Carolyn B. (2002). Pollutant export from various land uses in the Upper Neuse River Basin. Water Environment Research, 74(1), 100-108.
Ling, Ge, & El-Kadi, Aly I. (1998). A lumped parameter model for nitrogen transformation in the unsaturated zone. Water Resources Research, 34(2), 203-212.
Maciolek JA, Brock RE (1974) Aquatic survey of the Kona coast ponds, Hawai‘i Island. Sea Grant Advisory Report, UNIHI-SEAGRANT-AR-74-04. 73 pp.
Markewitz, Daniel, Davidson, Eric, Moutinho, Paulo, & Nepstad, Daniel. (2004). Nutrient loss and redistribution after forest clearing on a highly weathered soil in Amazonia. Ecological Applications, 14(sp4), 177-199.
Maynard, Jeffrey, Conklin, Eric, Minton, Dwayne, Most, Rebecca, Couch, Courtney S, Williams, Gareth J, . . . Walsh, William Arthur. (2016). Relative resilience potential and bleaching severity in the West Hawai'i Habitat Focus Area in 2015.
Minton, D., Conklin, E., Weiant, P., and Wiggins, C. (2012). 40 Years of Decline on Puako’s Coral Reefs: A review of Historical and Current Data (1970-2010), The Nature Conservancy. 140pp.
Ochoa-Izaguirre MJ, Soto-Jiménez MF (2015) Variability in nitrogen stable isotope ratios of macroalgae: consequences for the identification of nitrogen sources. J Phycol 51(1): 46-65
Officer CB (1979) Discussion of the behaviour of nonconservative dissolved constituents in estuaries. Estuar Coast Mar Sci 9(1):91- 4
Oki, Delwyn S. (1999). Geohydrology and numerical simulation of the ground-water flow system of Kona, island of Hawaii: Geological Survey (US).
Oki DS, Tribble GW, Sourza WR, Bolke EL (1999). Groundwater resources in Kaloko-Honokohau National Historic Park, Island of Hawai‘i, and numerical simulations of the effect of groundwater withdrawls. USGS Water-Resources Investigations Report 99-4070

Parnell A, Inger CR, Bearhop S, Jackson AL (2010) Source partitioning using stable isotopes: coping with too much variation. PLoS ONE 5, e9672

Peterson, R. N., Burnett, W. C., Glenn, C. R., & Johnson, A. G. (2009). Quantification of point-source groundwater discharges to the ocean from the shoreline of the Big Island, Hawaii. Limnology and Oceanography, 54(3), 890-904. doi: 10.4319/lo.2009.54.3.0890

Phillips, Brandt, Reddick & Associates (Hawai‘i) Inc. (1986) Final environmental impact statement, Kūki‘o Beach Development. http://oeqc2.doh.hawaii.gov/EA_EIS_Archive/1986-05-DD-HA-FEIS-Kukio-Beach-Development.pdf

Rodgers KS, Jokiel PL, Brown EK, Hau S, Sparks R (2015) Over a decade of change in spatial and temporal dynamics of Hawaiian coral reef communities. Pac Sci: 69(1):1–13

Rubin K, Doo B (2004) Hualālai Volcano. Hawai‘i Center for Volcanology webdevelopment. http://www.soest.hawaii.edu/GG/HCV/hualalai.html

Sharp JH, Carlson CA, Peltzer ET, Castle-Ward DM, Savidge KB, Rinker KR (2002) Final dissolved organic carbon broad community intercalibration and preliminary use of DOC reference materials. Mar Chem 77(4):239-53

Sharp, R. , Tallis, H.T., Ricketts, T, Guerry, A.D., Wood, S.A., Chaplin-Kramer, R, . . . Bierbower, W. . (2015). InVEST 3.2 User's Guide. The Natural Capital Project: Stanford University, University of Minnesota, The Nature Conservancy, and World Wildlife Fund.

Smith CM, Smith JE (2006) Algal blooms in North Kihei: An assessment of patterns and processes relating nutrient dynamics to algal abundance. City and County of Maui Report.

Smith JE, Runcie JW, Smith CM (2005) Characterization of a large-scale ephemeral bloom of the green alga Cladophora sericea on the coral reefs of West Maui, Hawai’i. Mar Ecol Prog Ser 302:77-91

Smith, J. E., Brainard, R., Carter, A., Grillo, S., Edwards, C., Harris, J., ... & Vroom, P. S. (2016). Re-evaluating the health of coral reef communities: baselines and evidence for human impacts across the central Pacific. Proc. R. Soc. B, 283(1822), 20151985.

Stearns, Harold T, & Macdonald, Gordon A. (1946). Geology and ground-water resources of the island of Hawaii: Honolulu Advertising.

Street, Joseph H, Knee, Karen L, Grossman, Eric E, & Paytan, Adina. (2008). Submarine groundwater discharge and nutrient addition to the coastal zone and coral reefs of leeward Hawai'i. Marine Chemistry, 109(3), 355-376.

Swart PK, Evans S, Capo T, Altabet MA (2014) The fractionation of nitrogen and oxygen isotopes in macroalgae during the assimilation of nitrate. Biogeosciences 11:6147–6157

USEPA (2017) Nutrient pollution. Sources and solutions. https://www.epa.gov/nutrientpollution/sources-and-solutions

van Beukering P, Cesar HS (2004) Ecological economic modeling of coral reefs: Evaluating tourist overuse at Hanauma Bay and algae blooms at the Kihei Coast, Hawai'i. Pac Sci 58(2):243-60

Pacific Island Benthic Habitat Mapping Center (2018) West Hawai‘i dominate substrate – 5 meter grid. http://www.soest.hawaii.edu/pibhmc/cms/data-by-development/main-hawaiian-islands/hawaii-big-island/hawaii-habitat/

Wiegner TN, Mokiao-Lee AU, Johnson EE (2016) Identifying nitrogen sources to thermal tide pools in Kapoho, Hawai'i, U.S.A, using a multi-stable isotope approach. Mar Pollut Bull 103:63–71

Yoshioka R, Kim CJS, Tracey A, Most R, Harvell CD (2016) Linking sewage pollution and water quality to spatial patterns of Porites lobata growth anomalies in Puakō, Hawai‘i. Mar Pollut Bull 104:313-321

Young, William J, Marston, Frances M, & Davis, Richard J. (1996). Nutrient exports and land use in Australian catchments. Journal of Environmental Management, 47(2), 165-183.

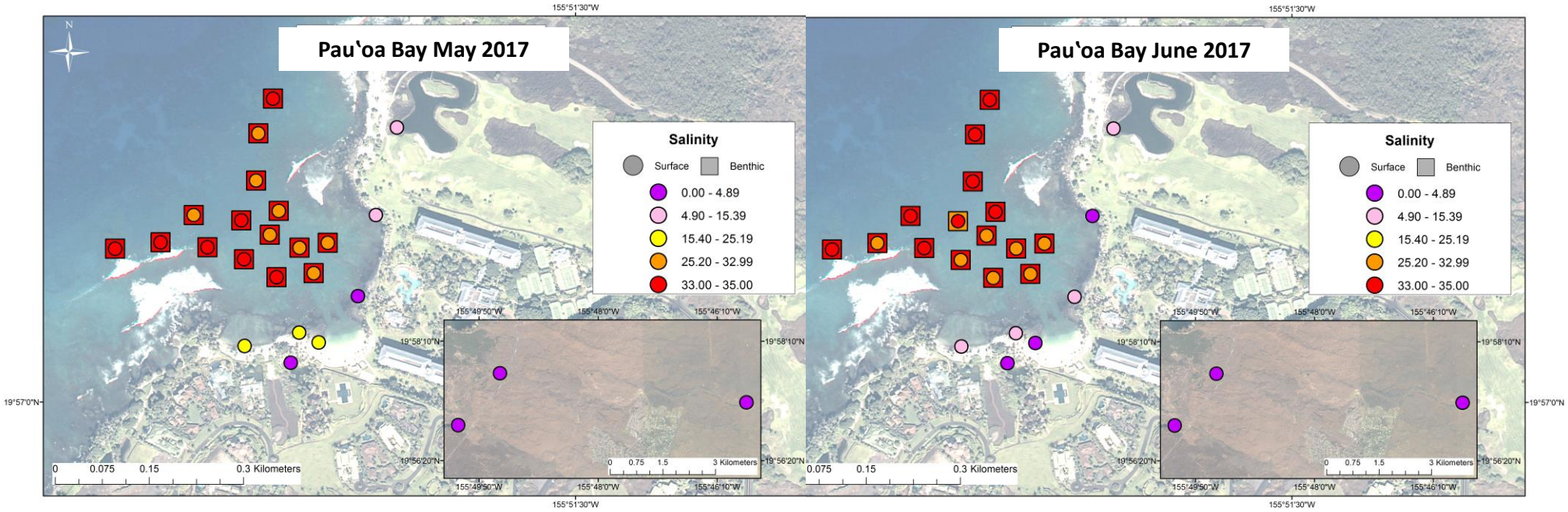

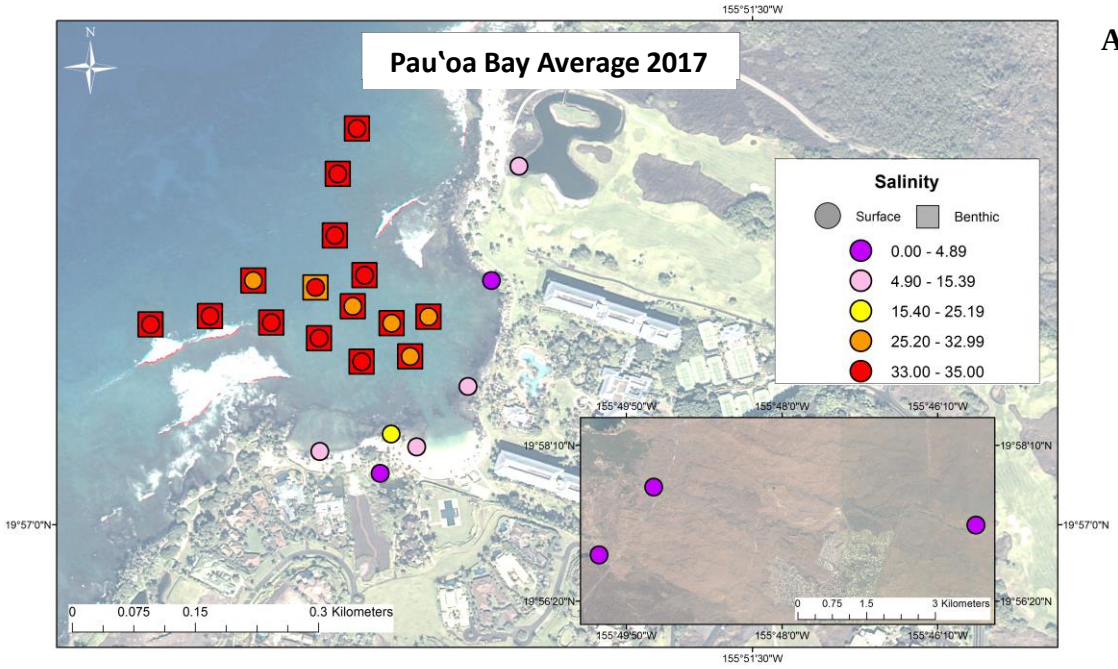

Appendix 1. Salinity concentration maps for Pauʻoa Bay, Hawaiʻi.

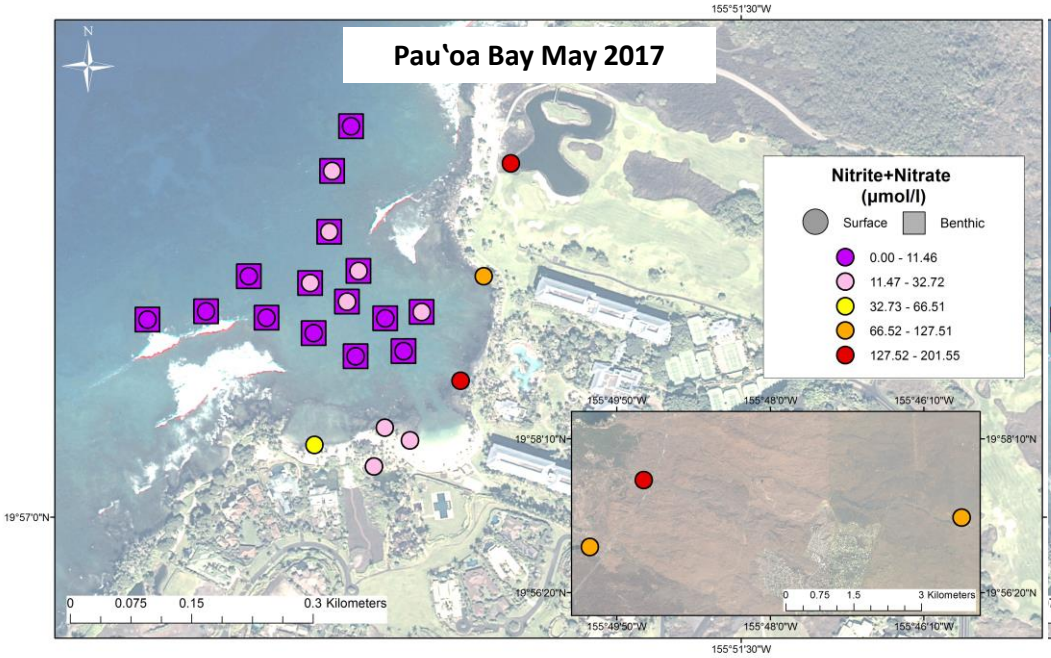

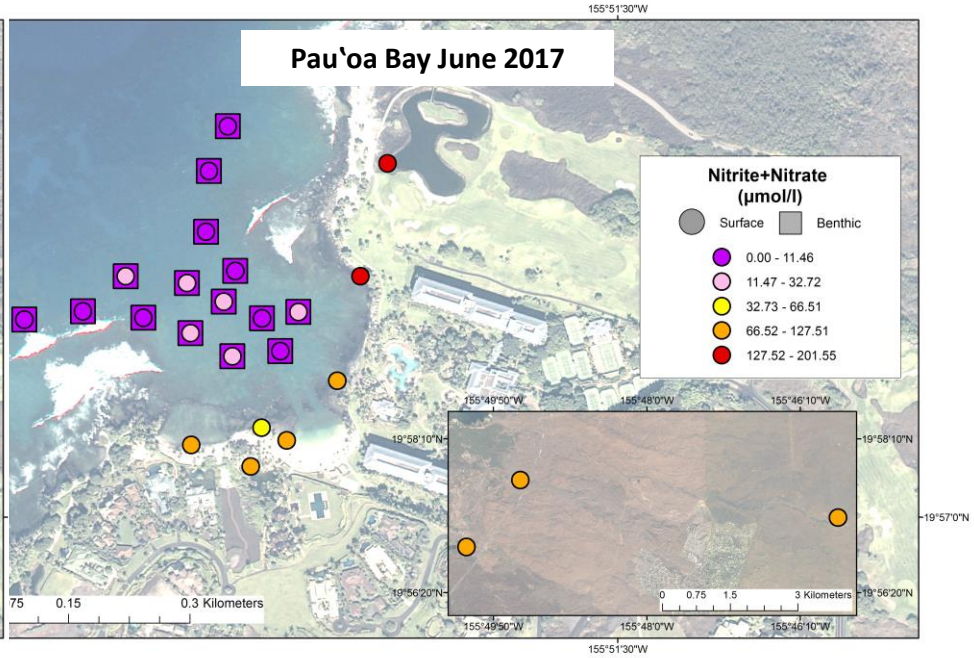

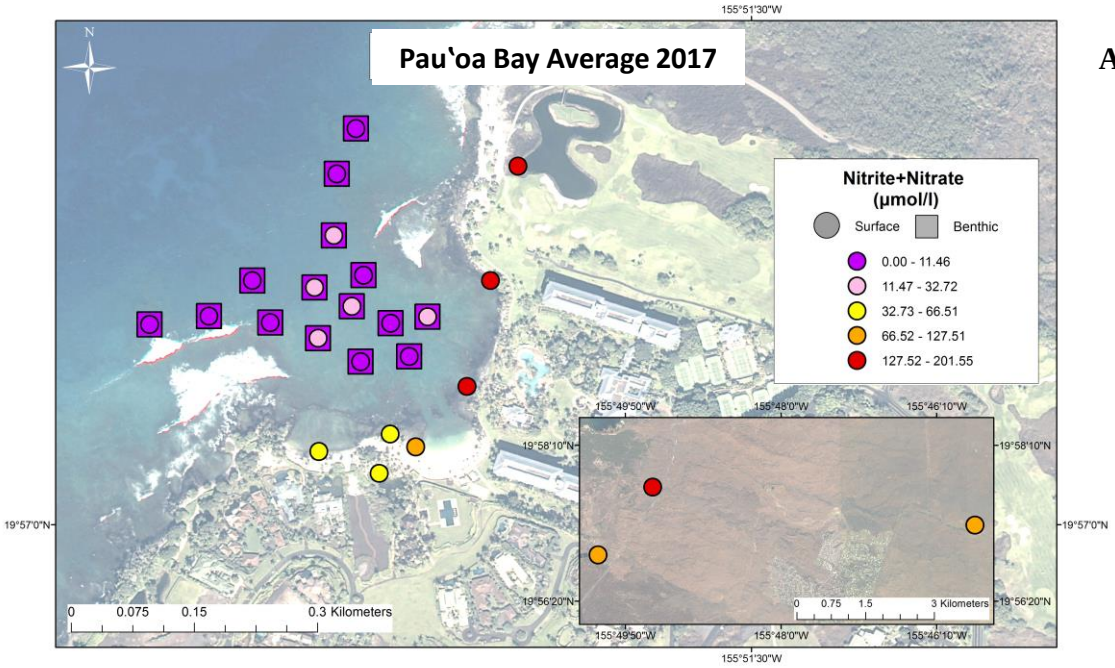

Appendix 2. NO_3^- +NO_2^- concentration maps for Pauʻoa Bay, Hawaiʻi.

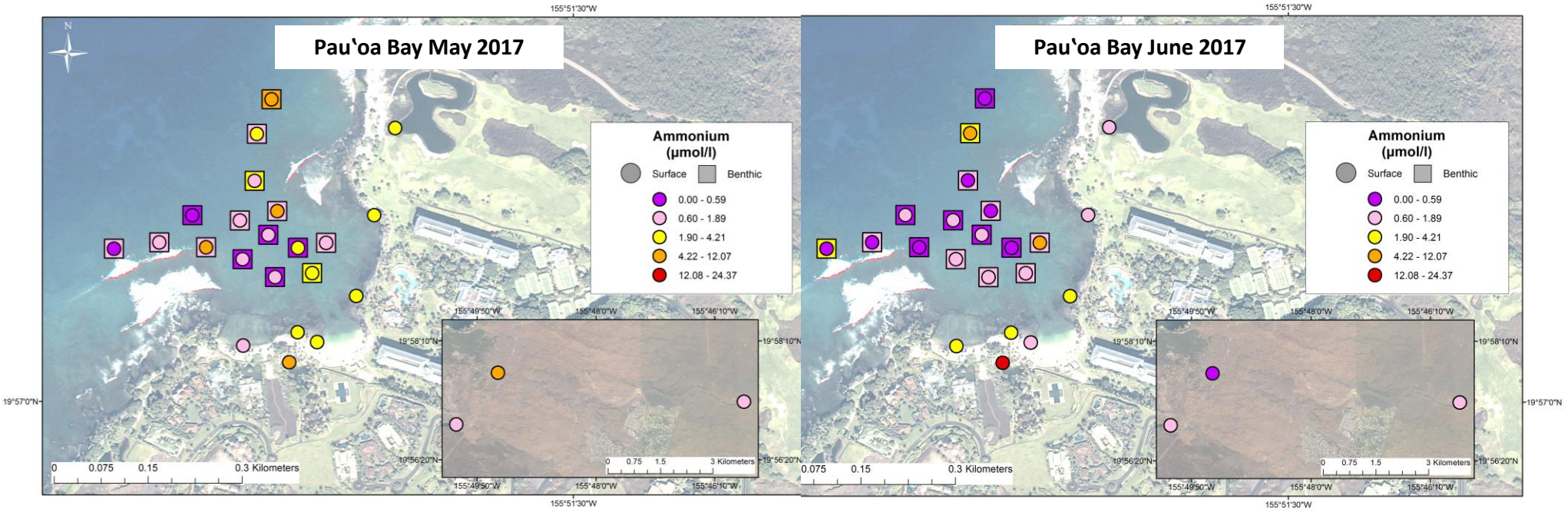

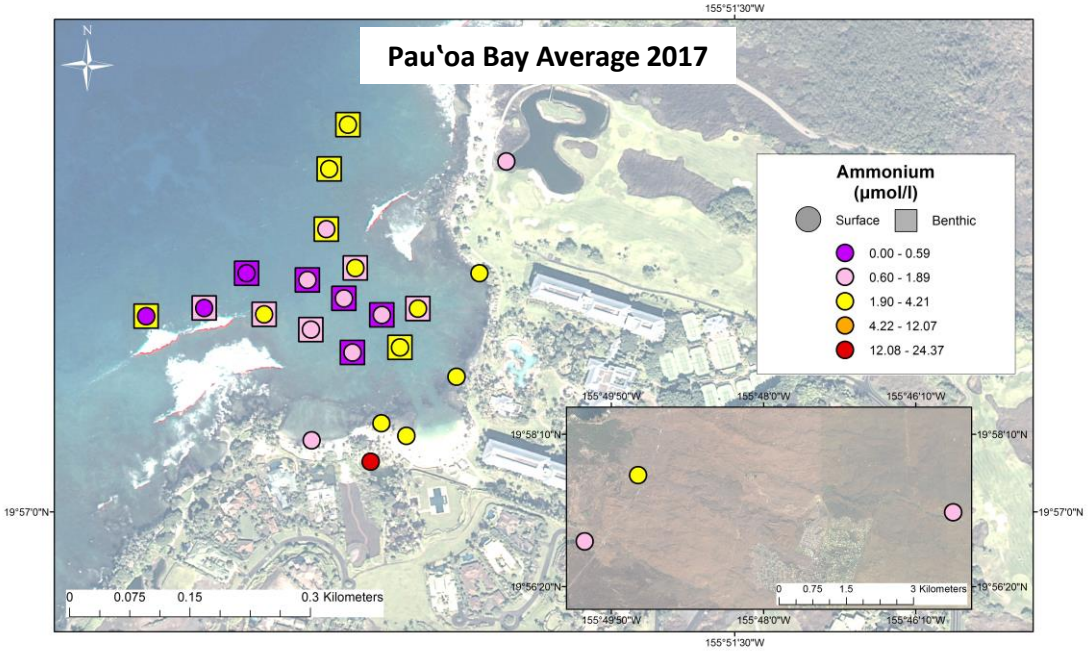

Appendix 3. NH_4^+ concentration maps for Pauʻoa Bay, Hawaiʻi.

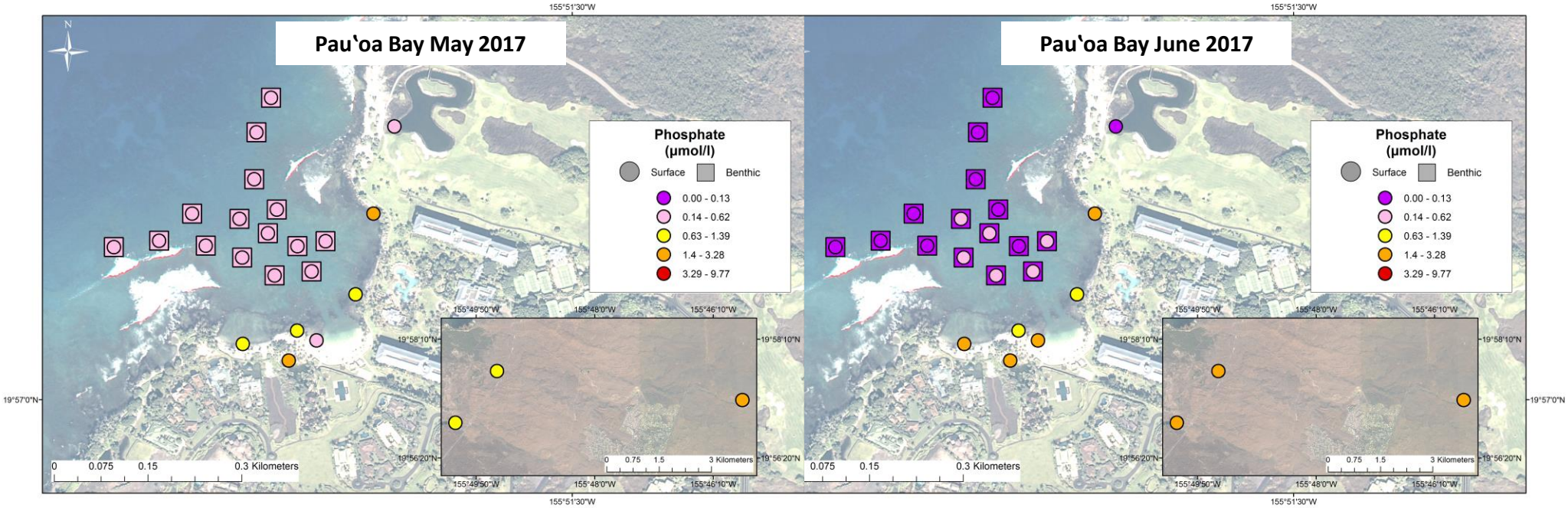

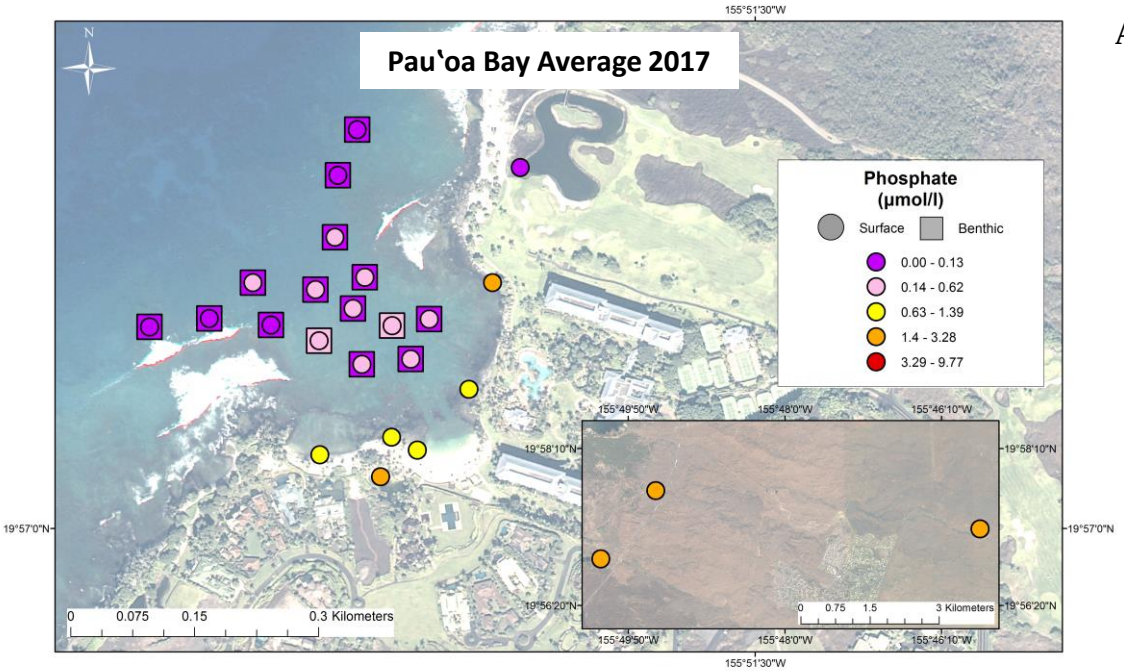

Appendix 4. PO_4^{3-} concentration maps for Pauʻoa Bay, Hawaiʻi.

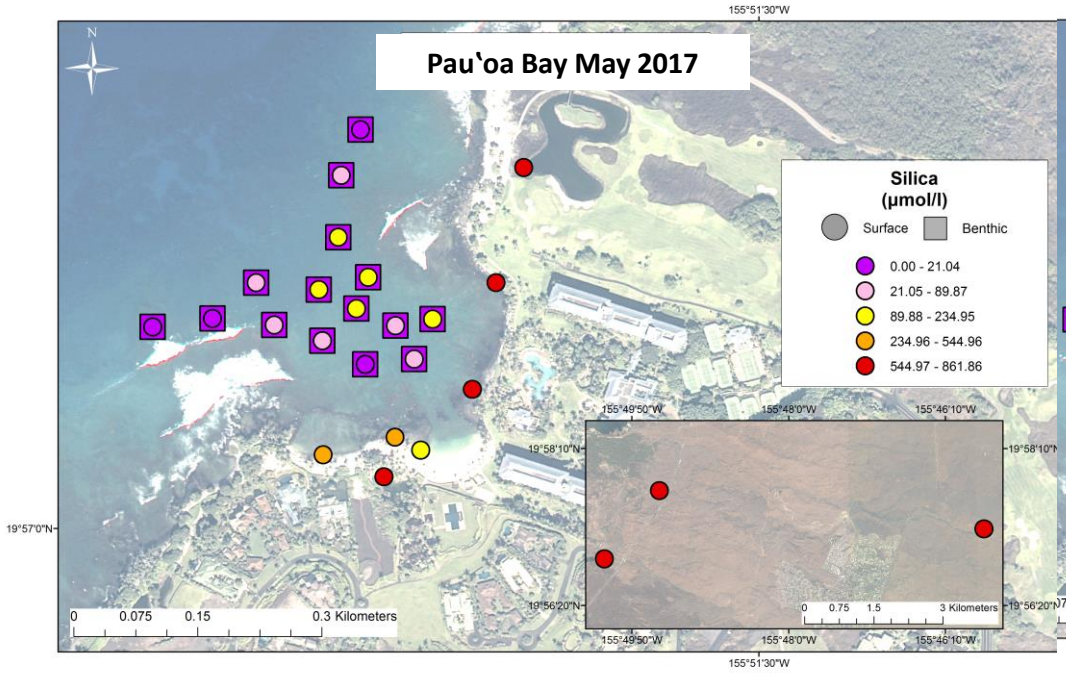

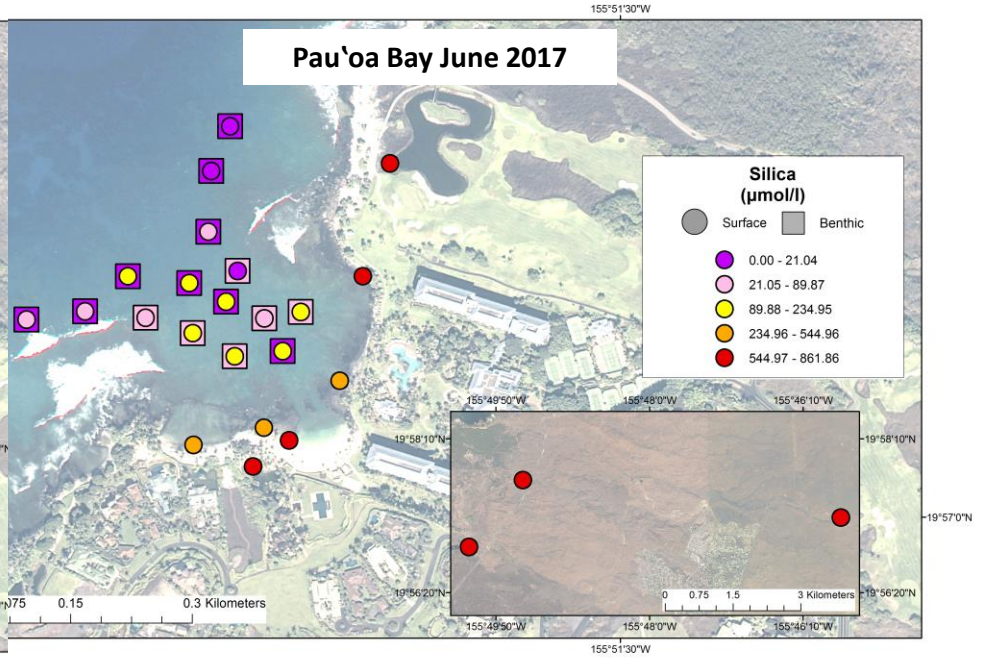

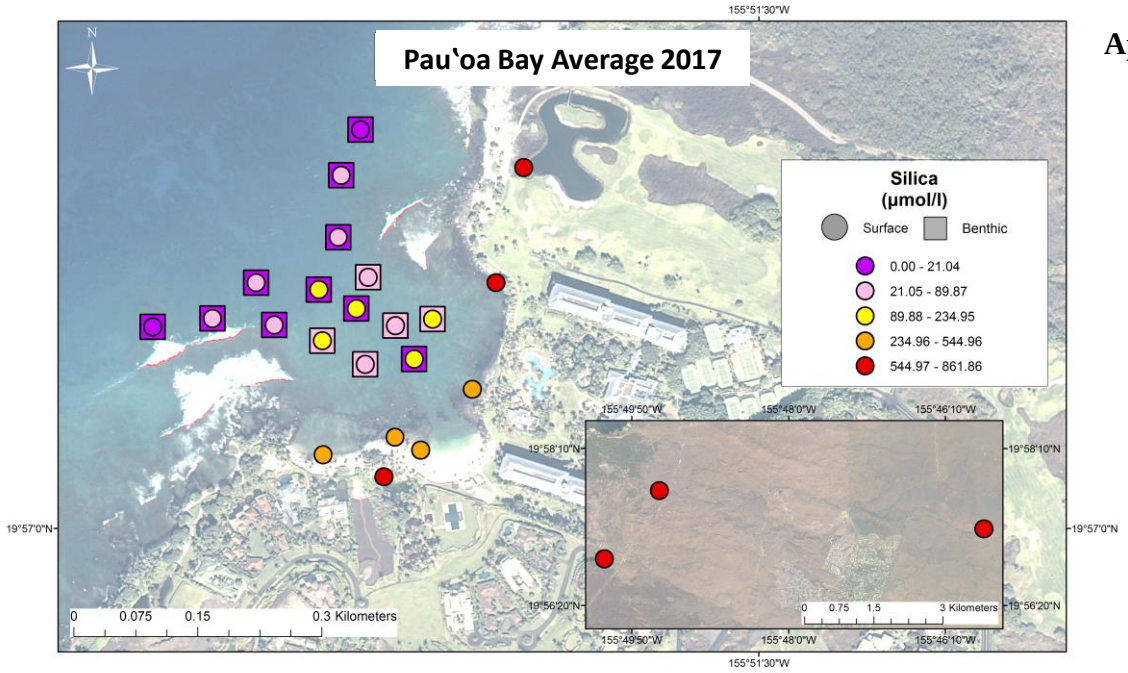

Appendix 5. H_4SiO_4 concentration maps for Pauʻoa Bay, Hawaiʻi.

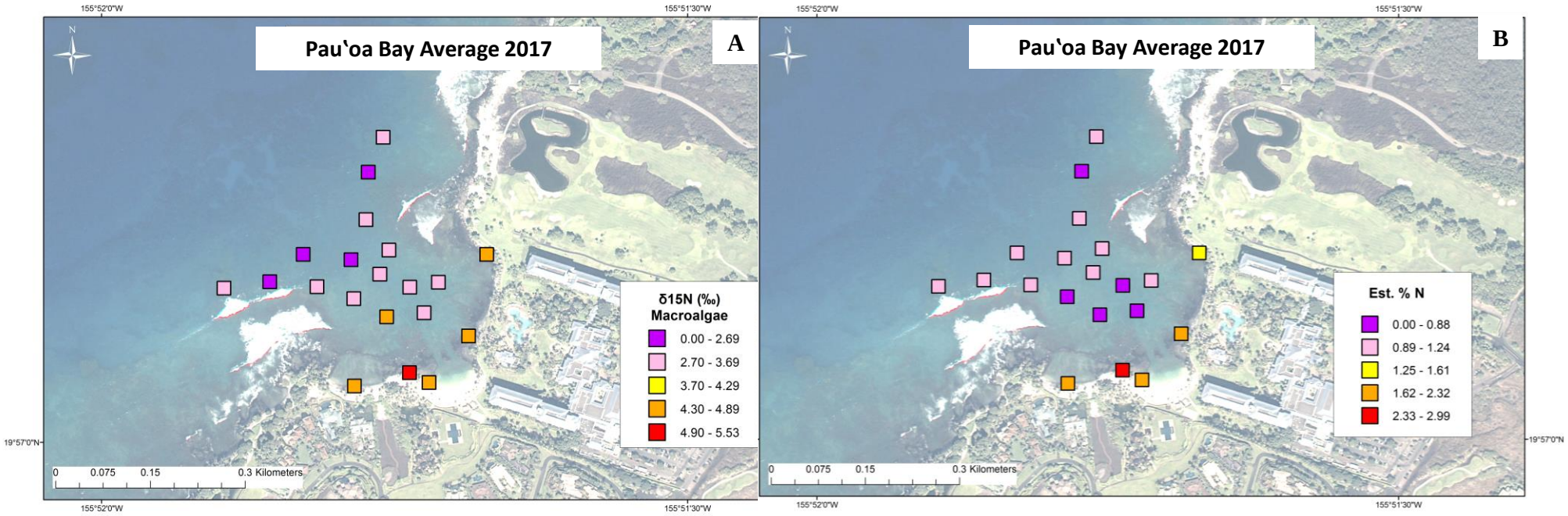

Appendix 6. Average $\delta^{15}N$ (A) and %N (B) macroalgae tissue maps for Pauʻoa Bay, Hawaiʻi.

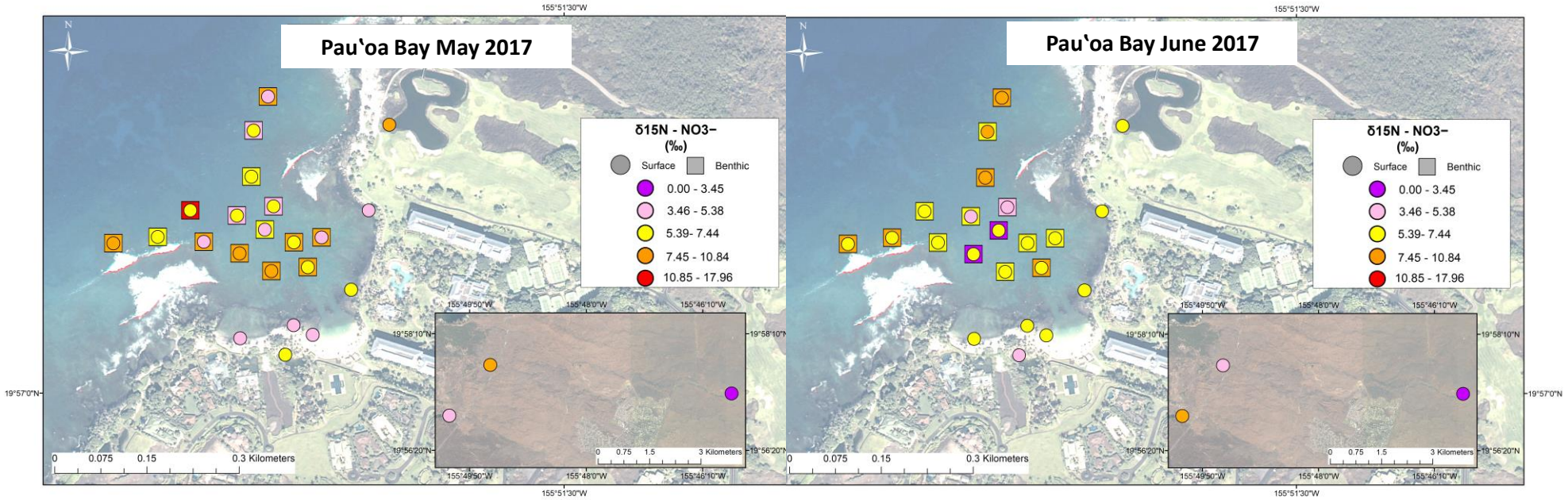

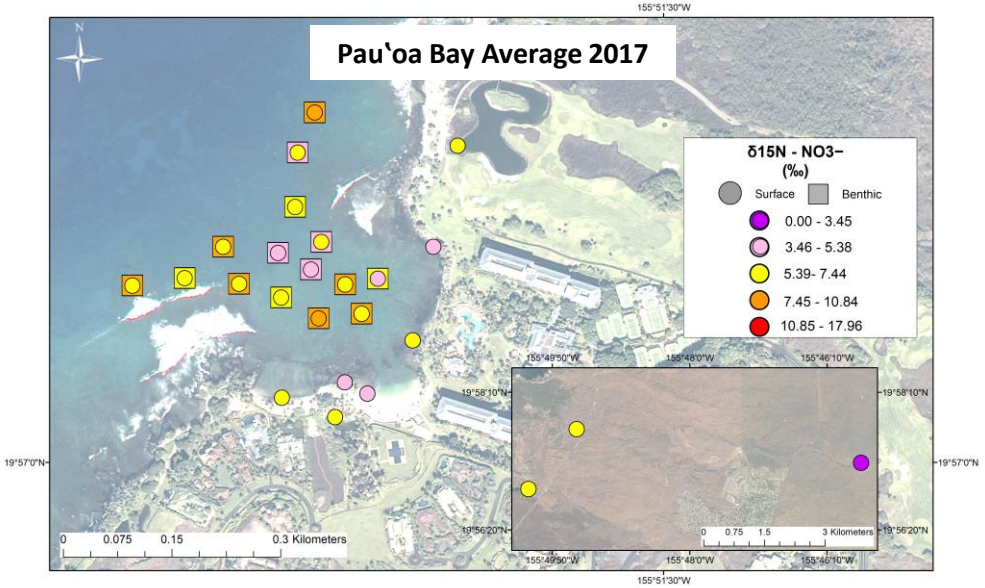

Appendix 7. $\delta^{15}N\text{-}NO_3^-$ concentration maps for Pauʻoa Bay, Hawaiʻi.

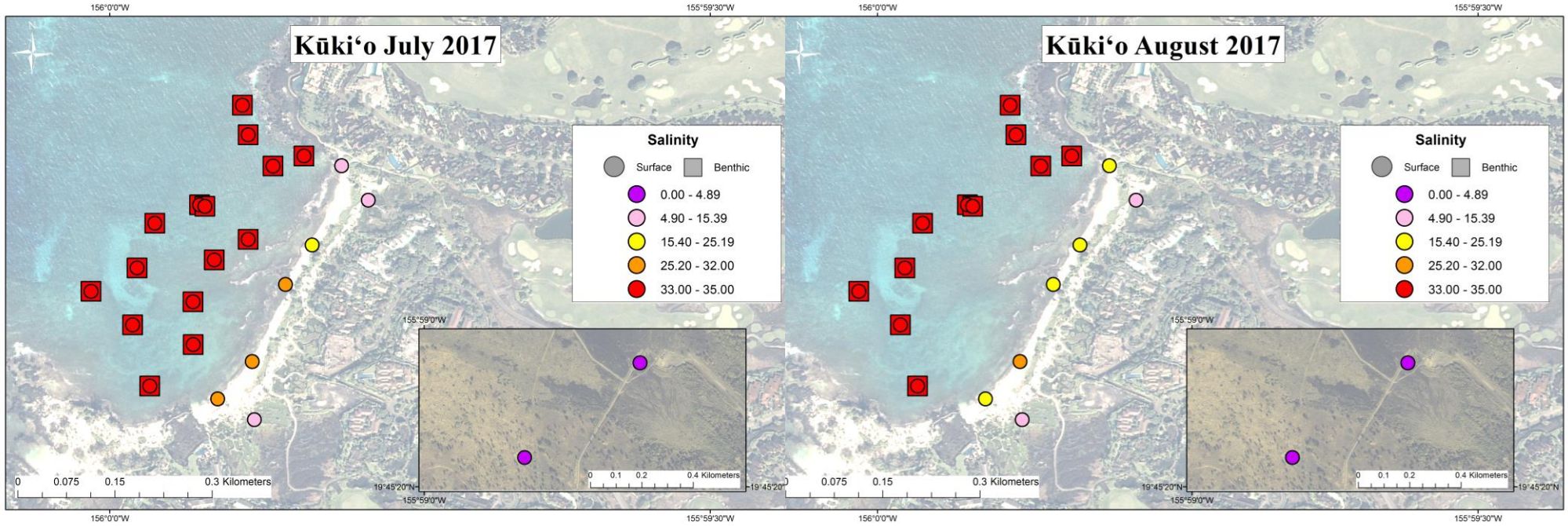

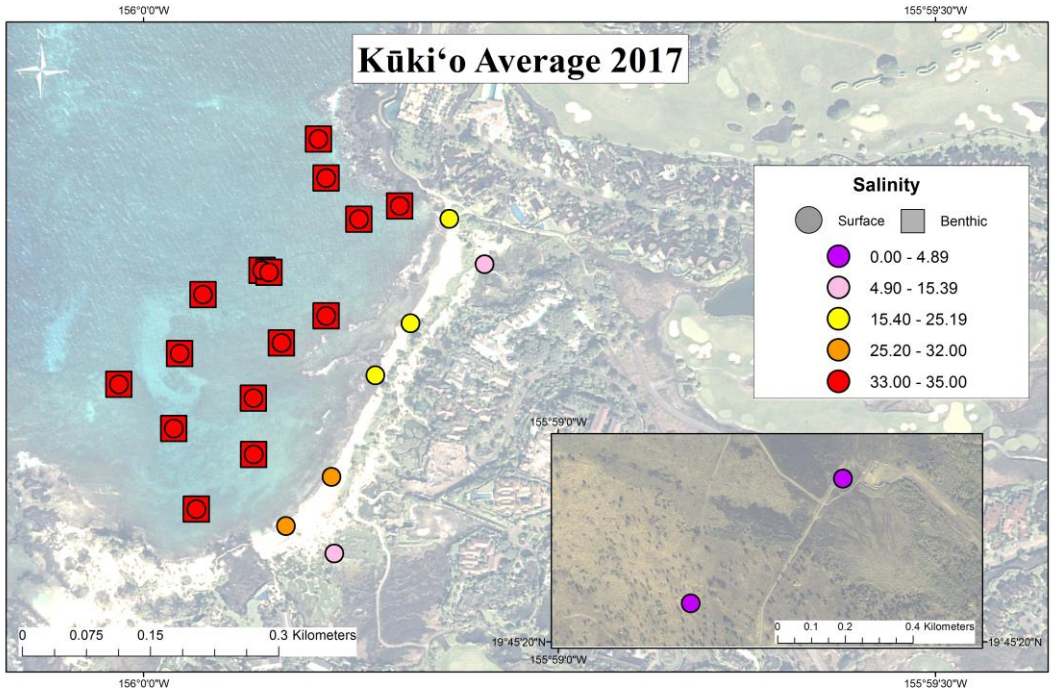

Appendix 8. Salinity maps for Kūkiʻo Bay, Hawaiʻi.

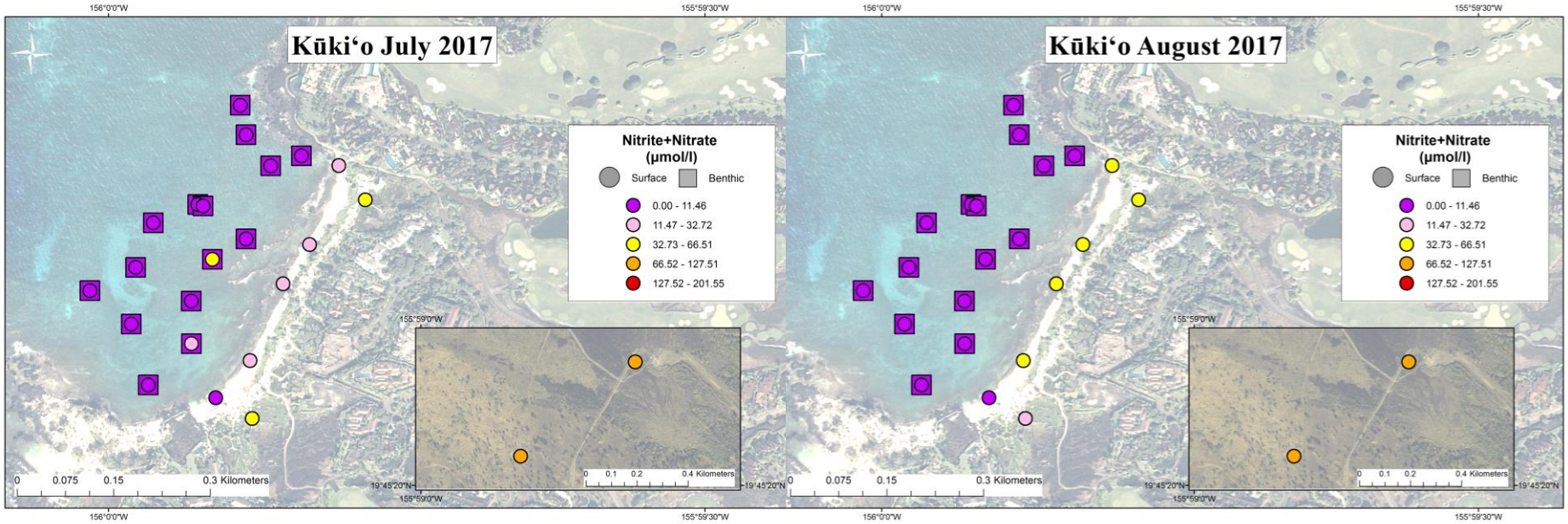

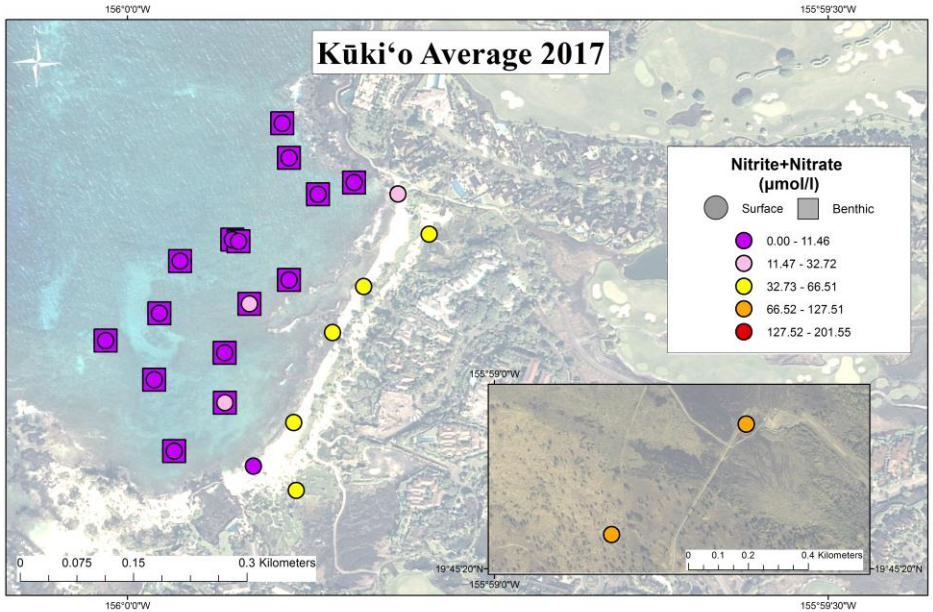

Appendix 9. NO_3^-+NO_2^- maps for Kūkiʻo Bay, Hawaiʻi.

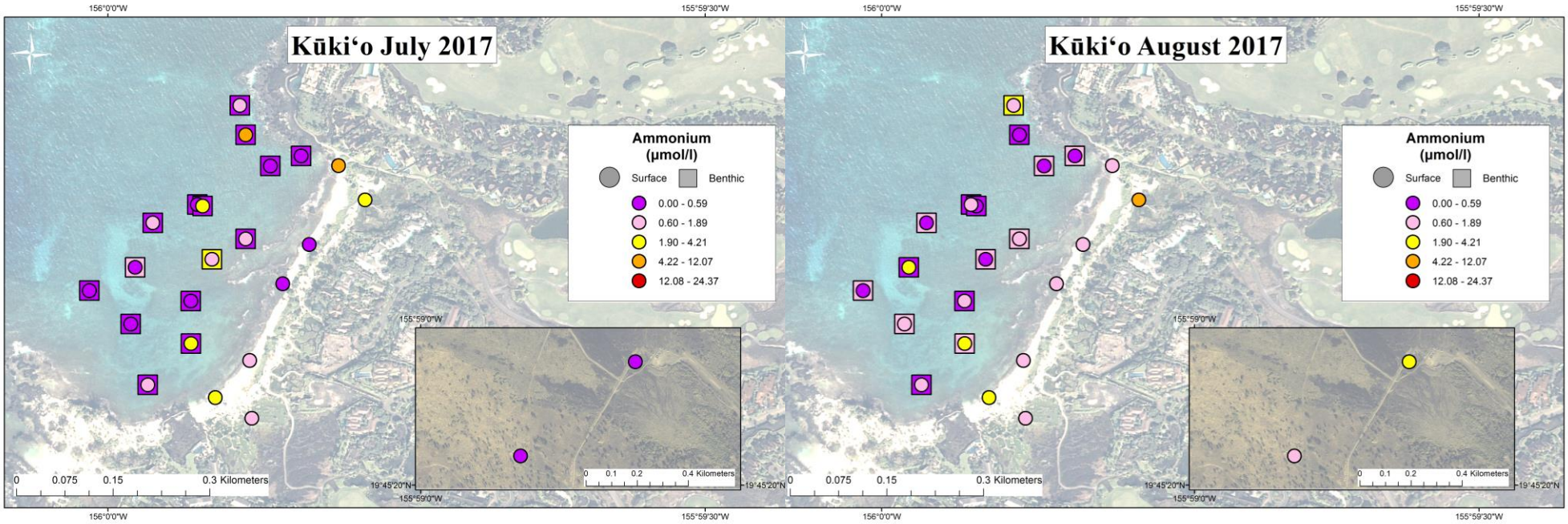

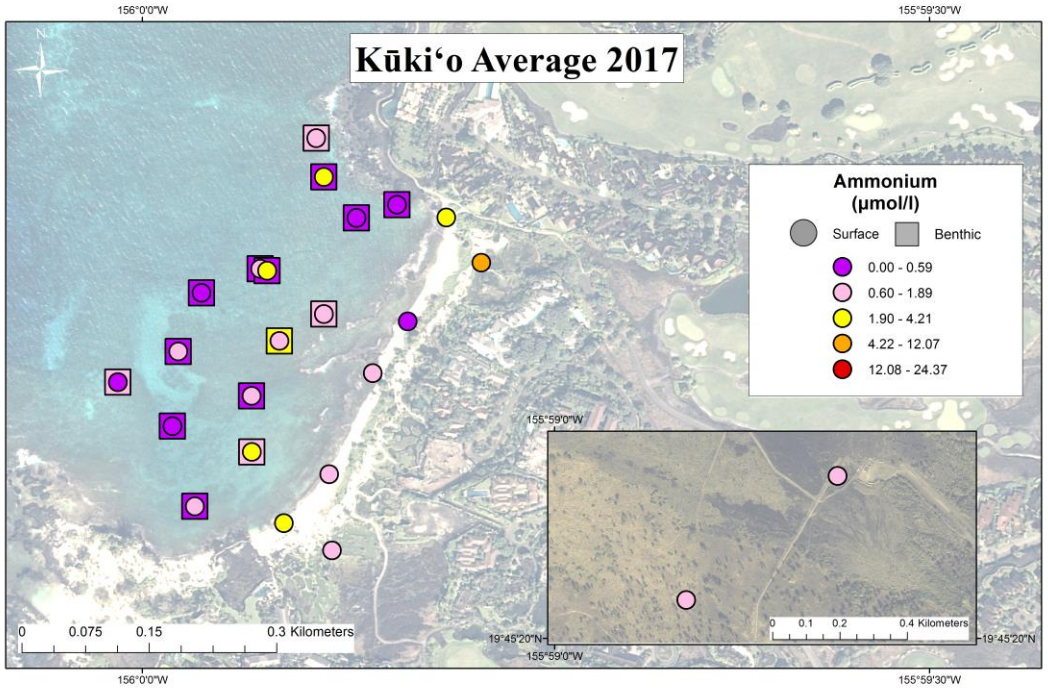

Appendix 10. NH_4^+ maps for Kūkiʻo Bay, Hawaiʻi.

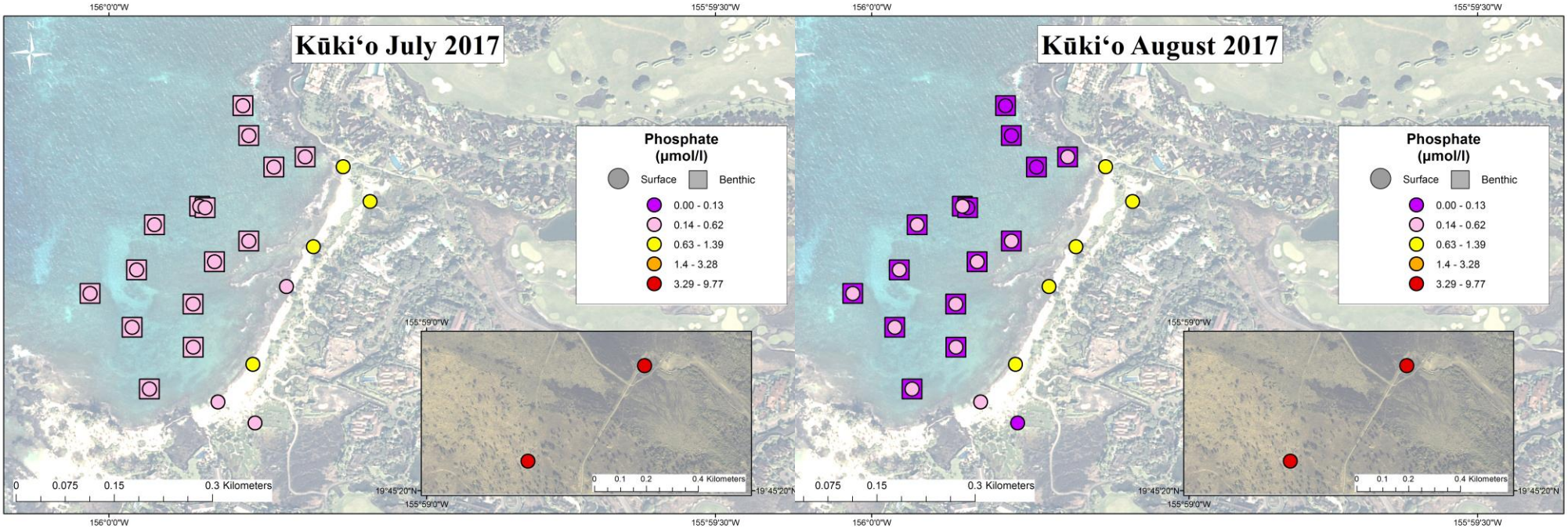

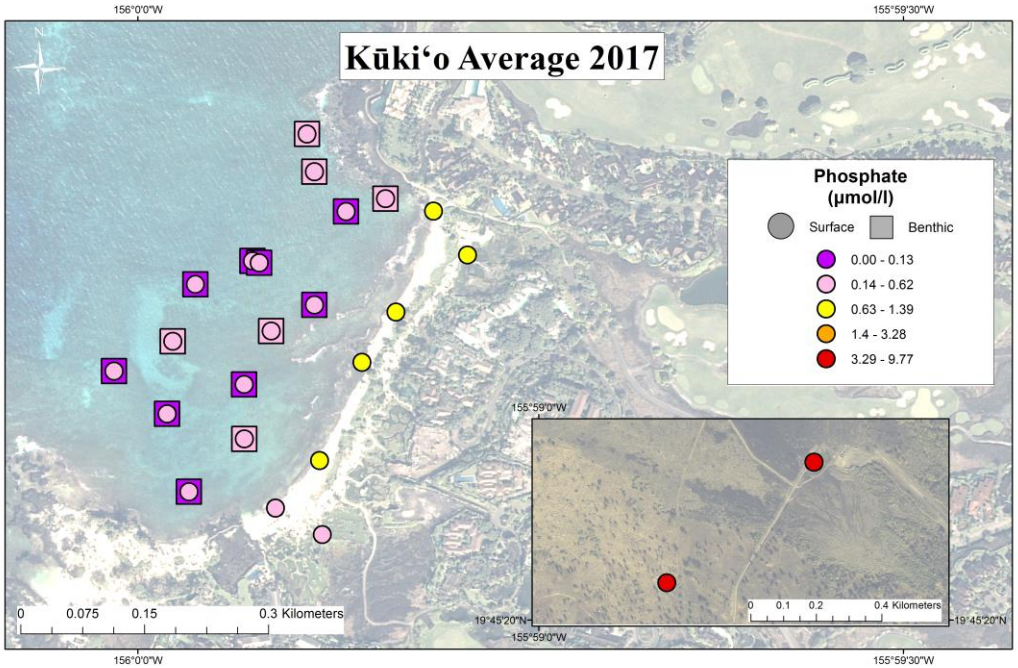

Appendix 11. PO_4^{3-} maps for Kūkiʻo Bay, Hawaiʻi.

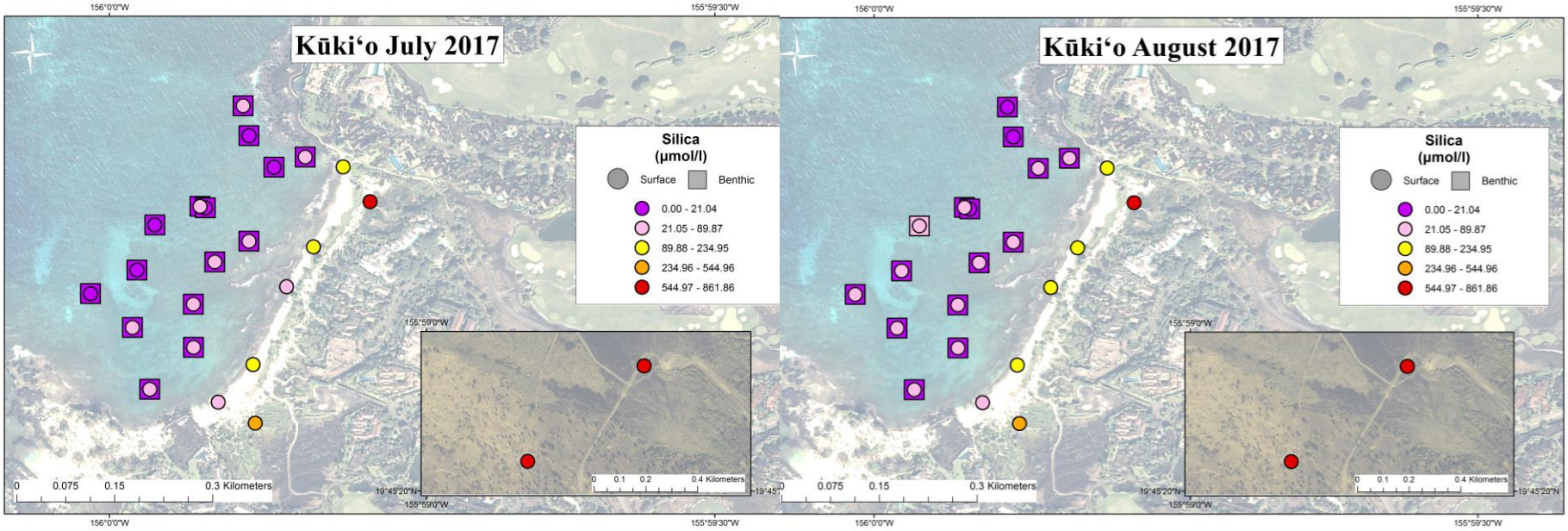

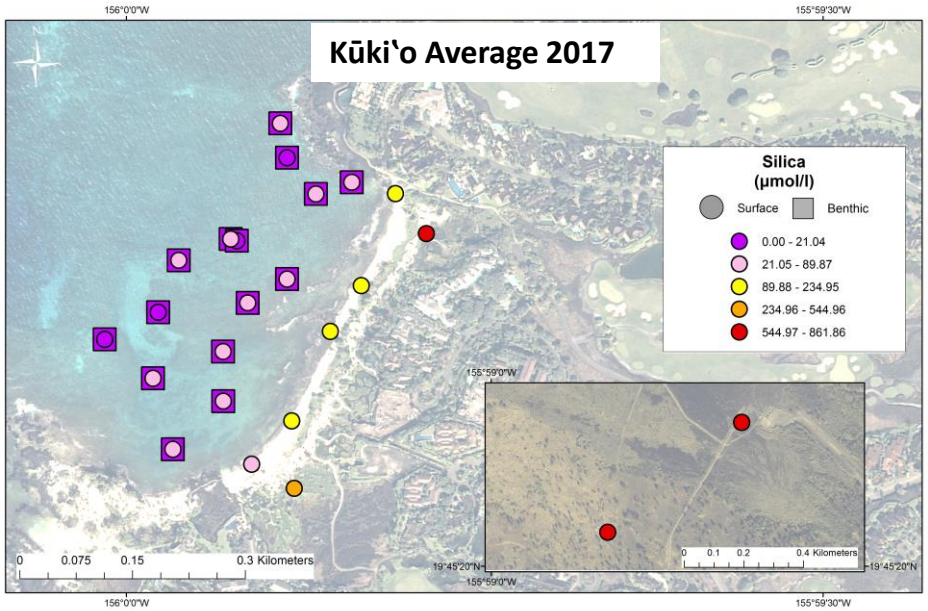

Appendix 12. H_4SiO_4 maps for Kūkiʻo Bay, Hawaiʻi.

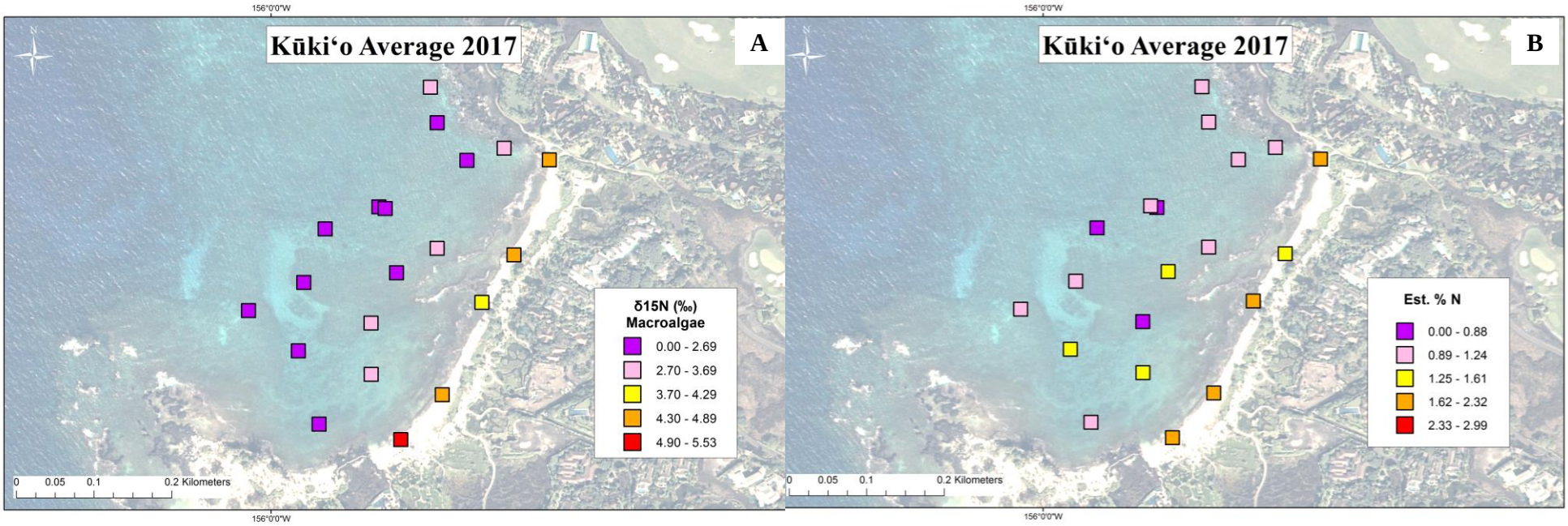

Appendix 13. Average $\delta^{15}N$ (A) and %N (B) in macroalgal tissue maps for Kūkiʻo Bay, Hawaiʻi.

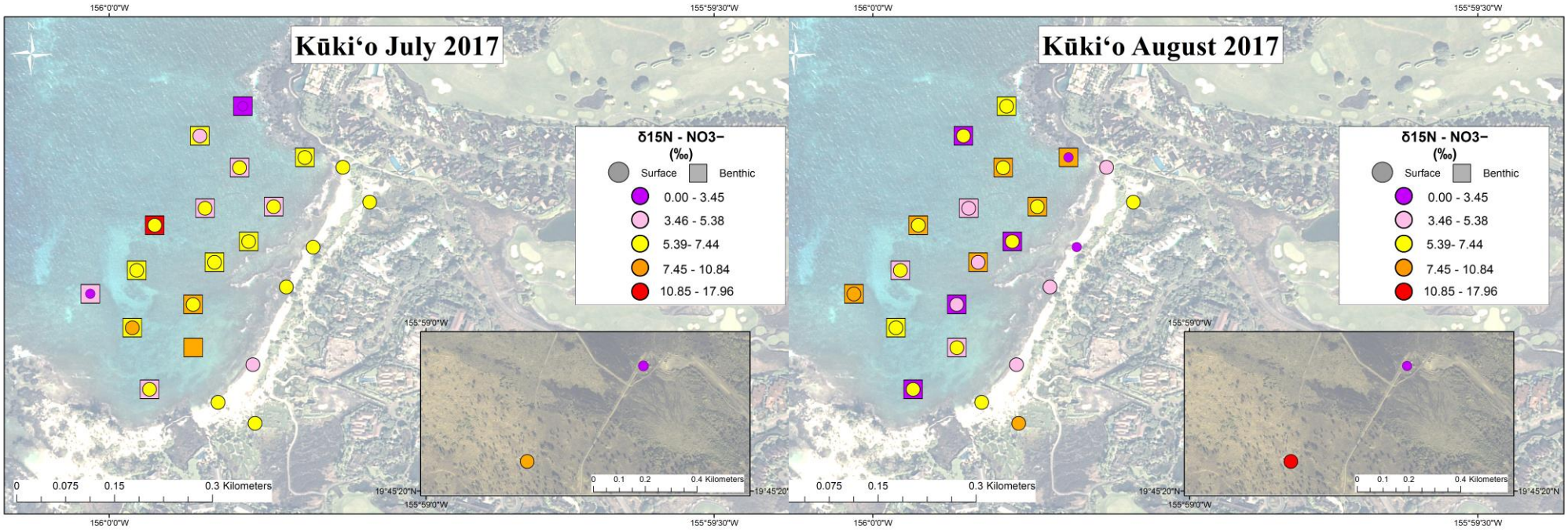

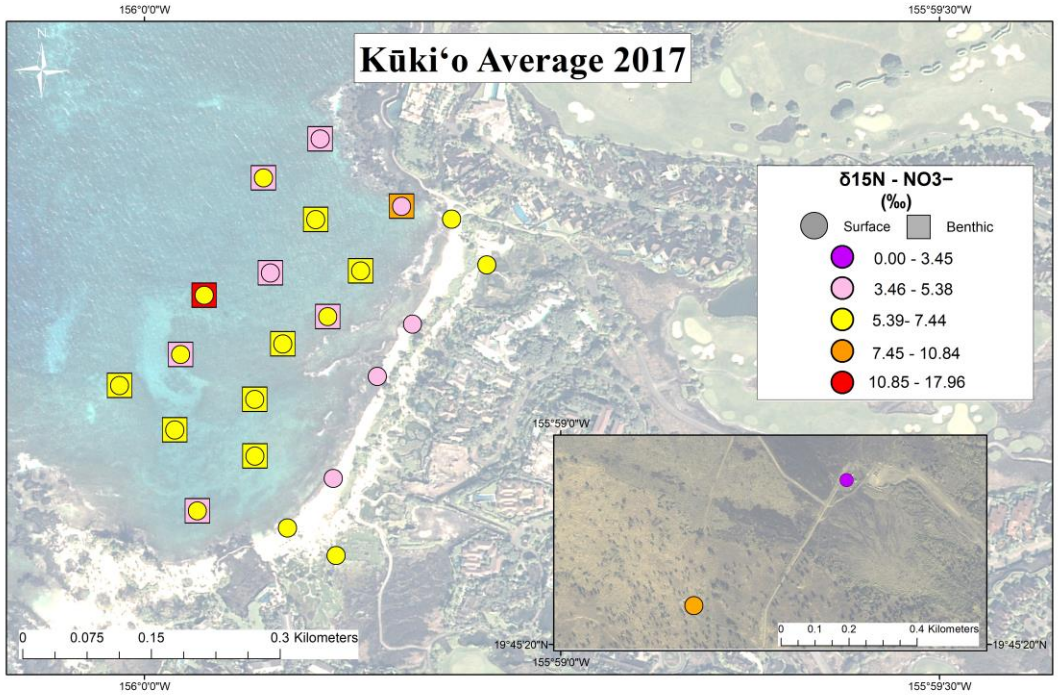

Appendix 14. $\delta^{15}N\text{-}NO_3^-$ concentration maps for Kūkiʻo Bay, Hawaiʻi.

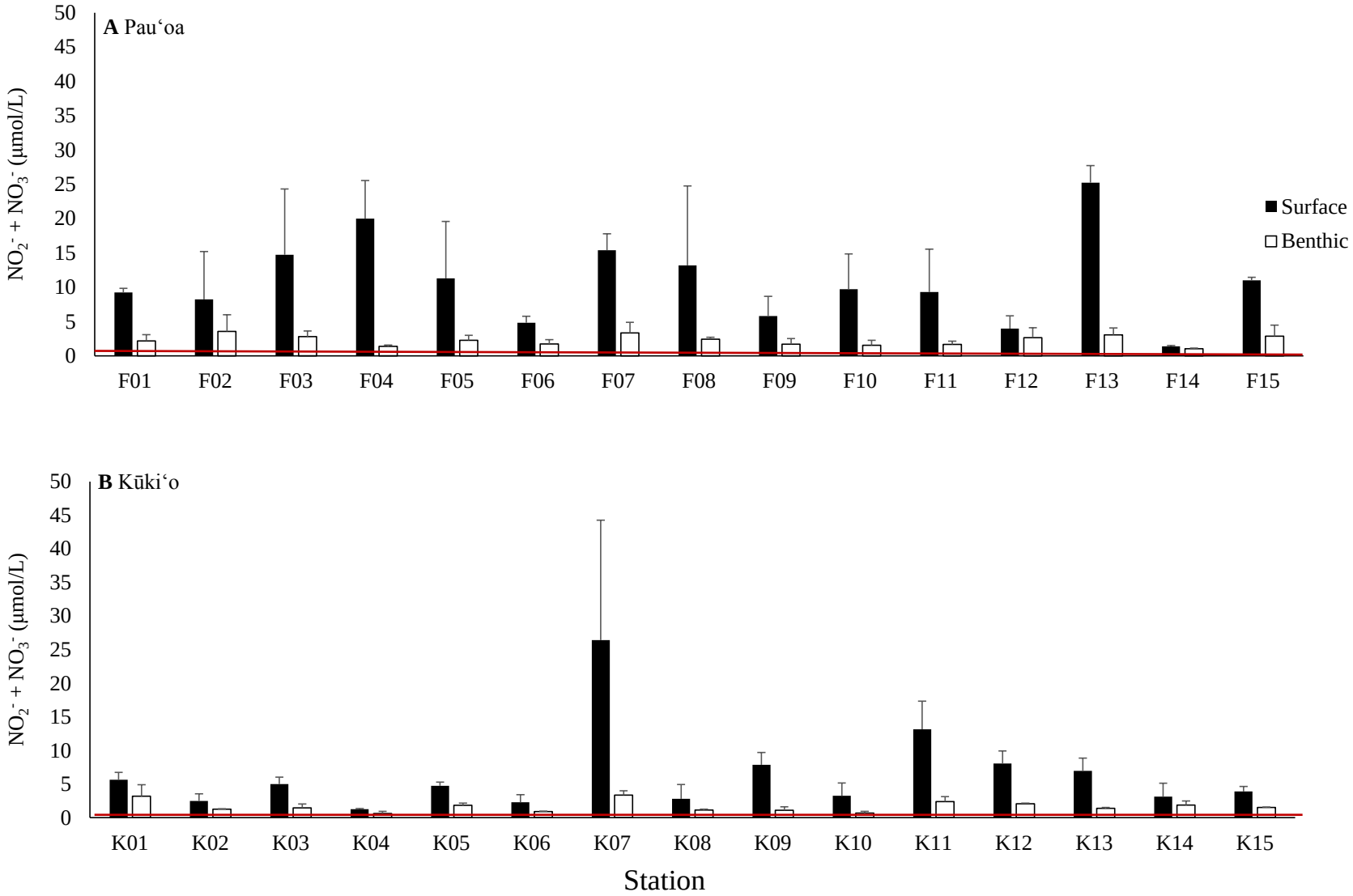

Appendix 15. Average (±SE) NO_3^-+NO_2^- concentrations at (A) Pauʻoa and (B) Kūkiʻo Bays, Hawaiʻi. Red line represents HDOH Kona (west) coast of Hawaiʻi Island standards for all marine waters Loa Point to Malae point, excluding Kawaihae and Honokohau harbors, including all areas from the shoreline at mean lower low water to a distance of 100 m seaward. The standard shown in the figure (0.32 µmol/L) applies to areas where marine water salinity is greater than 32 ppt. P13 at Pauʻoa Bay is the only station where the surface salinity was less than 32 ppt. Note, standard only applies to surface water samples, not benthic ones.

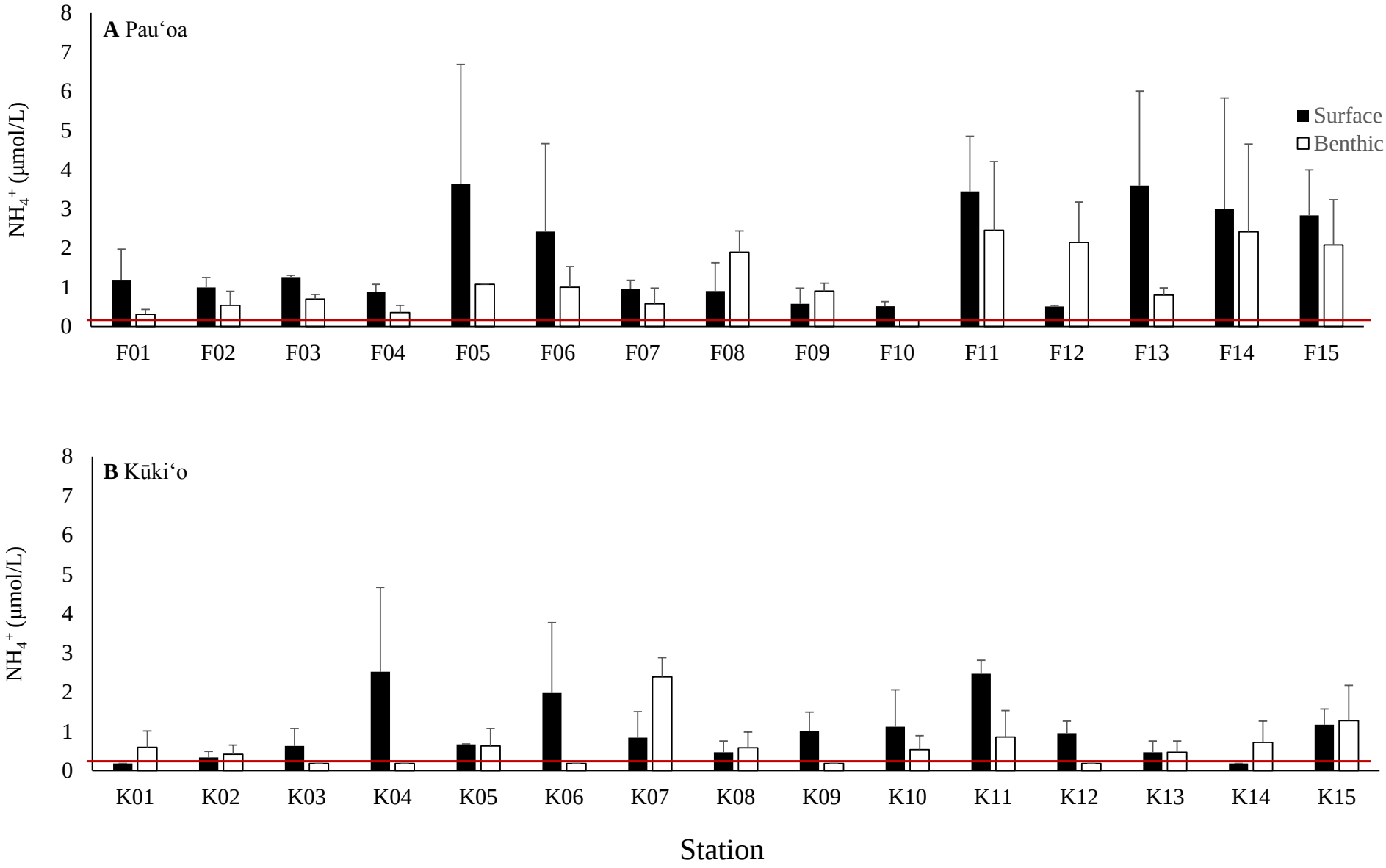

Appendix 16. Average (±SE) NH_4^+concentrations at (A) Pauʻoa and (B) Kūkiʻo Bays, Hawaiʻi. Red line represents HDOH Kona (west) coast of Hawaiʻi Island standards for all marine waters Loa Point to Malae point, excluding Kawaihae and Honokohau harbors, including all areas from the shoreline at mean lower low water to a distance of 100 m seaward. The standard shown in the figure (0.18 µmol/L) applies to areas where marine water salinity is greater than 32 ppt. P13 at Pauʻoa Bay is the only station where the surface salinity was less than 32 ppt. Note, standard only applies to surface water samples, not benthic ones.

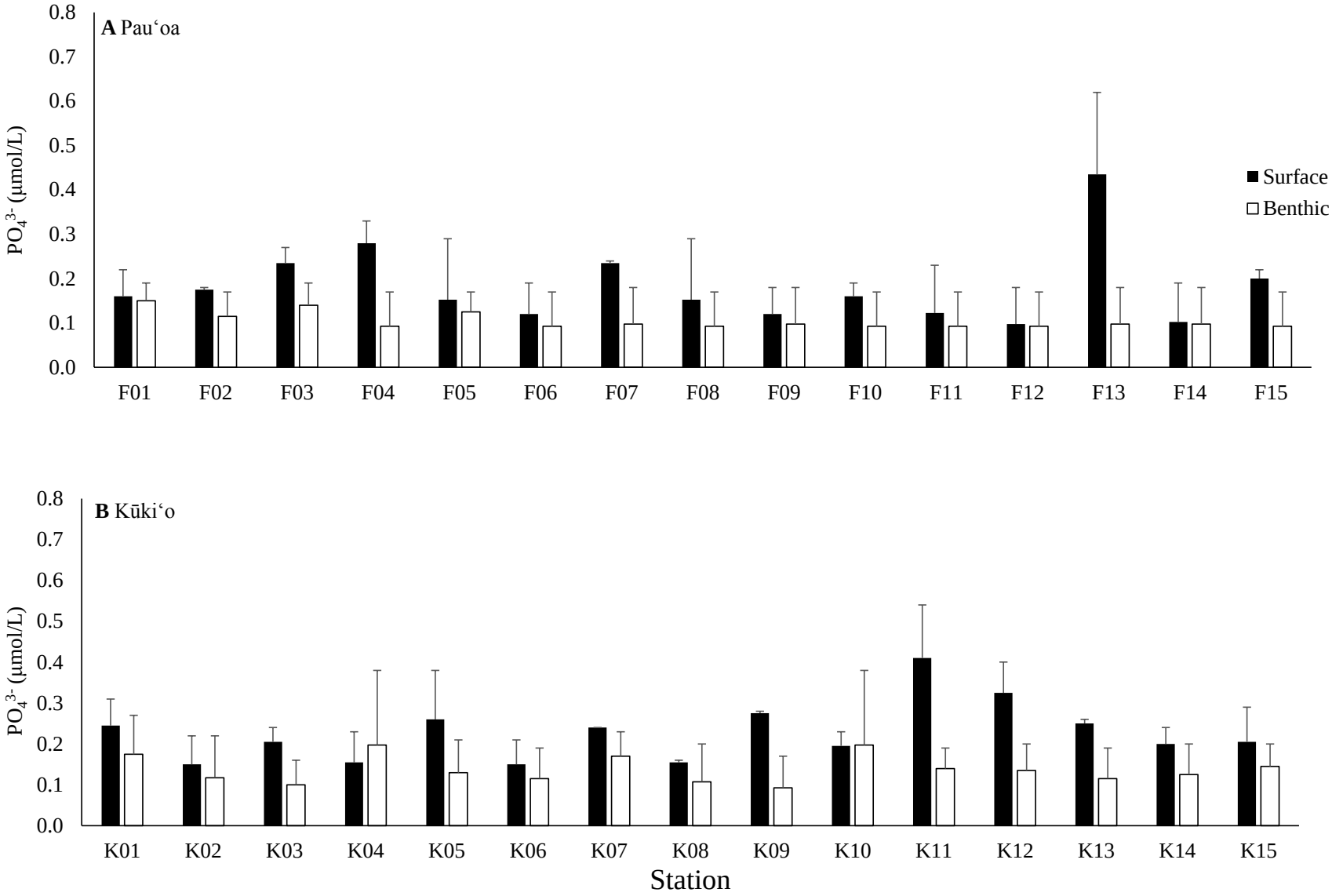

Appendix 17. Average (±SE) PO_4^{3-} concentrations at (A) Pauʻoa and (B) Kūkiʻo Bays, Hawaiʻi. Red line represents HDOH Kona (west) coast of Hawaiʻi Island standards for all marine waters Loa Point to Malae point, excluding Kawaihae and Honokohau harbors, including all areas from the shoreline at mean lower low water to a distance of 100 m seaward. The standard shown in the figure (0.16 µmol/L) applies to areas where marine water salinity is greater than 32 ppt. P13 at Pauʻoa Bay is the only station where the surface salinity was less than 32 ppt. Note, standard only applies to surface water samples, not benthic ones.

Appendix 18. Average ± SE salinity, $NO_2^- + NO_3^-$ (µmol/L), NH_4^+ (µmol/L), PO_4^{3-} (µmol/L), H_4SiO_4 (µmol/L), %N and $\delta^{15}N$ in macroalgae (‰), and $\delta^{15}N$- and $\delta^{18}O$-NO_3^- (‰) for shoreline (PSH1 – PSH5), offshore (surface and benthic, P01-P15), anchialine pond (PAP1 – PAP2), and well (PML1, PML5, PHHS5) stations at Pau'oa. Macroalgal tissue was collected once. Stations and parameters without SE indicate single samples.

Station	Depth	Salinity	$NO_2^-+NO_3^-$	NH_4^+	PO_4^{3-}	H_4SiO_4	%N (algae)	$\delta^{15}N$ (algae)	$\delta^{15}N$ (NO_3^-)	$\delta^{18}O$ (NO_3^-)
PSH1		13.1 ± 5.5	59.13 ± 14.48	1.84 ± 0.41	1.23 ± 0.35	490 ± 49	2.10 ± 0.22	4.45 ± 0.22	5.48 ± 0.52	0.61 ± 0.91
PSH2		18.9 ± 3.6	42.12 ± 11.98	2.50 ± 0.28	0.89 ± 0.20	364 ± 23	2.46 ± 0.56	4.97 ± 0.56	4.70 ± 0.74	1.95 ± 2.20
PSH3		11.1 ± 10.7	68.87 ± 48.96	2.03 ± 0.69	1.20 ± 0.77	454 ± 271	2.00	4.65	5.27 ± 0.98	0.22 ± 0.76
PSH4		7.9 ± 4.4	137.81 ± 63.74	3.41 ± 0.13	1.17 ± 0.22	504 ± 130	1.73 ± 0.59	4.53 ± 0.00	6.13 ± 0.35	0.80 ± 2.17
PSH5		34.3 ± 3.4	3.14 ± 43.04	1.53 ± 1.37	0.09 ± 0.06	5 ± 44	1.61 ± 0.99	3.40 ± 0.58	5.02 ± 0.72	10.65 ± 0.60
P01	Surface	32.7 ± 0.1	9.23 ± 0.61	1.20 ± 0.79	0.16 ± 0.06	75 ± 15	n/a	n/a	6.36 ± 0.84	6.87 ± 1.24
	Benthic	34.4 ± 0.2	2.17 ± 0.90	0.31 ± 0.13	0.15 ± 0.04	27 ± 23	0.78	3.50	8.91 ± 1.81	10.41 ± 6.23
P02	Surface	33.2 ± 1.0	8.24 ± 6.95	1.00 ± 0.25	0.18 ± 0.00	49 ± 47	n/a	n/a	7.63 ± 1.67	9.27 ± 6.04
	Benthic	34.1 ± 0.4	3.56 ± 2.43	0.54 ± 0.36	0.12 ± 0.06	23 ± 20	0.80	4.40	8.50 ± 1.50	11.04 ± 7.09
P03	Surface	33.1 ± 0.8	14.74 ± 9.56	1.26 ± 0.05	0.24 ± 0.04	93 ± 43	n/a	n/a	6.77 ± 0.81	1.25 ± 1.13
	Benthic	34.3 ± 0.0	2.79 ± 0.83	0.70 ± 0.12	0.14 ± 0.05	33 ± 23	0.88	3.30	5.96 ± 3.25	1.08 ± 7.38
P04	Surface	32.4 ± 0.4	20.00 ± 5.55	0.89 ± 0.19	0.28 ± 0.05	142 ± 41	n/a	n/a	5.36 ± 1.16	1.54 ± 0.89
	Benthic	34.6 ± 0.1	1.39 ± 0.19	0.36 ± 0.18	0.09 ± 0.08	10 ± 10	1.00	2.90	4.06 ± 3.38	9.30 ± 2.91
PO5	Surface	33.2 ± 0.8	11.28 ± 8.31	3.64 ± 3.05	0.15 ± 0.14	73 ± 52	n/a	n/a	5.94 ± 0.97	3.62 ± 0.39
	Benthic	34.4 ± 0.0	2.27 ± 0.73	1.08 ± 0.01	0.13 ± 0.05	21 ± 21	1.02	3.50	4.89 ± 0.36	7.21 ± 1.53
P06	Surface	33.6 ± 0.1	4.83 ± 0.93	2.43 ± 2.25	0.12 ± 0.07	35 ± 2	n/a	n/a	5.47 ± 0.43	4.19 ± 0.21
	Benthic	34.7 ± 0.0	1.75 ± 0.62	1.01 ± 0.53	0.09 ± 0.08	15 ± 14	1.18	3.30	8.57 ± 1.89	13.68 ± 4.88
P07	Surface	34.1 ± 0.9	15.39 ± 2.38	0.97 ± 0.22	0.24 ± 0.00	122 ± 24	n/a	n/a	5.36 ± 0.50	1.66 ± 0.25
	Benthic	32.6 ± 2.0	3.35 ± 1.53	0.58 ± 0.40	0.10 ± 0.08	11 ± 9	1.19	2.50	5.06 ± 1.46	8.42 ± 0.18
PO8	Surface	33.5 ± 1.1	13.19 ± 11.56	0.91 ± 0.73	0.15 ± 0.04	63 ± 38	n/a	n/a	7.30 ± 1.57	8.36 ± 7.64
	Benthic	34.6 ± 0.0	2.42 ± 0.29	1.90 ± 0.54	0.09 ± 0.08	2 ± 1	0.99	3.60	7.09 ± 1.54	16.25 ± 0.05
P09	Surface	33.4 ± 0.7	5.80 ± 2.87	0.58 ± 0.40	0.12 ± 0.06	34 ± 15	n/a	n/a	6.22 ± 0.69	7.73 ± 1.90
	Benthic	34.8 ± 0.0	1.71 ± 0.82	0.91 ± 0.21	0.10 ± 0.08	4 ± 3	1.15	2.60	6.75 ± 1.02	6.58 ± 5.86
P10	Surface	32.8 ± 0.4	9.71 ± 5.14	0.52 ± 0.12	0.16 ± 0.03	69 ± 29	n/a	n/a	5.70 ± 0.24	3.61 ± 0.75
	Benthic	34.8 ± 0.0	1.54 ± 0.72	0.18 ± 0.00	0.09 ± 0.08	3 ± 2	1.08	2.10	10.82 ± 3.52	13.34 ± 0.55
P11	Surface	33.7 ± 0.7	9.32 ± 6.23	3.45 ± 1.41	0.12 ± 0.11	34 ± 31	n/a	n/a	6.99 ± 1.27	7.02 ± 5.67
	Benthic	34.6 ± 0.1	1.67 ± 0.46	2.46 ± 1.75	0.09 ± 0.08	1 ± 0	0.60	2.50	5.02 ± 1.10	9.28 ± 7.64
P12	Surface	34.2 ± 0.2	3.97 ± 1.88	0.52 ± 0.03	0.10 ± 0.08	17 ± 8	n/a	n/a	7.27 ± 0.81	5.27 ± 1.78
	Benthic	34.7 ± 0.1	2.65 ± 1.44	2.15 ± 1.03	0.09 ± 0.08	1 ± 1	1.23	3.10	9.89 ± 0.40	17.02 ± 4.74
P13	Surface	31.6 ± 0.2	25.24 ± 2.50	3.60 ± 2.41	0.44 ± 0.19	133 ± 11	n/a	n/a	5.16 ± 0.71	0.17 ± 2.46
	Benthic	33.9 ± 0.2	3.05 ± 1.00	0.81 ± 0.19	0.10 ± 0.08	21 ± 8	1.01	3.30	7.44 ± 0.30	6.75 ± 1.52
P14	Surface	34.5 ± 0.1	1.38 ± 0.13	3.01 ± 2.83	0.10 ± 0.09	1 ± 0	n/a	n/a	7.96 ± 2.79	7.37 ± 4.59
	Benthic	34.6 ± 0.1	1.05 ± 0.08	2.42 ± 2.24	0.10 ± 0.08	2 ± 2	0.99	3.10	9.83 ± 0.53	19.90 ± 5.60
P15	Surface	32.6 ± 0.2	11.01 ± 0.45	2.84 ± 1.16	0.20 ± 0.02	90 ± 11	n/a	n/a	6.22 ± 0.51	2.53 ± 1.62
	Benthic	34.1 ± 0.1	2.85 ± 1.61	2.09 ± 1.16	0.09 ± 0.08	12 ± 6	0.57	3.50	10.01 ± 0.82	13.39 ± 0.38
PAP1		3.9 ± 0.9	43.15 ± 29.40	16.61 ± 7.8	2.49 ± 0.80	669 ± 31	n/a	n/a	5.95 ± 1.04	0.64 ± 1.29
PAP2		10.5 ± 0.2	147.89 ± 2.99	1.69 ± 0.5	0.12 ± 0.11	633 ± 42	n/a	n/a	6.90 ± 0.72	-0.09 ± 0.02
PML1		1.4 ± 0.8	137.30 ± 18.68	2.65 ± 2.5	1.43 ± 0.24	789 ± 1	n/a	n/a	6.96 ± 1.79	2.24 ± 2.79
PML5		2.1 ± 0.1	102.12 ± 7.22	1.09 ± 0.5	1.54 ± 0.42	783 ± 37	n/a	n/a	6.38 ± 1.98	0.66 ± 3.04
PHWS5		0.2 ± 0.0	101.78 ± 4.20	0.85 ± 0.2	2.27 ± 0.02	733 ± 51	n/a	n/a	2.31 ± 0.05	-0.26 ± 0.47

Appendix 19. Average ± SE salinity, $NO_2^- + NO_3^-$ (µmol/L), NH_4^+ (µmol/L), PO_4^{3-} (µmol/L), H_4SiO_4 (µmol/L), %N and $\delta^{15}N$ in macroalgae (‰), and $\delta^{15}N$- and $\delta^{18}O$-NO_3- (‰) for shoreline (KSH1 – KSH5), offshore (surface and benthic, K01-K15), anchialine pond (KAP1 – KAP2), and well (KWHS3 – KWHS5) stations at Kūkiʻo. Macroalgal tissue was collected during the study. Stations and parameters without SE indicate single samples.

Station	Depth	Salinity	$NO_2^- + NO_3^-$	NH_4^+	PO_4^{3-}	H_4SiO_4	%N (algae)	$\delta^{15}N$ (algae)	$\delta^{15}N$ (NO_3^-)	$\delta^{18}O$ (NO_3^-)
KSH1		27.7 ± 3.2	9.39 ± 1.97	2.21 ± 0.28	0.38 ± 0.12	53 ± 17	1.78 ± 0.34	5.37 ± 0.11	6.28 ± 0.30	5.47 ± 0.87
KSH2		27.2 ± 0.1	35.80 ± 4.73	0.80 ± 0.12	0.93 ± 0.00	151 ± 5	2.14 ± 0.74	4.34 ± 0.26	4.94 ± 0.01	6.41 ± 3.82
KSH3		24.3 ± 1.0	36.95 ± 22.29	0.73 ± 0.35	0.71 ± 0.29	155 ± 80	1.99 ± 0.55	4.27 ± 0.24	4.87 ± 0.97	2.91 ± 1.37
KSH4		21.2 ± 3.1	39.14 ± 11.45	0.40 ± 0.22	1.06 ± 0.20	183 ± 25	1.45 ± 0.15	4.64 ± 0.17	4.52 ± 1.19	2.56 ± 0.98
KSH5		17.4 ± 4.2	32.02 ± 5.39	3.15 ± 2.10	0.83 ± 0.02	174 ± 9	1.67 ± 0.18	4.76 ± 0.26	5.45 ± 0.78	2.03 ± 1.04
K01	Surface	33.7 ± 0.2	5.64 ± 1.10	0.18 ± 0.00	0.25 ± 0.07	32 ± 5	n/a	n/a	4.81 ± 2.42	0.39 ± 2.14
	Benthic	34.2 ± 0.0	3.21 ± 1.70	0.60 ± 0.42	0.18 ± 0.10	11 ± 0	1.16	3.60	7.93 ± 0.74	7.53 ± 4.97
K02	Surface	34.1 ± 0.1	2.48 ± 1.06	0.34 ± 0.16	0.15 ± 0.07	22 ± 6	n/a	n/a	6.45 ± 0.94	7.33 ± 2.45
	Benthic	34.4 ± 0.1	1.27 ± 0.06	0.42 ± 0.24	0.12 ± 0.10	3 ± 3	1.21	2.30	7.23 ± 2.32	11.92 ± 6.18
K03	Surface	33.8 ± 0.1	5.00 ± 1.03	0.63 ± 0.45	0.21 ± 0.04	34 ± 8	n/a	n/a	5.51 ± 0.08	6.53 ± 0.23
	Benthic	34.3 ± 0.1	1.47 ± 0.57	0.18 ± 0.00	0.10 ± 0.06	6 ± 1	1.14	2.50	6.27 ± 2.24	10.73 ± 1.65
K04	Surface	34.4 ± 0.0	1.26 ± 0.10	2.52 ± 2.14	0.16 ± 0.08	10 ± 8	n/a	n/a	5.54 ± 0.16	8.28 ± 2.77
	Benthic	34.4 ± 0.0	0.64 ± 0.31	0.18 ± 0.00	0.20 ± 0.18	3 ± 0	1.23	2.20	4.35 ± 1.11	9.23 ± 1.89
K05	Surface	34.0 ± 0.7	4.74 ± 0.56	0.67 ± 0.02	0.26 ± 0.12	33 ± 3	n/a	n/a	5.98 ± 0.05	5.49 ± 0.28
	Benthic	34.3 ± 0.1	1.86 ± 0.31	0.63 ± 0.45	0.13 ± 0.08	10 ± 1	1.22	3.00	4.40 ± 1.32	9.66 ± 2.89
K06	Surface	34.7 ± 0.2	2.31 ± 1.12	1.98 ± 1.80	0.15 ± 0.06	10 ± 6	n/a	n/a	5.37 ± 0.83	5.19 ± 0.53
	Benthic	34.3 ± 0.2	0.90 ± 0.08	0.18 ± 0.00	0.12 ± 0.08	5 ± 1	0.55	1.60	5.25 ± 0.06	4.91 ± 6.57
K07	Surface	33.9 ± 0.2	26.40 ± 17.84	0.84 ± 0.66	0.24 ± 0.00	39 ± 11	n/a	n/a	5.63 ± 0.84	3.99 ± 1.64
	Benthic	34.2 ± 0.3	3.38 ± 0.63	2.39 ± 0.50	0.17 ± 0.06	6 ± 1	1.39	2.10	7.20 ± 0.80	9.07 ± 4.67
K08	Surface	34.3 ± 0.5	2.80 ± 2.15	0.47 ± 0.29	0.16 ± 0.01	29 ± 26	n/a	n/a	5.72 ± 0.05	4.71 ± 0.47
	Benthic	34.6 ± 0.3	1.14 ± 0.14	0.58 ± 0.40	0.11 ± 0.09	14 ± 11	0.79	2.00	13.41 ± 4.46	20.02 ± 2.53
K09	Surface	33.8 ± 0.6	7.87 ± 1.85	1.02 ± 0.48	0.28 ± 0.01	45 ± 4	n/a	n/a	5.41 ± 0.15	5.38 ± 0.30
	Benthic	34.2 ± 0.1	1.10 ± 0.51	0.18 ± 0.00	0.09 ± 0.08	5 ± 0	0.78	2.80	6.05 ± 2.60	6.55 ± 2.57
K10	Surface	34.2 ± 0.3	3.27 ± 1.92	1.12 ± 0.94	0.20 ± 0.04	15 ± 12	n/a	n/a	5.98 ± 0.01	7.46 ± 2.20
	Benthic	34.5 ± 0.1	0.68 ± 0.29	0.54 ± 0.36	0.20 ± 0.18	3 ± 1	1.11	1.80	4.76 ± 1.08	8.51 ± 0.54
K11	Surface	33.6 ± 0.7	13.17 ± 4.19	2.47 ± 0.35	0.41 ± 0.13	42 ± 7	n/a	n/a	5.78	4.37
	Benthic	34.1 ± 0.2	2.38 ± 0.76	0.86 ± 0.68	0.14 ± 0.05	7 ± 2	1.61	3.40	7.20 ± 2.19	12.98 ± 2.33
K12	Surface	33.8 ± 0.0	8.05 ± 1.89	0.95 ± 0.31	0.33 ± 0.08	43 ± 4	n/a	n/a	5.62 ± 0.17	9.05 ± 3.69
	Benthic	34.1 ± 0.0	2.09 ± 0.08	0.18 ± 0.00	0.14 ± 0.07	11 ± 1	1.17	1.90	3.60 ± 0.83	3.62 ± 3.57
K13	Surface	33.7 ± 0.1	6.97 ± 1.91	0.47 ± 0.29	0.25 ± 0.01	47 ± 18	n/a	n/a	7.02 ± 0.92	9.97 ± 5.08
	Benthic	34.3 ± 0.2	1.40 ± 0.13	0.47 ± 0.29	0.12 ± 0.08	11 ± 3	1.46	2.40	5.66 ± 0.13	11.71 ± 1.23
K14	Surface	34.2 ± 0.3	3.14 ± 1.98	0.18 ± 0.00	0.20 ± 0.04	15 ± 11	n/a	n/a	5.40 ± 2.23	7.33 ± 3.00
	Benthic	34.5 ± 0.0	1.89 ± 0.60	0.72 ± 0.54	0.13 ± 0.08	5 ± 0	1.24	1.60	6.86 ± 1.61	14.86 ± 1.75
K15	Surface	34.0 ± 0.0	3.90 ± 0.76	1.17 ± 0.40	0.21 ± 0.09	21 ± 4	n/a	n/a	3.73 ± 3.52	7.81 ± 3.87
	Benthic	34.3 ± 0.0	1.53 ± 0.05	1.27 ± 0.90	0.15 ± 0.06	9 ± 3	1.00	3.00	4.21 ± 1.58	9.07 ± 1.88
KAP1		6.7 ± 0.4	49.62 ± 16.90	0.90 ± 0.28	0.27 ± 0.26	510 ± 34	n/a	n/a	6.55 ± 1.05	7.65 ± 2.92
KAP2		7.0 ± 0.7	50.67 ± 4.95	8.03 ± 4.04	1.28 ± 0.01	617 ± 20	n/a	n/a	5.95 ± 0.35	6.27 ± 3.82
KWHS3		0.8 ± 0.1	72.91 ± 1.76	0.82 ± 0.64	9.73 ± 0.04	741 ± 121	n/a	n/a	10.09 ± 7.86	16.89 ± 13.69
KHWS5		1.4 ± 0.1	74.26 ± 3.00	1.58 ± 1.03	6.71 ± 0.25	739 ± 123	n/a	n/a	1.93 ± 0.32	0.89 ± 1.32

Appendix 20. Probability (percent) of total time salinity was within a given range at each station. Values of 0.0% represent positive occurrences of salinity in that range, but during <0.05% of the deployment.

Pauʻoa Bay

Salinity Range	FO1	FO2	FO4	FO5	FO7	FO8	FO9	FO10	FO11	FO12	FO15
[35.0-35.5]	-	-	0.8	-	-	2.8	-	-	0.0	0.0	-
[34.5-35.0)	0.1	0.5	39.7	0.3	28.6	34.5	2.1	7.1	6.3	0.4	1.1
[34.0-34.5)	27.6	42.7	48.2	20.0	68.4	53.0	96.7	86.7	31.7	10.1	44.8
[33.5-34.0)	69.3	53.2	9.5	77.6	2.8	8.5	1.2	6.2	40.6	68.8	52.4
[33.0-33.5)	3.0	3.6	0.8	2.0	0.2	1.2	-	0.0	16.5	19.0	1.6
[32.5-33.0)	-	0.0	0.9	-	0.0	-	-	-	4.5	1.6	0.0
[32.0-32.5)	-	-	0.1	-	-	-	-	-	0.3	0.0	-
[31.5-32.0)	-	-	0.0	-	-	-	-	-	-	-	-
[31.0-31.5)	-	-	-	-	-	-	-	-	-	-	-
[30.5-31.0)	-	-	-	-	-	-	-	-	-	-	-
[30-30.5)	-	-	-	-	-	-	-	-	-	-	-

Kūkiʻo Bay

Salinity Range	KU01	KU02	KU04	KU07	KU08	KU09	KU10	KU11	KU12	KU13	KU14	KU15
[35.0-35.5]	-	-	11.6	-	-	-	-	-	-	-	-	-
[34.5-35.0)	0.2	76.5	80.8	0.0	0.0	0.3	0.1	-	0.2	-	-	74.0
[34.0-34.5)	74.1	23.0	7.5	85.4	51.9	65.3	74.5	13.6	13.4	97.7	90.2	21.1
[33.5-34.0)	18.6	0.4	0.1	11.9	34.8	29.2	25.4	58.2	63.5	2.3	9.8	1.7
[33.0-33.5)	6.7	0.0	-	2.4	10.1	2.0	0.0	22.8	16.0	0.0	-	0.9
[32.5-33.0)	0.4	0.0	-	0.1	2.8	1.2	-	3.1	6.1	-	0.0	0.3
[32.0-32.5)	0.0	0.0	-	0.0	0.3	1.0	-	2.3	0.8	-	-	0.6
[31.5-32.0)	-	-	-	0.0	0.0	0.5	-	-	0.0	-	-	0.2
[31.0-31.5)	-	-	-	0.0	-	0.4	-	-	0.0	-	-	0.7
[30.5-31.0)	-	0.0	-	-	0.0	0.1	-	-	0.0	-	-	0.4
[30-30.5)	-	-	-	-	-	0.1	-	-	-	-	-	0.2

Appendix 21

Land Use Land Cover Description	Land Use Code	Load N (kg/ha)	Efficiency N	Critical Length	Vegetation Present?	Proportion Subsurface N	Comments
Background	0	0	0.75	50	0	1	
Unclassified	1	0	0.75	50	0	1	
Developed High Intensity	2	10	0.1	50	0	1	
Developed Medium Intensity	3	7.5	0.15	50	0	1	
Developed Low Intensity	4	5	0.25	50	0	1	
Developed Open Space	5	50	0.1	1000	1	1	Considering as landscaping.
Cultivated Crops	6	100	0.75	50	1	1	Mostly coffee and mixed vegetables near Captain Cook
Pasture/Hay	7	1	0.9	50	1	1	Considers nutrient load from goats and cattle (although very rocky terrain on the Big Island) (formerly 20 kg/ha)
Grassland/Herbaceous	8	3.1	0.99	50	1	1	Often very sparse in west Hawai‘i
Deciduous Forest	9	4.7	0.8	50	1	1	n/a
Evergreen Forest	10	11.3	0.99	50	1	1	Citing Ostertag for the native forest nutrient load; Very low erosion because of the type of forest; Predominant forest is south at Napo'opo'o

Land Use Land Cover Description (cont)	Land Use Code	Load N (kg/ha)	Efficiency N	Critical Length	Vegetation Present?	Proportion Subsurface N	Comments
Kiawe Forest	11	55	0.99	50	1	1	Cited at http://www.ncbi.nlm.nih.gov/pmc/articles/PMC98982/
Scrub/Shrub	12	5.5	0.99	50	1	1	Mostly low grass and shrubs at Puu Waawaa
Palustrine Forested Wetland	13	1.62	0.99	50	1	1	This is how Waipio Valley is classified - which is essentially lo'i and floodplain.
Palustrine Scrub/Shrub Wetland	14	1.62	0.99	50	1	1	
Palustrine Emergent Wetland	15	1.62	0.99	50	1	1	
Estuarine Forested Wetland	16	1.62	0.99	50	1	1	
Estuarine Scrub/Shrub Wetland	17	1.62	0.99	50	1	1	
Estuarine Emergent Wetland	18	1.62	0.99	50	1	1	
Unconsolidated Shore	19	0	0.75	50	0	1	
Bare Land	20	0	0	50	0	1	Here, meaning new volcanic rock
Open Water	21	2.6	0.1	50	0	1	
Palustrine Aquatic Bed	22	1.62	0.75	50	1	1	
Golf courses	23	200	0.1	50	1	1	

Land Use Land Cover Description (cont)	Land Use Code	Load N (kg/ha)	Efficiency N	Critical Length	Vegetation Present?	Proportion Subsurface N	Comments
Impervious Urban	30	17.1	0.1	50	0	1	
Impervious Ag	31	7.5	0.75	50	0	1	
Cultivated Crops, Coffee	40	140	0.86	50	1	1	Did not separate out Cultivated Crops and Coffee for the Kona coffee farms
Cultivated Crops, Fallow	41	3.1	0.64	50	1	1	
Grazing land	50	47.1	0.6	50	1	1	Same as pasture - left over from Maui
Cultivated Crops, Pineapple	51	424	0.75	50	1	1	
Cultivated Crops, Sugarcane	52	350	0.6	50	1	1	
Ag Subdivision	60	17.1	0.75	50	1	1	n/a for Hawai‘i
Cess pools	62	2000	0.1	1000	1	1	Buffered by 10m; Approximately 15kg per year for each cess pool. This is an underestimate.
Big Island Country Club	70	100	0.1	50	1	1	Previous versions of the model used golf course numbers by golf course. The highest is approximately 500 kg/ha as documented for west Hawai‘i hotels.
Hualalai Golf Club	71	100	0.1	50	1	1	
Kūki‘o Golf Course	72	100	0.1	50	1	1	
Makalei Golf Club	73	100	0.1	50	1	1	

Land Use Land Cover Description (cont)	Land Use Code	Load N (kg/ha)	Efficiency N	Critical Length	Vegetation Present?	Proportion Subsurface N	Comments
Mauna Lani Golf Course	74	100	0.1	50	1	1	
Waikoloa Beach Course	75	100	0.1	50	1	1	
Waikoloa Kings' Course	76	100	0.1	50	1	1	
Mauna Kea Golf Course	77	100	0.1	50	1	1	
Hapuna Golf Course	78	100	0.1	50	1	1	
Waikoloa Village Golf Course	79	100	0.1	50	1	1	
Lawns and Gardens	80	50	0.1	50	1	1	See lawns citation in Falinski, 2016
Hotel Trees and Shrubs	81	50	0.1	50	1	1	See lawns citation in Falinski, 2016
Agroforestry	112	22.6	0.9	50	1	1	For ulu, etc.
Loi	114	100	0.999	50	1	1	Deenik et al
Bare Soil	120	3.1	0.9	50	1	1	Areas of bare soil, not volcanic rock associated with Kohala. Giving it the same as grassland because am not sure how much nuts are in soil